SM REPORT 85-30

DESIGN OF ONE-KILOMETER-LONG ANTENNA STICKS AND SUPPORT STRUCTURE FOR A GEOSYNCHRONOUS SATELLITE

Thesis by

Janet Elizabeth Freeman

In Partial Fulfillment of the Requirements

for the Degree of

Aeronautical Engineer

California Institute of Technology

Pasadena, California

1986

(Submitted December 16, 1985)

ACKNOWLEDGEMENTS

I wish to express my appreciation to my adviser, Dr. Charles Babcock, for his patience, support, and keen technical insight. Our many discussions have been valuable learning experiences. My thanks also to the other members of my Engineer committee, Dr. Thomas Caughey and Dr. Peter Thompson, for their help in defining the technical problems of my research; Marta Nyiri, for word processing assistance and patient scheduling of appointments with Dr. Babcock; Betty Wood, for help with drawings; Dr. Brad Sturtevant and Rolf Sondergaard, for making it possible to transfer word processing files created on my personal computer to the GALCIT Word Processor; and the students and staff of GALCIT, for lively technical discussions and friendship.

I am grateful to my employer, Hughes Aircraft Company, for providing support through a Staff Engineer Fellowship. Many people at Hughes have been helpful during the course of my research, but a few deserve special recognition: Dr. Leo Stoolman, for encouragement and assistance in ways too numerous to list; my department manager Bob Drean and the Systems Labs management, for being understanding and supportive; Charles Edelsohn, for providing a thesis topic and charge number; Dr. John Velman and Dr. William Sargent, for illuminating technical discussions; Dr. James McEnnan, for providing access to and tutorial for his spacecraft dynamics computer program; Donna Williams, for dealing with administrative details; Dr. Zig Bleviss, for general encouragement; and the members of the Advanced System Design Department, for making me feel like a member of the team, even when I was at Hughes only one day a week.

Special thanks to Professor Babcock and Caltech for enabling me to complete the last term of my research through a Graduate Research Assistantship.

This work is dedicated to Mike Smith, who supplied understanding, solace, encouragement, and an occasional well-timed shove to a moody and irritable grad student throughout the long months.

ABSTRACT

This study develops a preliminary structural design for three one-kilometer-long antenna sticks and an antenna support structure for a geosynchronous earth-imaging satellite. On each of the antenna sticks is mounted a linear array of over 16,000 antenna elements. The antenna sticks are parallel to each other, and are spaced 1 km apart so that they form the corners of an imaginary triangular tube. This tube is spinning about its long axis. Antenna performance requires that the position of each antenna element be known to an accuracy of 0.5 cm, and that the spacecraft's spin axis be parallel to the earth's spin axis within one degree. Assuming that the position of each joint on each antenna stick is known, the antenna sticks are designed as beams under a uniformly distributed acceleration (due to spacecraft spin) to meet the displacement accuracy requirements for the antenna elements. Both a thin-walled round tube and a three-longeron double-laced truss are considered for the antenna stick structure. A spacecraft spinrate is chosen by considering the effects of environmental torques on the precession of a simplified spacecraft. A preliminary truss-like support structure configuration is chosen, and analyzed in quasi-static equilibrium with control thrusters firing to estimate the axial loads in the structural members. The compressive loads found by this analysis are used to design the support structure members to be buckling-critical three-longeron double-laced truss columns. Some tension-only members consisting of Kevlar cord are included in the design to eliminate the need for bulkier members. The lateral vibration modes of the individual structural members are found by conventional analysis--the fundamental frequencies are as low as 0.0066 Hz. Finite element dynamic analyses of the structure in free vibration confirm that simplified models of the structure and members can be used to determine the structural modes and natural frequencies for design purposes.

CONTENTS

FIGURES

TABLES

NOMENCLATURE*

a = column imperfection (m)

a_R = translational acceleration induced by a control thruster acting on the rigid body model (m/s^2)

a_T = transverse acceleration due to satellite spinrate, acting at antenna sticks (m/s^2)

A_d = cross-sectional area of truss column diagonal (m^2)

A_l = cross-sectional area of truss column longeron (m^2)

A_r = amplitude of mode shape $Y_r(x)$ (m)

A_s = cross-sectional area of antenna stick (m^2)

b = number of bays in a truss column (dimensionless)

c = speed of light (3×10^8 m/s^2)

C_d = coefficient of diffuse reflection (dimensionless)

C_o = opacity (dimensionless)

C_s = coefficient of specular reflection (dimensionless)

$\overrightarrow{df_s}$ = differential solar radiation force (N)

dA = elemental surface area of spacecraft (m^2)

dF_G = gravitational force acting on spacecraft (N)

D_l = outer diameter of a tubular longeron in a truss column (m)

D_d = outer diameter of a tubular diagonal in a truss column (m)

$E(x)$ = Young's Modulus (N/m^2)

E_o = Young's Modulus, uniform over entire beam length (N/m^2)

f = frequency of antenna radiation (Hz)

F = momentum flux from the sun (4.4×10^{-6} $kg/m/s^2$)

---

* SI units (length = meters, mass = kilograms, time = seconds, force = Newtons) are used throughout, and are indicated in parantheses.

F_R = inertial reaction force acting on a point mass to maintain equilibrium in the presence of applied translational acceleration a_R (N)

F_u = component of force F in the u-direction (N)

F_{ui} = applied load in the u-direction at point mass i in the rigid body model (N)

$F_{\theta u}$ = inertial reaction force acting on a point mass to maintain equilibrium in the presence of applied angular acceleration Ω_u (N)

G = gravitational constant (6.672×10^{-11} N-m^2/kg^2)

H = a measure of width or outer diameter of an antenna stick (m)

H_s = distance between longerons in antenna stick truss column (m)

H_{cm} = distance between longerons in cross member (m)

H_{dm} = distance between longerons in diagonal member (m)

I(x) = area moment of inertia of a cross-section (m^4)

I_d = area moment of inertia of a truss column diagonal (m^4)

I_l = area moment of inertia of a truss column longeron (m^4)

I_o = area moment of inertia of a cross section, uniform over entire beam length (m^4)

I_u = mass moment of inertia of a point mass about principal body axis u (kg-m^2)

I_{uB} = mass moment of inertia of a rigid body about principal body axis u (kg-m^2)

L = antenna stick segment half-lenth (m)

2L = antenna stick segment length (m)

m(x) = mass per unit length (kg/m)

m_{cm} = mass of structural cross member (kg)

m_{dm} = mass of structural diagonal member (kg)

m_e = mass of earth (5.979×10^{24} kg)

m_i = mass of interest in gravity equation (kg)

m_r = ratio of antenna element mass per unit length over antenna stick mass per unit length (dimensionless)

m_s = mass of antenna stick (kg)

M_{max} = maximum moment in a beam (N-m)

M_u = moment acting on rigid body model to create rotation about u-axis (N-m)

$\vec{N}$ = unit outward normal vector of area dA

P = axial load acting on a column (N)

P_E = Euler buckling load of a column (N)

P_d = axial load in a truss column diagonal (N)

P_i = axial tensile load in massless connecting member i of rigid body model (N)

P_l = axial load in a truss column longeron (N)

P_{To} = load carried by tension-only structural member (N)

$Q(x)$ = transverse load per unit length acting on a beam (N/m)

Q_o = uniformly distributed transverse load per unit length acting on a beam (N/m)

r_i = distance of mass m_i from center of earth (m)

r_d = radius of solid-rod longeron in a truss column (m)

r_l = radius of solid-rod diagonal in a truss column (m)

$\vec{R}$ = vector from spacecraft's center of mass to area dA (m)

R = static distance of antenna sticks from spacecraft spin axis (577.35 m)

$\vec{S}$ = unit vector from spacecraft to the sun

t = wall thickness of a thin-walled tube (m)

t_m = minimum practical wall thickness of a graphite-epoxy thin-walled tube (0.381 mm)

T = load applied by a control thruster (N)

T_u = component in u-direction of load applied by a control thruster (N)

V_{max} = maximum shear load in a beam (N)

$w(x)$ = transverse displacement of a beam (m)

$w_o(x)$ = transverse displacement of a beam having E, I, and Q constant (m)

$Y_r(x)$ = mode shapes in free vibration

α = width of an imperfection in beam bending stiffness EI (dimensionless)

β = angle between vectors $\vec{S}$ and $\vec{N}$ (degrees)

δ = amplitude of an imperfection in beam bending stiffness EI (dimensionless)

ϵ = displacement error (m)

λ = wavelength of antenna radiation (m)

ρ_s = mass density of antenna stick material (kg/m^3)

ϕ = angle between diagonal of a truss column and a line drawn perpendicular to the two adjoining longerons (degrees)

ν = Poisson's ratio

$\vec{\tau}_s$ = solar radiation torque acting on spacecraft (N-m)

ω_r = natural frequencies in free vibration (rad/sec or Hz)

Ω = spacecraft spinrate (rad/sec or rev/min)

$\dot{\Omega}_u$ = angular acceleration about axis u induced in rigid body model by moment M_u (rad/sec)

Chapter 1
INTRODUCTION

Geosynchronous orbits (at an altitude of approximately 37,000 km) are commonly used for a variety of satellite applications. A spacecraft in geosynchronous orbit has a constant view of the same spot of the earth, which is ideal for an earth imaging spacecraft that "takes pictures" of the earth's surface. Such a spacecraft might be composed in part of a large antenna structure that supports a linear array of antenna elements.

A developmental design for a geosynchronous earth-observation satellite uses 15 GHz phased array antennas for earth imaging. Each antenna is a one-kilometer-long "stick" (as opposed to a dish), along which more than 16,000 6-cm-long antenna elements are distributed. The antenna elements lie in a straight line, each element not quite touching its neighboring element(s).

The three antenna sticks form the three corners of an imaginary triangular tube, such that each stick is parallel to and spaced 1 km from the other two at all points along its length (Figure 1-1). To perform the earth imaging task, the "tube" is spinning about its axis with a minimum spinrate Ω of 1 rev/hr.

1.1. Satellite Performance Requirements.

The location of each antenna element must be known to an accuracy of one-quarter wavelength (0.5 cm) to obtain the desired image resolution. Because the antenna elements are mounted on the surface of the antenna sticks, displacement of any part of an antenna stick results in displacement of antenna elements. Image resolution requirements therefore necessitate that the displacement of each antenna stick must be

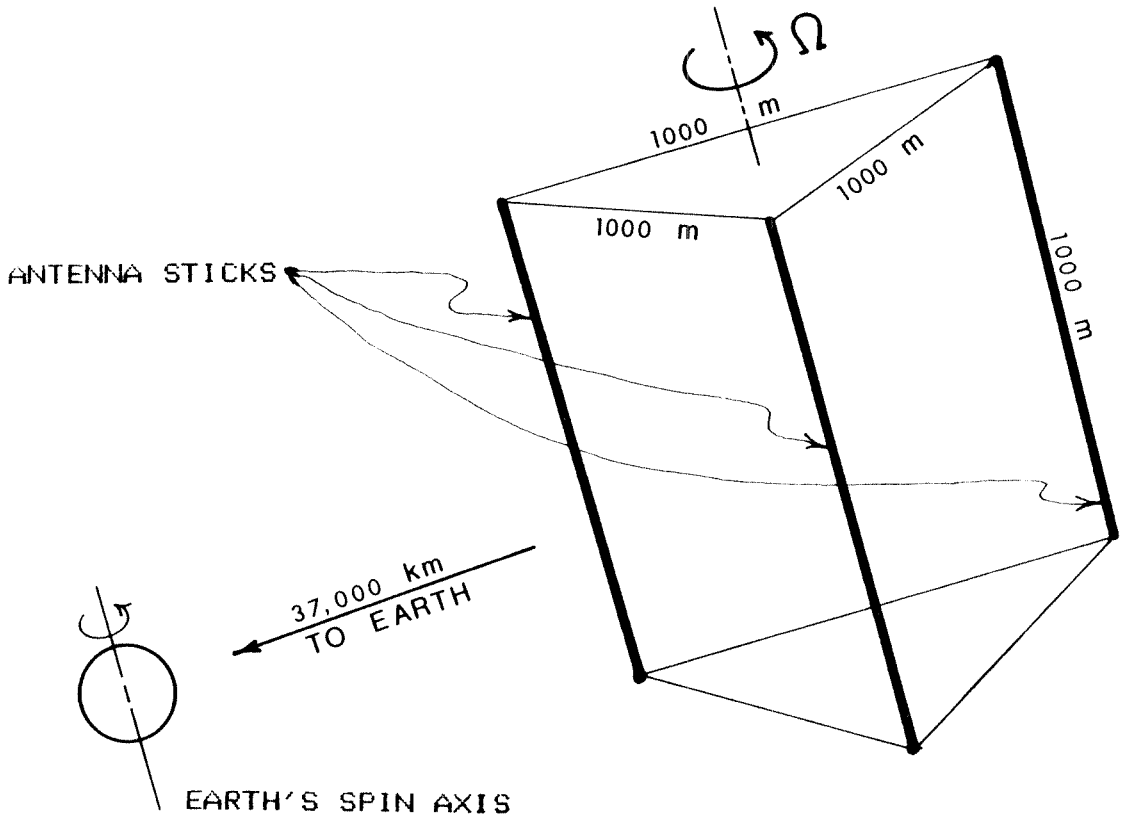

FIGURE 1-1. ANTENNA STICK CONFIGURATION.

known to an accuracy of one-quarter wavelength (0.5 cm). Note that no limit has been placed on the absolute displacement of the antenna sticks or elements.

Pointing accuracy of the spacecraft must be maintained so that the satellite views the desired area on the earth's surface. The tightest pointing requirements occur in the plane formed by the earth's spin axis and the spacecraft center of mass. In this plane, the spacecraft's spin axis must remain perpendicular to the earth's equatorial plane within one degree. Precession of the spacecraft's spin axis[1] must therefore not be allowed to exceed one degree.

Although additional performance requirements certainly exist to guide the design of a complex satellite antenna system, the displacement and pointing accuracy requirements were considered to be the most critical during the early development of this particular design.

1.2. Design Approach.

This research develops a structural design for an antenna system that consists of the three antenna sticks and a truss-like support structure.

The environment at geosynchronous altitude is relatively benign compared to low-earth-orbit altitudes. The predominant loads acting on a large structure in geosynchronous orbit are solar radiation pressure, the earth's gravity, and any loads used for spacecraft stability and attitude control.

---

1. This assumes that nutation is negligible compared to precession. In this application, precession is the angle between the angular momentum vector of the spacecraft and the line that (1) passes through the spacecraft center of mass and (2) is perpendicular to the earth's equatorial plane. Nutation is the angle between the spacecraft angular momentum vector and spacecraft spin axis.

The antenna sticks are sized in Chapter 2 as beams under a uniformly distributed load to meet displacement accuracy requirements. The displacement of each antenna stick is affected by the spinrate of the spacecraft as well as transients such as control thrusters. The antenna elements can be represented as a mass per unit length of 0.82 kg/m distributed uniformly along each stick. The spinning motion of the spacecraft creates a transverse acceleration $\Omega^2 R$ that acts on the uniformly distributed mass of the stick and antenna elements to create a uniformly distributed transverse load. Given the position of the antenna stick joints, beam theory provides a means of determining the transverse displacement of a beam. The antenna sticks are therefore modelled as simply-supported beams under a uniform transverse load. If an imperfection is assumed to exist in the beam bending stiffness EI, the beam equation can be used to find a relationship between beam properties and displacement error. When this displacement error is set equal to the required antenna stick displacement accuracy, the dimensions of the beam are partially determined. The resulting design calculations show that a 250-meter-long antenna stick segment must have a diameter of approximately 0.71 m to meet the 0.5 cm displacement accuracy requirement when the spacecraft spinrate is 1 rev/hr.

The spinrate Ω of the spacecraft is selected in Chapter 3 by considering the effects of solar pressure and gravity gradient torques on spacecraft precession. At this point, the "spacecraft" consists of the three antenna sticks. Once a spinrate has been selected, the remaining beam dimensions can be determined.

A preliminary design for a truss-like support structure is proposed in Chapter 4. Axial loads induced in truss members by control thruster firing are estimated with rigid body dynamics and a finite element quasi-static analysis. Both the diagonal members and the majority of cross members in the support structure are designed as truss columns using concepts of structural efficiency to minimize

spacecraft mass. The remaining cross members are tension-only members, essentially thin Kevlar cords.

In Chapter 5, conventional analysis is used to determine the vibrational modes and natural frequencies of the proposed antenna sticks and support structure members. A finite element dynamic analysis of a simplified model then determines the frequencies and mode shapes of the antenna structure as a whole. A more complicated finite element model is used to demonstrate that the results of the simplified finite element model and conventional analysis are adequate for design purposes.

Chapter 6 briefly discusses design issues not considered in this preliminary analysis, and proposes possible "next steps" in the design process.

Chapter 2
SIZING THE ANTENNA STICKS

Antenna performance requires that the location of each antenna element be known to an accuracy of one-quarter wavelength. Because the antenna elements are mounted on the antenna sticks, the location of the antenna elements is known if the location of each point along each antenna stick is known. As shown below, beam theory can be used to determine the location of each point along the length of an antenna stick provided the positions of the ends of the antenna stick are known. This approach assumes that the largest load on the antenna sticks is produced by centrifugal outward acceleration (from the spacecraft spinning about its axis), acting on the mass of the antenna sticks and antenna elements.

Assume that joints in the overall antenna structure are hinged. If these joints were fixed in space, then the antenna sticks could be modelled as simply-supported beams, with each joint acting as a simple support. The spinning motion of the spacecraft creates a transverse acceleration that acts on the uniformly distributed mass of the stick and antenna elements[1] to create a uniformly distributed transverse load. Given the dimensions, material properties, and transverse loading of the sticks and the location of the joints, the transverse displacement of each point along a stick's length can be found from the solution of the beam equation. The beam equation is

$$\frac{d^2}{dx^2}\left[E(x)I(x)\frac{d^2}{dx^2}w(x)\right] = Q(x) \qquad (2.1)$$

where

$w(x)$ = transverse displacement of beam (m)

1. The antenna elements can be represented as a mass per unit length of 0.82 kg/m distributed uniformly along each stick.

$E(x)I(x)$ = bending stiffness of beam ($N\text{-}m^2$)
$Q(x)$ = distributed load per unit length (N/m).

The solution for a simply-supported beam of length 2L with a uniformly distributed load per unit length Q_o and both E and I constant ($EI = E_oI_o$) is

$$w_o(x) = \frac{Q_oL^4}{24E_oI_o}\left[\frac{x^4}{L^4} - \frac{4x^3}{L^3} + \frac{8x}{L}\right] \tag{2.2}$$

The effect of the displacement of a joint on the transverse displacement of a stick can be found from superposition. Thus if Q_o, E_oI_o, 2L and the joint locations are known, the location of any part of an antenna stick can be found.

Equation (2.2) gives the transverse displacements of the antenna sticks. If the maximum displacement found by Equation (2.2) is set equal to 0.5 cm, the dimensions of the antenna stick can be determined such that a displacement accuracy of 0.5 cm is assured. However, the dimensions found by this method are unreasonably large: a 250-m-long thin-walled cylinder antenna stick segment would require a diameter of 80 m. Therefore, another method must be used to determine antenna stick dimensions.

Performance depends on the accuracy of the displacement computation, not the actual displacement. If an imperfection is assumed to exist in the beam bending stiffness EI, the beam equation can be used to find a relationship between beam properties and the accuracy, or displacement error, of the displacement computation. When the maximum displacement error given by this relationship is set equal to the required antenna stick displacement accuracy, the dimensions of the beam are partially determined.

2.1. Stick Displacement Error is Sensitive to Beam Bending Stiffness.

Suppose that Q_o and 2L are known exactly, but that EI actually has a step increase of magnitude δ and width 2α in the center of the beam (Figure 2-1). This is a simple model of the effect a manufacturing tolerance (or error) or a variation in material properties might have on beam properties. The bending stiffness has a symmetry around the beam center at x = L, so we can simplify the problem by solving the beam equation (2.1) over the interval x = 0 to x = L instead of over the entire length of the beam. Consider this beam to be composed of two different beams, Beam 1 and Beam 2. Beam 1 has a bending stiffness of $EI = E_o I_o$, displacement $w_1(x)$, and exists over the interval x = 0 to $x = L(1-\alpha)$. Beam 2 has a bending stiffness of $EI = E_o I_o(1+\delta)$, displacement $w_2(x)$, and exists over the interval of $x = L(1-\alpha)$ to x = L. By continuity, both beams must have the same displacement and first three derivatives at $x = L(1-\alpha)$. These conditions, combined with the simple support at end x = 0 and the symmetry condition at x = L, result in eight boundary conditions

$$w_1(L - L\alpha) = w_2(L - L\alpha) \tag{2.3a}$$

$$w_1'(L - L\alpha) = w_2'(L - L\alpha) \tag{2.3b}$$

$$w_1''(L - L\alpha) = w_2''(L - L\alpha) \tag{2.3c}$$

$$w_1'''(L - L\alpha) = w_2'''(L - L\alpha) \tag{2.3d}$$

$$w_1(0) = 0 \tag{2.3e}$$

$$w_1''(0) = 0 \tag{2.3f}$$

$$w_2'(L) = 0 \tag{2.3g}$$

FIGURE 2-1. POSTULATED STEP IMPERFECTION IN BEAM BENDING STIFFNESS EI. Width of step is 2α, amplitude of step is δ.

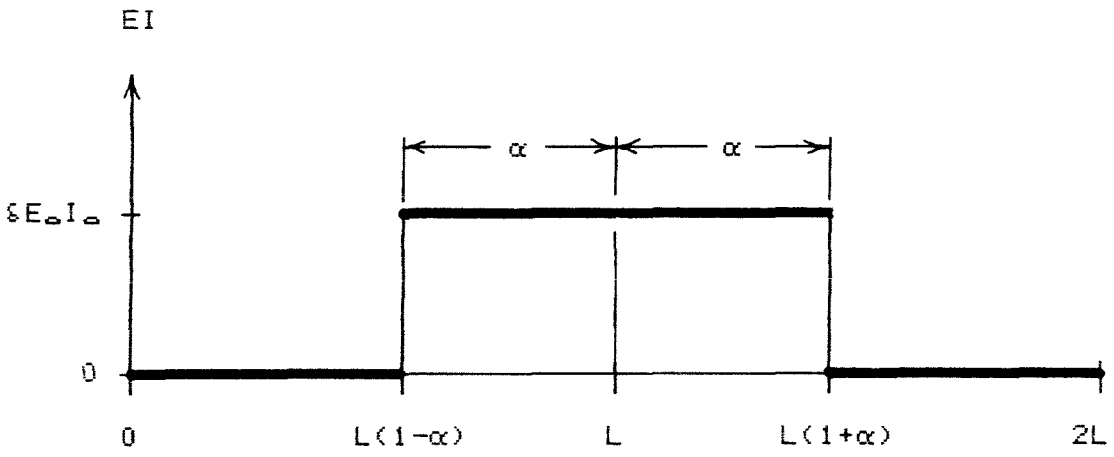

$$w_2'''(L) = 0 \qquad (2.3h)$$

which can be used to solve the beam equation (2.1) for both $w_1(x)$ and $w_2(x)$. The completed sensitivity study is detailed in Appendix A.

A comparison of the magnitudes of $w_1(x)$ and $w_2(x)$ with $w_o(x)$ (Equation 2.2) for varying ranges of α and x show that the maximum displacement error ϵ occurs at x = L when $\alpha = 1.0$, and is given by

$$\epsilon = \frac{5Q_o L^4}{24E_o I_o} \frac{\delta}{(1+\delta)} = \frac{\delta}{(1+\delta)} w_o(L) \qquad (2.4)$$

where

ϵ = displacement error at x = L (m)
2L = beam length (m)
δ = (amplitude of imperfection in EI)/$E_o I_o$ (dimensionless)

When displacement error ϵ is set equal to the required antenna element displacement accuracy, then Equation (2.4) can be used to determine some parameters of the antenna stick design.

2.2. Stick Dimensions and Mass Are Determined by Cross-. Sectional Area and Area Moment of Inertia.

Antenna performance specifications for this application require that the position of each of the antenna elements be known to a quarter wavelength ($\lambda/4$). Since wavelength is $\lambda = c/f$, where c is the speed of light in m/s and f is the wave frequency in Hz, then the displacement error ϵ must be less than or equal to c/4f. Assume that the distributed load Q_o results from the centrifugal acceleration a_T of the rotating satellite acting on the mass per unit length of the antenna elements and stick. The transverse antenna stick acceleration $a_T = \Omega^2 R$ is assumed to be uniform along the length of the stick, where R is the distance (577.35 m) from the rotational axis to the antenna stick

center of mass, and Ω is the spinrate in rad/sec. Assume also that the mass per unit length of the uniformly-distributed antenna elements is some fraction m_r of the mass per unit length m_s of the antenna stick. Then Equation (2.4) gives

$$\frac{c}{4f} \geq \epsilon = \frac{5}{24} \frac{\rho_s A_s}{E_o I_o} (1 + m_r) \Omega^2 R L^4 \frac{\delta}{(1+\delta)} \qquad (2.5)$$

where

f = wave frequency (Hz)
c = speed of light (3×10^8 m/s)
ρ_s = density of antenna stick material (kg/m^3)
A_s = cross-sectional area of antenna stick (m^2)
m_r = (antenna element mass)/(antenna stick mass).

Equation (2.5) shows that the maximum error ϵ in the transverse displacement measurement increases with the fourth power of beam length. Thus the sensitivity of displacement error to the variations in EI can be reduced by dividing the one-kilometer-long antenna stick into several shorter segments. Equation (2.5) also shows that maximizing the ratios E_o/ρ_s and I_o/A_s will help to reduce sensitivity. Graphite-reinforced-epoxy composite has a high specific stiffness ($E_o/\rho_s = 7.724 \times 10^7$ m^2/s^2 for $E_o = 110.2$ GPa and $\rho_s = 1522$ kg/m^3) and can be constructed to have a coefficient of thermal expansion near zero; all subsequent calculations will assume that graphite epoxy is the antenna stick material. The ratio of I_o/A_s varies with the structural design used for the antenna stick. If we assume E_o/ρ_s is given, then the value of I_o/A_s must increase to maintain the same displacement accuracy when the percent imperfection δ in EI increases.

The values of I_o/A_s that will insure the displacement accuracy requirement will be met can be found, allowing a load margin of 1.5, by rearranging (2.5) to get

$$\frac{I_o}{A_s} \geq (1.5)\ \frac{4f}{c}\ \frac{5}{24}\ \frac{\rho_s}{E_o}(1 + m_r)\ \Omega^2 RL^4\ \frac{\delta}{(1 + \delta)} \qquad (2.6)$$

The effect of changes in L and δ on I_o/A_s is shown in Figure 2-2.

2.3. Choosing a Structural Shape.

2.3.1. Thin-Walled Tube. If the antenna stick shape is assumed to be a thin-walled tube, I_o/A_s can be expressed simply in terms of the outer dimensions of the antenna stick. For example,

$$I_o/A_s = H^2/6 \quad \text{for a square tube} \qquad (2.7a)$$

$$I_o/A_s = H^2/8 \quad \text{for a round tube} \qquad (2.7b)$$

where H for a square tube is the width of the tube side, and H for a round tube is the tube outer diameter. A square or rectangular tube possesses a useful flat surface for mounting antenna elements. However, the flat sides of such a tube are more susceptible to local buckling from bending and shear stresses in the tube than is the curved surface of a round tube. Local buckling is unacceptable. Therefore, a round thin-walled tube is used in the initial sizing of the antenna sticks. For a round tube, H can be found by combining Equations (2.6) and (2.7b) and rearranging to obtain

$$H \geq \sqrt{10\ \frac{f}{c}\ \frac{\rho_s}{E_o}\ (1+m_r)\Omega^2 RL^4\ \frac{\delta}{(1+\delta)}} \qquad (2.8)$$

The mass of an antenna stick composed of a single thin-walled tube (without antenna elements) is given by

$$m_s = \rho_s A_s 2s = \rho_s \pi H t 2s \qquad (2.9)$$

where H is the tube outer diameter given by Equation (2.8), and 2s is

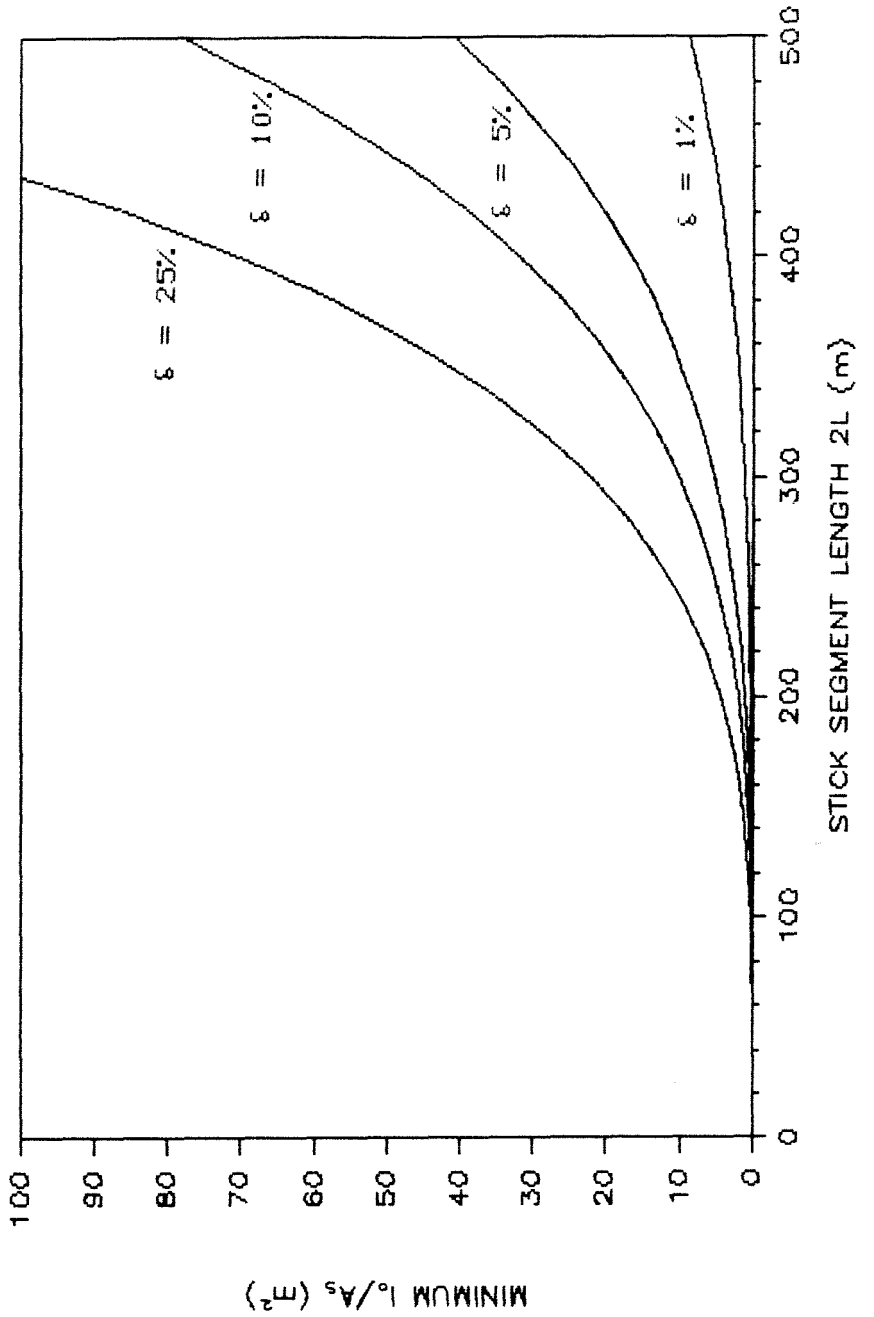

FIGURE 2-2. DEPENDENCE OF THE RATIO I_o/A_s ON ANTENNA STICK LENGTH 2L AND BENDING STIFFNESS IMPERFECTION δ.

the length of the antenna stick (2s = 1000 m).

2.3.2. Three-Longeron Double-Laced Truss. If the antenna stick shape is assumed to be a three-longeron double-laced truss column (Figure 2-3), antenna stick mass is reduced considerably. However, the calculations of the antenna stick dimensions from equation (2.6) are not so straightforward as when the antenna stick is assumed to be a thin-walled tube.

If we assume that the cross-sectional area A_d of the truss diagonals is approximately the same as the cross-sectional area A_l of the longerons, then the antenna stick cross-sectional area A_s is

$$A_s = 3A_l + 6A_d \approx 9A_l \tag{2.10}$$

A conservative estimate for the area moment of inertia I_o of the antenna stick can be found from A_l and the distance H between longerons as

$$I_o = \frac{A_l H^2}{2} \tag{2.11}$$

A value for H is found by combining (2.10) and (2.11) with (2.6) to get

$$H \geq \sqrt{22.5 \frac{f}{c} \frac{\rho_s}{E_o} (1 + m_r)\Omega^2 R L^4 \frac{\delta}{(1+\delta)}} \tag{2.12}$$

The value of H alone does not completely determine the geometry, however. From geometry and Figure (2-3), we see that

$$b = \frac{2L}{H \tan\phi} \tag{2.13}$$

where

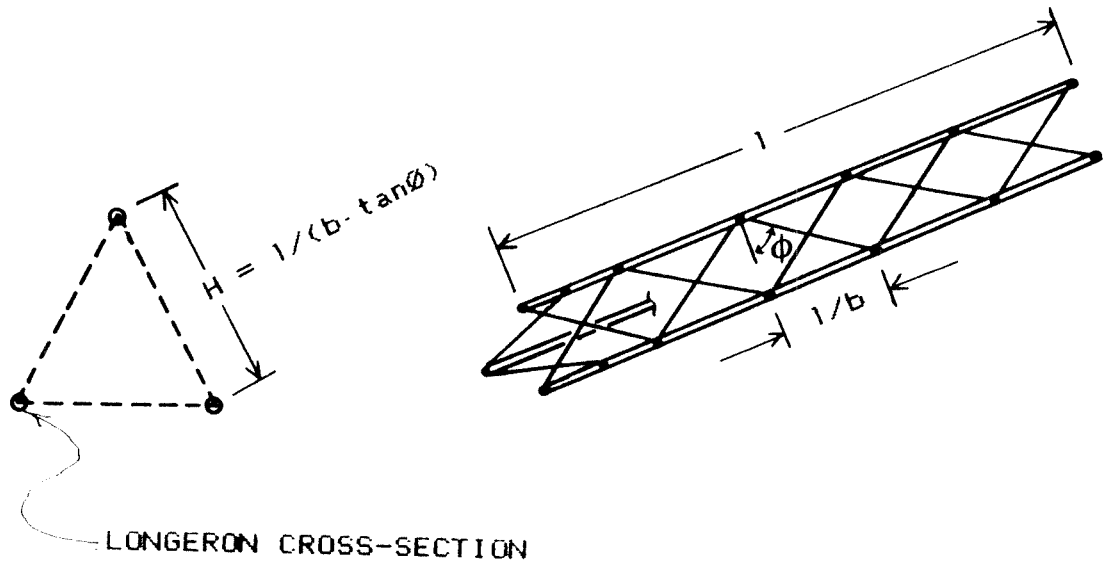

FIGURE 2-3. THREE-LONGERON DOUBLE-LACED TRUSS COLUMN. Note the absence of batens.

H = distance between longerons (m)
b = number of truss column bays (dimensionless)
2L = truss column length (m) = l in Figure (2-3)
ϕ = angle of truss diagonals, measured from a line perpendicular to the two longerons (degrees).

To insure that b is an integer, set

$$b = \text{INT}\left\{\frac{2L}{H\tan\phi}\right\} \tag{2.14}$$

where H is the value calculated in (2.12). Then the actual distance H_s between longerons based on an integer value of b and an assumed value of ϕ can be calcuated using (2.12) and (2.14) to produce

$$H_s = \frac{2L}{\tan\phi}\ \text{INT}\left[\frac{\tan\phi}{2L}\sqrt{22.5\ \frac{f}{c}\ \frac{\rho_s}{E_o}\ (1 + m_r)\Omega^2 RL^4\ \frac{\delta}{(1+\delta)}}\right] \tag{2.15}$$

We now have values for H, b and ϕ. To complete the truss design, we need values for D_l and D_d, the diameters of the truss longerons and truss diagonals, respectively.

Using the assumption that the antenna stick is a simply supported beam under a uniformly distributed transverse load per unit length Q_o, we find that the maximum moment in the antenna stick is

$$M_{max} = \frac{Q_o(2L)^2}{8} = \frac{Q_o L^2}{2} \tag{2.16}$$

The maximum load in a longeron segment is

$$P_l = \frac{M_{max} A_l}{I_o}\ \frac{H_s}{2\cos 30^o} = \frac{Q_o L^2 A_l H_s}{2\sqrt{3 I_o}} \tag{2.17}$$

The Euler buckling load in a longeron segment of length 2L/b (the

length of one bay) is

$$P_E = \frac{\pi^2 E_o I_l}{(2L/b)^2} \tag{2.18}$$

If we set P_E in (2.18) equal to 1.5*P_l in (2.17), which provides a safety factor of 1.5, and substitute $\rho_s(9A_l)(1+m_r)\Omega^2 R$ for the value of Q_o, the resulting equation is

$$\frac{\pi^2 E_o I_l}{(2L/b)^2} = \frac{1.5[\rho_s(9A_l)(1+m_r)\Omega^2 R]L^2 H_s A_l}{2\sqrt{3}(A_l H_s^2/2)} \tag{2.19}$$

This value can be combined with equation (2.13) to find the ratio

$$\frac{I_l}{A_l} = 9 \cdot \sqrt{3}\, \frac{\rho_s}{E_o}\, \frac{(1+m_r)\Omega^2 R L^3 \tan\phi}{\pi^2 b} \tag{2.20}$$

Assuming a wall thickness t for each longeron, the cross-sectional area A_l of a longeron is $A_l = \pi D_l t$, and the area moment of inertia I_l of a longeron is $I_l = \pi D_l^3 t/8$. Thus the ratio I_l/A_l reduces to

$$\frac{I_l}{A_l} = \frac{D_l^2}{8} \tag{2.21}$$

Substituting this into (2.20), we find that the diameter of the longerons is given by

$$D_l = \sqrt{72 \cdot \sqrt{3}\, \frac{\rho_s}{E_o}\, \frac{(1+m_r)\Omega^2 R L^3 \tan\phi}{\pi^2 b}} \tag{2.22}$$

A similar procedure can be used to determine the diameter of the truss diagonals. The maximum shear in a simply-supported beam under a under a uniform transverse load is

$$V_{max} = Q_o L \tag{2.23}$$

The resulting maximum load in the truss diagonals is

$$P_d = \frac{V_{max}}{4\cos\phi\cos 30^o} = \frac{Q_o L}{2\sqrt{3}\cos\phi} \tag{2.24}$$

Set the Euler buckling load of one diagonal equal to $1.5*P_d$ to get

$$\frac{\pi^2 E_o I_d}{(2L/b\sin\phi)^2} = \frac{1.5[\rho_s(9A_d)(1+m_r)\Omega^2 R]L}{2\sqrt{3}\cos\phi} \tag{2.25}$$

This can be rewritten in the form I_d/A_d as before. Assuming a wall thickness t for each diagonal, the ratio I_d/A_d reduces to $D_d^2/8$, and the diameter of each diagonal is given by

$$D_d = \sqrt{72\cdot\sqrt{3}\,\frac{\rho_s}{E_o}\,\frac{(1+m_r)\Omega^2 R L^3}{\pi^2 b^2 \sin^2\phi\cos\phi}} \tag{2.26}$$

The mass on an antenna stick composed of a three-longeron double-laced tubular truss (without antenna elements) is given by

$$m_s = \rho_s 3\pi t(D_i + 2D_d/\sin\phi)2s \tag{2.27}$$

where D_i and D_d are given by (2.22) and (2.26), and 2s is the length of the antenna stick.

0.1. An Increase in Spinrate Increases Stick Dimensions and Mass.

Assume that each antenna stick is divided by hinged joints into segments of length 2L. Before the antenna stick mass and dimensions can be determined, values are needed for 2L, Ω, t, m_r, and δ (recall that the values E_o = 110.2 GPa and ρ_s = 1522 kg/m^3 were chosen in Section 2.2). Values for segment length 2L and spinrate will be chosen in subsequent chapters; at this point in the calculations, we will

consider a range of values for these two parameters.

If we assume that local buckling does not occur in the thin-walled tube, we can use a minimum wall thickness (limited by manufacturing considerations) of t_m = 0.381 mm (.015") for all tubes. This corresponds to 2 or 3 plys of graphite-epoxy prepreg. However, a manufacturing tolerance of .025 mm (.001") in wall thickness would result in a 6.6% error in the area moment of inertia I of a tube (since $I = \pi D^3 t$ for a thin-walled tube). A value of δ = 10% is therefore used as a conservative estimate of the imperfection in antenna stick EI. A preliminary value of m_r can be found for any combination of Ω, 2L, and δ by first calculating stick dimensions and mass with m_r set equal to zero. This gives a first estimate of antenna stick mass per unit length, from which a more realistic value of m_r can be calculated. Some values for antenna stick width H and mass m_s are given in Tables (2-1) and (2-2) for different stick segment lengths and spacecraft spinrates.

Plots of antenna stick mass as a function of spinrate for varying antenna stick segment lengths are shown in Figures (2-4) and (2-5) for a tubular antenna stick and a truss column antenna stick, respectively. The mass of the thin-walled tubular antenna stick increases with spinrate in a nearly linear fashion. The mass of the three-longeron truss antenna stick increases more rapidly with spinrate than does the tubular stick; however, the overall mass of the truss stick at a given spinrate is considerably less than the mass of the tubular stick.

TABLE 2-1. VALUES OF ANTENNA STICK MASS m_s AND DIAMETER H VS. SPINRATE Ω FOR VARYING STICK SEGMENT LENGTH 2L (ANTENNA STICK = THIN-WALLED ROUND TUBE)

2L =	200 m	250 m	500 m	200 m	250 m	500 m
Ω	m_s	m_s	m_s	H	H	H
1	929	1292	4173	0.510	0.709	2.291
2	1568	2265	7966	0.861	1.243	4.373
3	2188	3222	11753	1.201	1.768	6.452
4	2802	4173	15538	1.538	2.291	8.529
5	3412	5123	19323	1.873	2.812	10.607
6	4021	6071	23107	2.207	3.333	12.684
7	4629	7019	26891	2.541	3.853	14.761
8	5237	7966	30675	2.875	4.373	16.838
9	5844	8913	34458	3.208	4.893	18.915
10	6450	9860	38242	3.541	5.412	20.992
11	7057	10807	42026	3.874	5.932	23.069
12	7663	11753	45809	4.207	6.452	25.146
13	8269	12700	49593	4.539	6.971	27.223
14	8875	13646	53376	4.872	7.491	29.300
15	9481	14592	57160	5.205	8.010	31.376

Note: Ω is rev/hr, 2L is in meters, m_s is in kilograms, H is in meters.

TABLE 2-2. VALUES OF ANTENNA STICK MASS m_s AND TRUSS WIDTH H_s VS. SPINRATE Ω FOR VARYING STICK SEGMENT LENGTH 2L (ANTENNA STICK = THREE-LONGERON TRUSS)

2L =	200 m	250 m	500 m	200 m	250 m	500 m
Ω	m_s	m_s	m_s	H_s	H_s	H_s
1	399	440	563	7.22	9.02	16.98
2	502	541	711	8.25	10.07	19.25
3	571	616	866	8.88	10.83	21.65
4	626	676	1013	9.36	11.40	23.41
5	666	741	1216	9.62	12.03	26.24
6	706	790	1396	9.90	12.37	27.94
7	749	863	1648	10.19	13.12	30.93
8	790	920	1897	10.50	13.53	33.31
9	836	979	2188	10.83	13.97	36.08
10	883	1044	2533	11.17	14.43	39.36
11	935	1114	2831	11.55	14.93	41.24
12	985	1191	3152	11.95	15.46	43.30
13	1045	1269	3669	12.37	16.04	48.11
14	1106	1357	4082	12.83	16.65	50.94
15	1138	1457	4560	12.83	17.32	54.13

Note: Ω is in rev/hr, 2L is in meters, m_s is in kilograms, H_s is in meters.

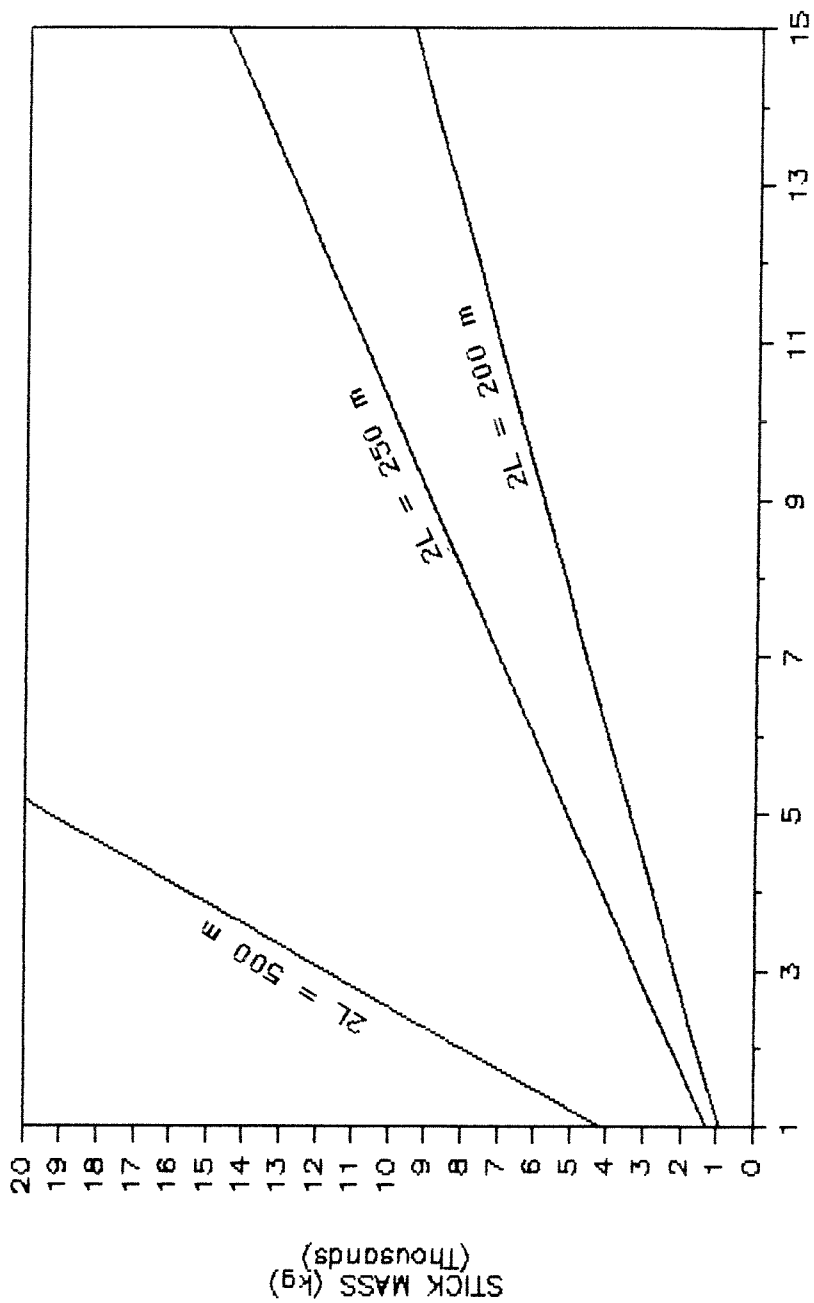

FIGURE 2-4. MASS OF THIN-WALLED ROUND TUBE ANTENNA STICK INCREASES AS SPINRATE INCREASES.

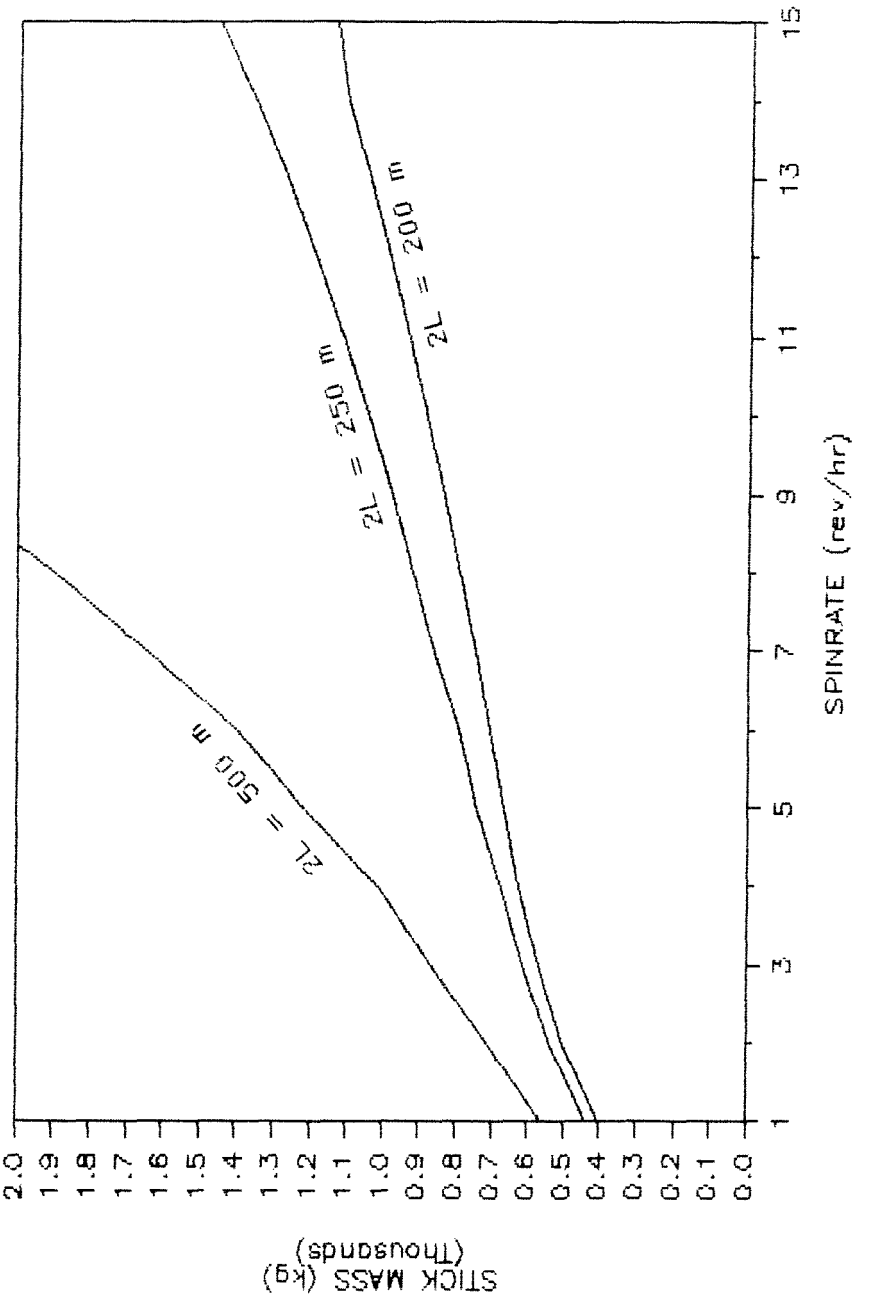

FIGURE 2-5. MASS OF TRUSS COLUMN ANTENNA STICK INCREASES AS SPINRATE INCREASES.

Chapter 3
SELECTING A STABLE SPINRATE

Large flexible space structures have low natural frequencies that are easily excited by any applied loads. Once excited, a structure may take hours or even days to damp out its vibrations. It is therefore desirable to apply as few loads to the structure as possible. In such cases, passive attitude control methods are preferable to the frequent use of attitude control thrusters or the cyclic excitations produced by inertia wheels.

Since the spacecraft must spin to perform its radiometry task, spin stabilization can be used as a passive method of attitude control. However, care must be taken in selecting a spinrate: as seen in Chapter 2, an increase in spinrate requires an corresponding increase in antenna stick mass (an undesirable effect). To be acceptable, a spinrate must meet stability requirements and yet keep spacecraft mass to a minimum.

3.1. Disturbance Torques, Precession, and Pointing.

One indication of spacecraft stability is precession, which is the angle between the spacecraft angular momentum vector and the desired angular momentum vector (normal to the earth's equatorial plane). Precession arises from disturbance torques; the most influential of these torques for a large satellite in geosynchronous orbit are solar radiation and the earth's gravitational field.

The differential solar radiation force $\vec{df_s}$ acting on an elemental area dA of the spacecraft is given by

$$\vec{df_s} = - C_o P \int \left\{ \left[(1-C_s)\vec{S} + 2(C_s \cos\beta + \frac{1}{3} C_d)\vec{N} \right] \cos\beta \right\} dA \qquad (3.1)$$

where

P = momentum flux from the sun (4.4×10^{-6} kg/m/s^2)
C_o = opacity
C_s = coefficient of specular reflection
C_d = coefficient of diffuse reflection
$\vec{S}$ = unit vector from the spacecraft to the sun
dA = elemental spacecraft area (m^2)
$\vec{N}$ = unit outward normal vector of dA
β = angle between $\vec{S}$ and $\vec{N}$

The solar radiation torque $\vec{\tau}_s$ acting on a spacecraft is given by

$$\vec{\tau}_s = \int \vec{R} \times d\vec{f}_s \tag{3.2}$$

where $\vec{R}$ is the vector from the spacecraft's center of mass to the elemental area dA, and $d\vec{f}_s$ is given by Equation (3.1).

The gravitational force is directed radially inward towards the earth, and is given by

$$dF_G = \frac{Gm_e dm}{r^2} \tag{3.3}$$

where

G = gravitational constant (6.672×10^{-11} N-m^2/kg^2)
m_e = mass of earth (5.979×10^{24} kg)
dm = incremental mass of interest (kg)
r = distance of dm from center of the earth (m).

For a satellite in geosynchronous orbit, the earth's oblateness can be neglected in gravity gradient computations.

Because some amount of precession is always present, all spin stabilized spacecraft require periodic attitude adjustments, which are implemented from earth by ground crews. The minimum time between attitude adjustments is usually three to four days, limited by the scheduling and expense of ground crew efforts.

Antenna performance requires that precession of the spacecraft be less than one degree at all times. This pointing requirement can be used as a measure of spacecraft stability for spinrate determination. If attitude adjustments occur once per week, and a 20% allowance is made for precession that might arise from sources other than solar pressure and gravity gradient effects, then precession must be less than 0.83 degrees in any one-week period.

3.2. 12 Rev/Hr Spinrate Meets Pointing Requirements.

The spacecraft can be modelled simplistically as a rigid body composed of three oriented cylinders (representing the three antenna sticks). Because the diameter and mass of a thin-walled cylindrical antenna stick vary with spinrate (Section 2.4.), the mass, cross-sectional area, and mass moments of inertia of the spacecraft model also vary with spinrate. The effects of gravity gradient and solar pressure acting on this spacecraft model over a given period of time can then be determined numerically for different spinrates.[1]

The precession after a 24-hour period at summer solstice of the rigid body spacecraft model is plotted in Figure (3-1) for different spacecraft spinrates. The spacecraft is assumed to be in geosynchronous orbit (completing one revolution around the earth in one standard solar day) with an initial declination of 90 degrees (spin axis initially perpendicular to the earth's equatorial plane). The 24-hour period covers 00:00 hours on 21-June-1980 to 00:00 hours on 22-June-1980; this is one possible time when the angle between the spacecraft and the solar radiation is most extreme, and therefore the solar pressure is greatest. For computation purposes, it is assumed that C_o = 1.00, C_s = 0.01, C_d = 0.09, and solar radiation at the spacecraft is equivalent to the radiation present at 1 A.U. Allowance is made for each cylinder shading the other two due to spacecraft rotation and

1. The numerical analysis uses a FORTRAN program written by Dr. James McEnnan of the Dynamics and Control Department in the Systems Laboratories, Hughes Aircraft Space and Communications Group.

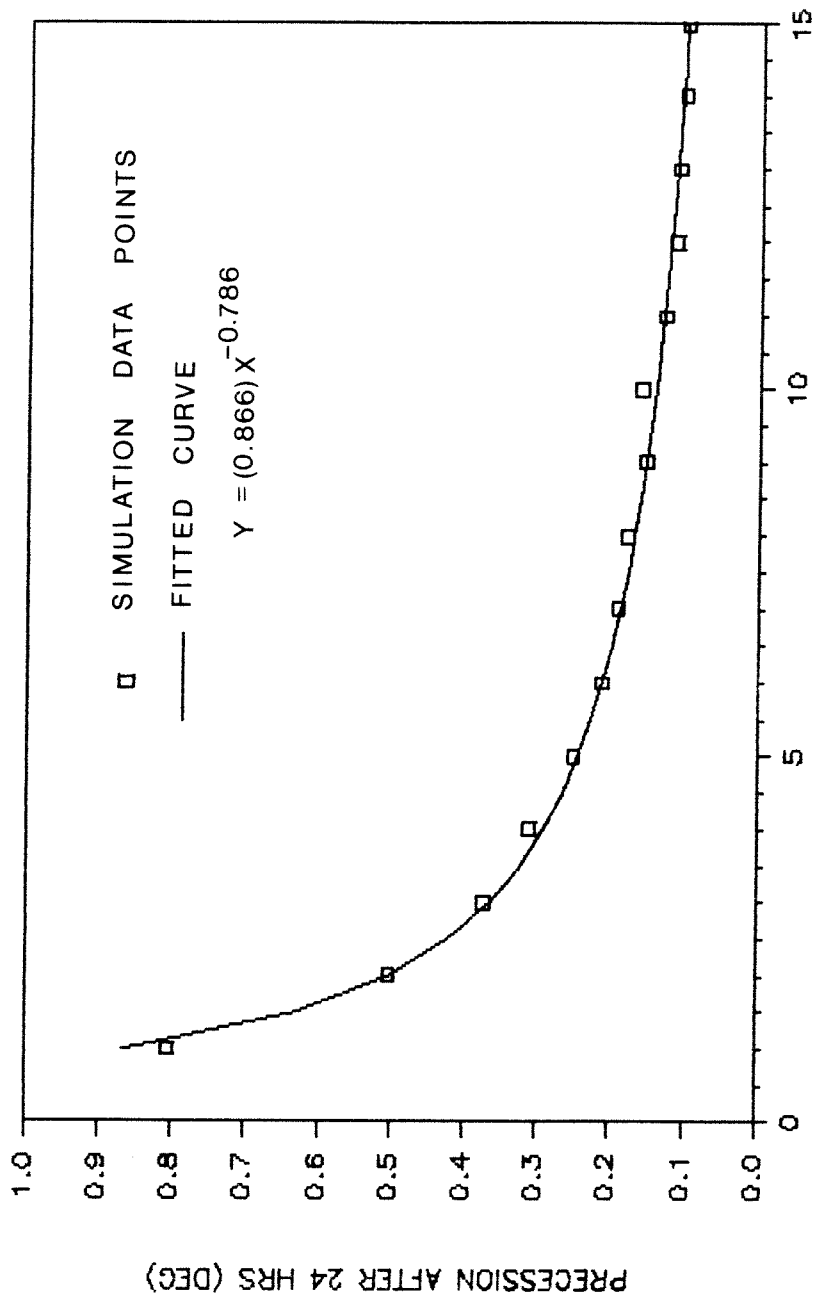

FIGURE 3-1. SPACECRAFT PRECESSION DECREASES AS SPINRATE INCREASES.

orbital path (shading reduces solar torque and shifts the center of pressure of the spacecraft). The integration step size for the computations is found by dividing the spin period in seconds by 40.

For each spinrate case, the precession angle increases in a nearly linear fashion with time. This is shown in Figure (3-2) for a spinrate of 12 rev/hr. The solar pressure effects are sufficient to move the center of mass of the spacecraft out of the earth`s equatorial plane. Gravity gradient effects then act on the unsymmetrical mass distribution to increase precession.

By extrapolation from Figure (3-2), the precession after a one-week period is 0.819 degrees for spinrate Ω = 12 rev/hr. This spinrate meets the pointing accuracy requirement with a 22% margin, and will be assumed in all following calculations.

The calculations in this section of the analysis were done early in the design study, and determine antenna stick dimensions assuming that the antenna stick segments are clamped on both ends (see data in Appendix B). Note that this differs from the simply-supported beam assumption used in Chapter 2. The spinrate selected from these calculations is satisfactory for a preliminary design. However, the completed preliminary structure should be used as the model in future design iterations to determine spacecraft precession.

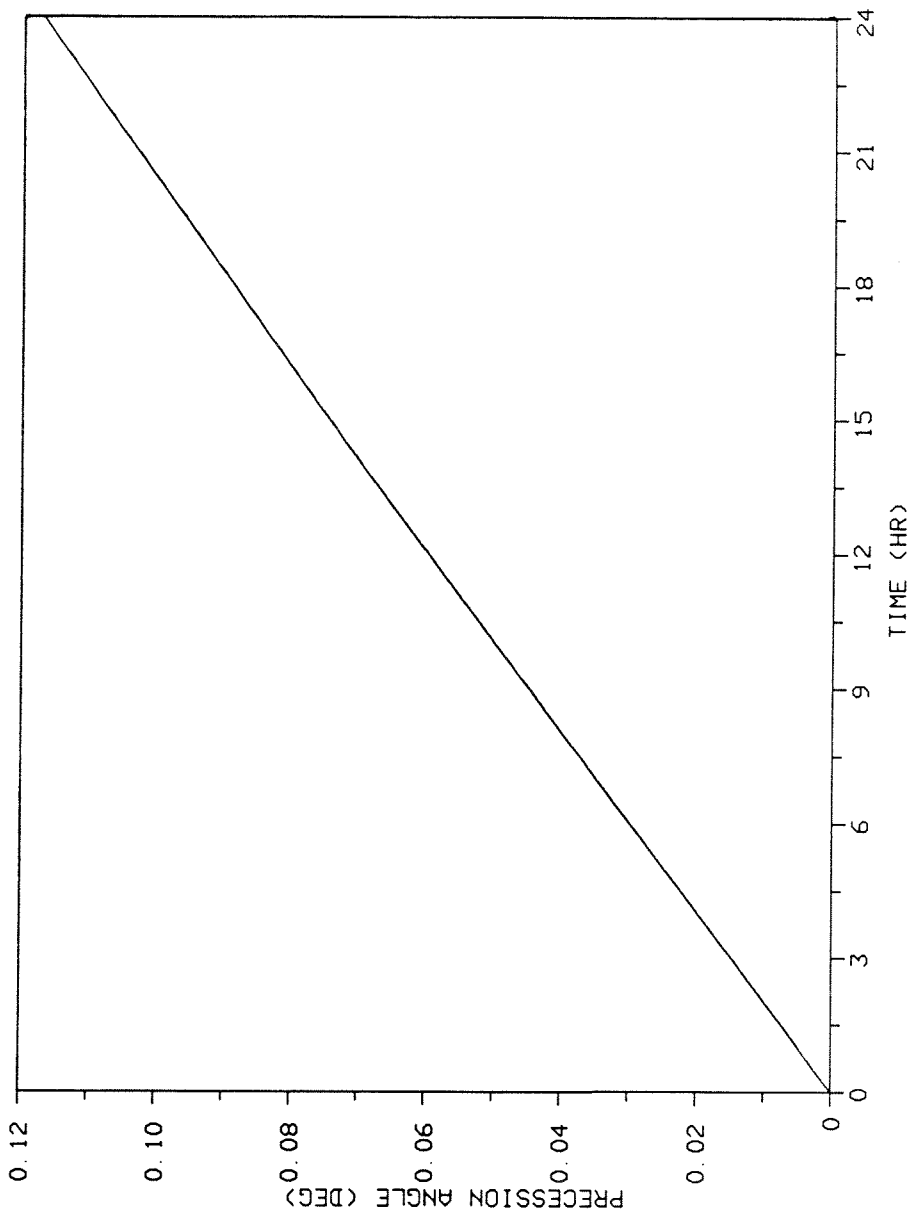

FIGURE 3-2. SPACECRAFT PRECESSION DURING 24-HOUR PERIOD (Ω=12 REV/HR).

Chapter 4
SIZING THE SUPPORT STRUCTURE

4.1. Preliminary Configuration.

The preliminary configuration chosen for the support structure is a basic triangular truss design (Figure 4-1). Cross members maintain the required 1 km spacing between the antenna sticks. Diagonal members[1] carry column shear loads to prevent collapse of the hinged structure. An antenna stick segment length of 250 m (2L = 250 m, or 4 segments) is used in the preliminary configuration.

Cross members connect each of the hinge points on each antenna stick to the other hinge points on its level (a level is located entirely in one x-y plane). The cross members at the z = -500, z = 0, and z = 500 levels can carry both tension and compression, while the cross members at the z = -250 and z = 250 levels are tension-only members to reduce overall spacecraft mass. Diagonal members connect antenna stick hinge points on the z = 0 level to hinge points on the z = -500 and z = 500 levels. Each diagonal member is capable of carrying both tension and compression.

The preliminary dimensions of an antenna stick composed of four segments (with a spacecraft spinrate Ω of 12 rev/hr) is calculated in Section 4.2 for both the thin-walled round tube and the three-longeron truss column designs. The axial loads carried by the diagonal members and tension-compression cross members of the support structure are estimated in Section 4.3; preliminary designs for these members are then calculated in Section 4.4.

---

1. Some confusion may arise over the use of the term "diagonal" in both the design of the antenna support structure and the design of the truss columns that are the members of the support structure. For clarity, the term "diagonal member" will refer solely to the column that is a component of the antenna support structure.

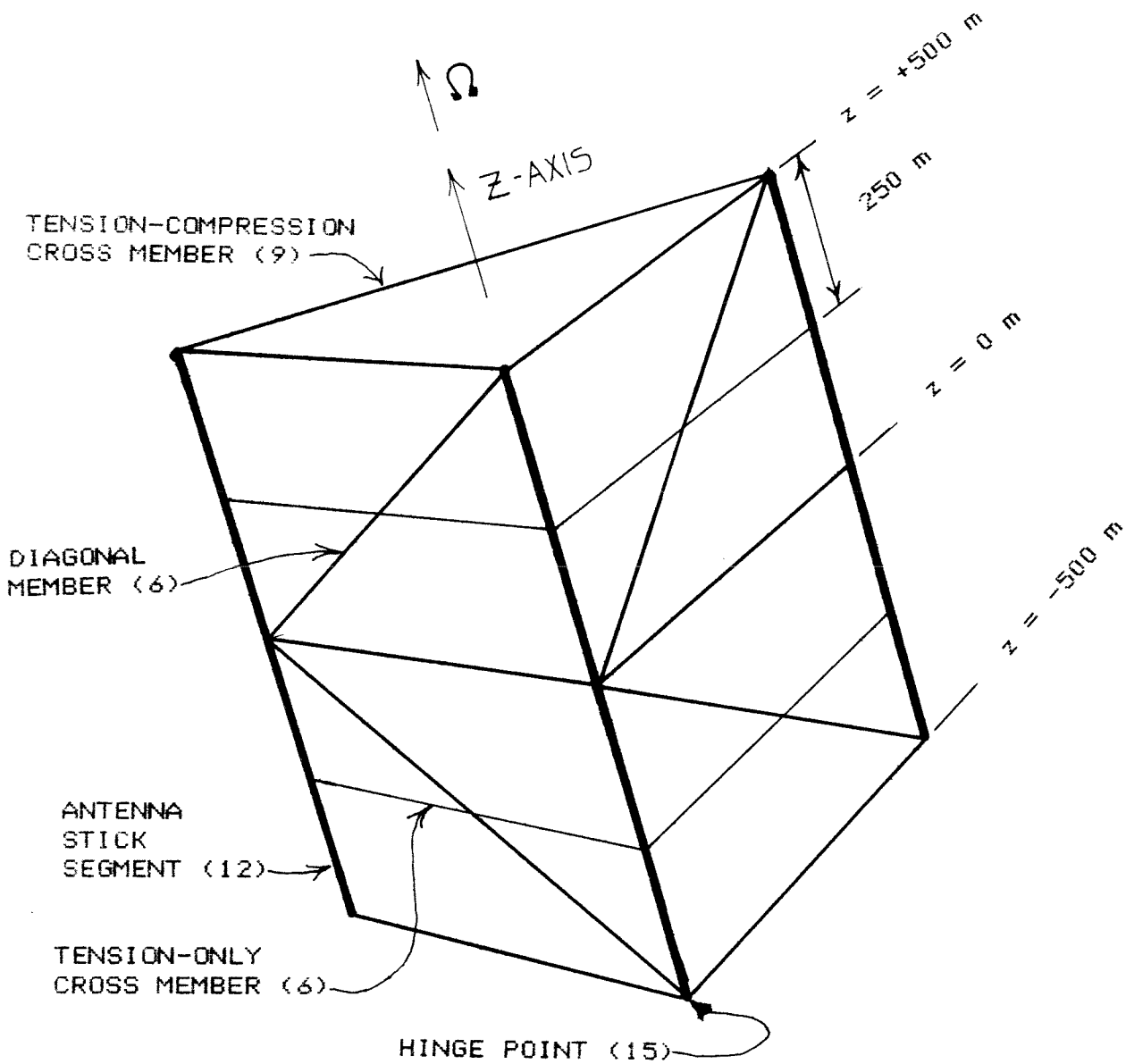

FIGURE 4-1. PRELIMINARY CONFIGURATION OF ANTENNA SUPPORT STRUCTURE. The cross members and diagonal members on the back side are omitted for clarity.

4.2. Antenna Stick Design for a 12 Rev/Hr Spinrate.

Table (2-1) in Chapter 2 gives values for diameter and mass (without antenna elements) of a thin-walled round tube antenna stick for various spacecraft spinrates and antenna stick segment lengths. With the stick segment length of 2L = 250 m chosen above and a spinrate of Ω = 12 rev/hr (chosen in Chapter 3), the table shows that the antenna stick must have a diameter of at least 6.452 m to keep displacement error less than the required 0.5 cm. If we choose the minimum allowable diameter, the antenna stick design parameters for a thin-walled round tube are

material	=	graphite-epoxy laminate
number of segments	= n =	4
segment length	= 2L =	250 m
diameter	= H =	6.452 m
wall thickness	= t_m =	0.381 mm
mass	= m_s =	11,753 kg

Table (2-2) shows antenna stick width and mass for a three-longeron double-laced truss antenna stick. If we choose the minimum allowable stick width for 2L = 250 m and Ω = 12 rev/hr, the antenna stick design parameters for a truss are

material	=	graphite-epoxy laminate
number of segments	= n =	4
segment length	= 2L =	250 m
truss width	= H_s =	15.46 m
number of bays	= b =	28
longeron diameter	= D_l =	6.943 cm
diagonal diameter	= D_d =	3.711 cm
angle of diagonals	= ϕ =	30^o
tube wall thickness	= t_m =	0.381 mm
mass	= m_s =	1191 kg

Note that both masses quoted above do not include the mass of joints or antenna elements.

4.3. Estimating Loads with Rigid-Body Lumped Mass Model.

The spacecraft requires control thrusters for periodic attitude adjustments and orbital maneuvers. The following analysis assumes that the most significant loads in the members of the antenna structure are induced by control thruster(s) applying loads at the antenna stick hinge points.

If the spacecraft is spun up by control thrusters after deployment (as opposed to spun up during deployment, or deployed after spin-up), some members of the support structure must carry compressive loads. Because the members are slender, the primary failure mode of the members is column buckling. The largest estimated compressive load induced in each type of member by control thruster firing can thus be used as a design load for that member. The worst-case compressive load in each type of member can be found from a quasi-static analysis of a rigid body model of the antenna support structure.

The tension-only cross members cannot carry compressive loads. For the purpose of estimating the worst-case compressive loads in the diagonal members and tension-compression cross members, the tension-only members are omitted from the rigid body model.

4.3.1. Nine-Mass Rigid Body Model.

The rigid-body model shown in Figure (4-2) is used to determine the member loads induced by control thruster firing. The model consists of nine identical point masses, each of which represents one-third of one antenna stick mass ($m_s/3$), interconnected by massless members which represent the antenna sticks, diagonal members, and tension-compression cross members of the antenna structure. Note that no members are included to represent the tension-only cross members. A corresponding finite element model consisting of nine nodes and 21

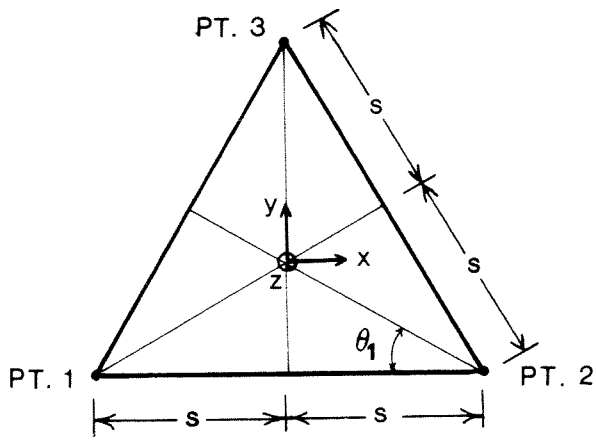

$s = 500$ m
$\theta_1 = 30°$
$\theta_2 = 49.107°$
$\theta_3 = 26.565°$
$\theta_4 = 45°$

TOP VIEW

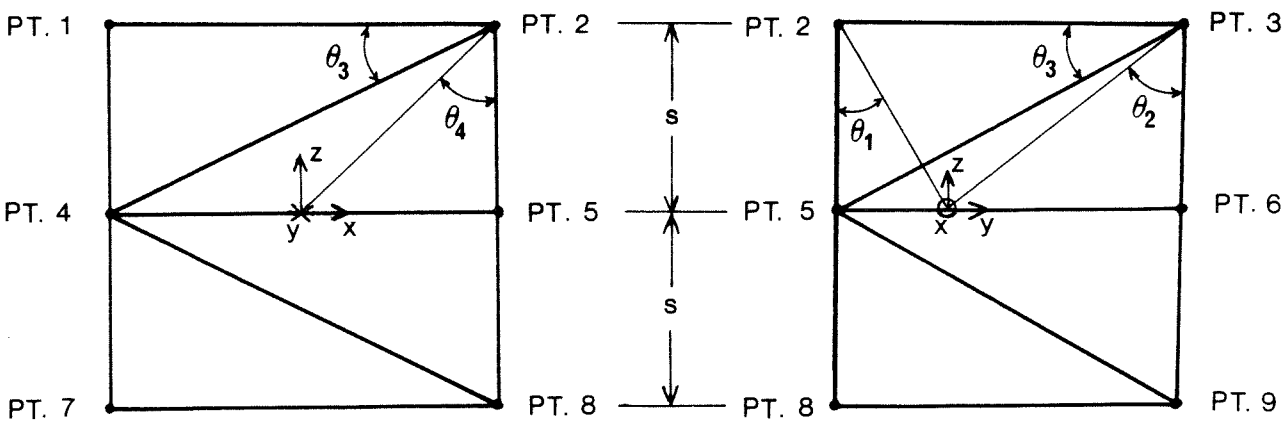

FRONT VIEW

RIGHT SIDE VIEW

FIGURE 4-2. NINE-MASS RIGID BODY MODEL, USED TO DETERMINE MEMBER LOADS IN ANTENNA SUPPORT STRUCTURE. Each point has a mass of $m_s/3$.

linear beam elements is used for verification of the analysis and for numerical evaluation of some load cases.

The point masses are placed at locations corresponding to the hinge points at the center and ends of each antenna stick. When the control thrusters are fired, they apply loads to the rigid structure. Inertial reaction loads then act on each mass to maintain quasi-static equilibrium of the rigid structure. These inertial reaction loads and the 27 equations of local equilibrium for the structure (equations for x, y, and z equilibrium at each of the nine point masses) determine the axial loads in the 21 massless interconnecting members of the model. The details of this procedure are given in Appendix C.

Three load cases are analyzed. In the first, control thrusters are assumed to be acting at hinge point 6 (on the center level) parallel to the x-, y-, and z-axes with loads of magnitude T_x, T_y, and T_z, respectively. A complete analysis gives the loads induced in each member in terms of the control thruster loads T_x, T_y, and T_z, so that the effect of each thruster can be isolated from the other two. The results agree with a finite element analysis run on SDRC's "SUPERB" software.

In the second case, the control thruster loads are assumed to be acting at hinge point 3 (on the top level) parallel to the x-, y-, and z-axes with loads of magnitude T_x, T_y, and T_z, respectively. The inertial reactions loads are determined analytically; the verified finite element model is then used to determine the member loads numerically.

The third case is a combination of the first two, and is evaluated numerically. It is included to indicate whether loads induced by control thrusters acting at different hinge points simultaneously are greater or less than loads induced by control thrusters acting on a single hinge point.

4.3.2. Worst-Case Loads in Members. Analysis indicates that only the cross members (and not the diagonal members) carry the loads created by the centrifugal acceleration $\Omega^2 R$ acting on the antenna sticks. The load induced in each cross member by this process is axial tension of magnitude $\sqrt{3} m_s \Omega^2 R/9$. If the spacecraft is not spinning at the time that the thrusters are firing (as is the case during after-deployment spin-up), this load is not present. Numeric values for the worst-case compressive loads in the members therefore assume that the spacecraft is not spinning ($\Omega = 0$).

The maximum compressive axial load for each type of member is given below. These values assume that each thruster exerts a force of one pound ($T_x = T_y = T_z = 4.45$ N), and that the spacecraft is not spinning ($\Omega = 0$).

	Compressive Load (N)
Antenna Stick	4.50
Cross Member	4.44
Diagonal Member	5.75

The worst-case compressive load for the antenna stick is induced by thrusters firing at point 6 only. However, the worst-case compressive loads for the cross member and the diagonal member are induced by thrusters firing at point 6 and point 3. This indicates that control thrusters acting on several hinge points at once may generate loads greater than those given above in cross members and diagonal members. To allow for the possibility that more severe loadings may occur, an additional multiplicative factor should be used with these results in the design of the members. A factor of 3 will be used for this purpose.

4.4. Minimum Mass Support Structure.

Now that estimates of worst-case compressive loads are available for the structural members, the members can be designed to prevent the primary failure mode of column buckling. The Euler buckling load of a simply-supported column is given by

$$P_E = \frac{\pi^2 EI}{l^2} \tag{4.1}$$

where E is the Young's modulus of the material (N/m^2), I is the area moment of inertia of the column cross-section (m^4), and l is the length of the column (m). To find a column design that will prevent buckling, the Euler buckling load is set equal to the largest expected axial compressive load (times some safety factor) that the column will experience. Note that larger values of EI allow a column of a given length to carry a greater load before buckling occurs. Since we also want to minimize the mass of the columns (to minimize overall spacecraft mass), a material with a large specific stiffness is desirable. Graphite-epoxy composite is therefore used in the design of the members of the support structure.

4.4.1. Structural Efficiency of a Truss in Buckling. Mikulas (reference 1) has outlined a method for designing a minimum mass three-longeron double-laced truss column (Figure 2-3). Assume a column has a straightness imperfection of magnitude a. A compressive axial load applied to the imperfect column induces a bending moment in the column; this moment induces axial loads in the longerons and diagonals of the column. The largest compressive load in a longeron is the sum of any applied axially compressive load P and the largest compressive load due to the bending moment that arises from the imperfection a.

The truss is composed of a number of bays b; each longeron is therefore divided into segments, and each segment is simply supported at each end by the joints that separate the bays. The design

parameters of the longeron for a given value of b can be determined by setting the largest compressive load in a longeron (times a safety factor) equal to the Euler buckling load of an individual longeron segment. A similar process involving the loads induced in the truss diagonals by the column shear can be used to size the diagonals. The number of truss bays is chosen by iteration to produce the minimum overall truss mass for a given diagonal angle ϕ.

Assume that the same material is used for both the longerons and the diagonals (note that the Mikulas truss has no batens). The designer chooses values for the following:

P = column axial compressive load (N)
l = column length (m)
a = column imperfection (m)
E = Young's modulus of material (N/m^2)
ρ = material density (kg/m^3)
b = number of truss bays (dimensionless)
ϕ = angle of diagonals (degrees)

The resulting parameters are then derivable:

l/b = bay length (m)
l/btan ϕ = spacing between longerons (m) = H_s
l/bsin ϕ = length of diagonals (m) = l_d

The radius r_l and mass m_l of each solid-rod longeron are given by

$$r_l^6 - \frac{2b^2 P \tan^2\phi}{\pi^3 E} r_l^4 - \frac{4lP}{3\pi^3 Eb}\left(\frac{l}{b} + 2ba\sqrt{3}\tan\phi\right) r_l^2 + \frac{2}{3}\left(\frac{Pl\tan\phi}{\pi^3 E}\right)^2 = 0 \qquad (4.2)$$

$$m_l = \rho\pi r_l^2 l \qquad (4.3)$$

The resulting Euler buckling load P_E of the column, load P_d in the diagonals, mass m_d of each diagonal, and radius r_d of each diagonal are given by

$$P_E = \frac{\pi^2 E I_c}{l^2} = \frac{\pi^2 E A_l}{2b^2 \tan^2\phi} = \frac{\pi^3 E r_l^2}{2b^2 \tan^2\phi} \tag{4.4}$$

$$P_d = \frac{P\pi a/l}{2\sqrt{3}\cos\phi(1-P/P_E)} \tag{4.5}$$

$$m_d = 2\rho l_d^2 \left\{\frac{P_d}{\pi E}\right\}^{1/2} \tag{4.6}$$

$$r_d = \sqrt{m_d/\pi\rho l_d} \tag{4.7}$$

The mass m of the complete column is the mass of three longerons plus the mass of 6b diagonals (the truss has b bays, with 6 diagonals per bay). The column mass is then

$$m = 1.15(3m_l + 6bm_d) \tag{4.8}$$

which assumes an additional 15% of column mass for the mass of the joints. The procedure is repeated with different values of b and ϕ until the minimum mass column is found. Note that (4.2) can be solved as a cubic equation in r_l^2; the solution is taken to be the positive root with the highest value. This procedure is used to design truss columns for the tension-compression cross members and diagonal members of the antenna structure.

4.4.2. Design of Cross Member Truss Column. The dependence on number of bays b and angle ϕ of the mass of a truss column cross member is shown in Figure (4-3). The longerons and diagonals of the truss are assumed to be solid rods made of graphite-epoxy composite (E = 110.2 GPa, ρ = 1522 kg/m^3). The axial load P is taken from the lumped mass rigid body model results given above, so that P = 3*(4.44 N) = 13.32 N. The column length l is 1000 m. The value of a/l is assumed to be 0.0025, which is a recommended value in civil engineering. For a column 1000 m long, this indicates a deviation in straightness of 2.5 m from centerline. As indicated in Figure (4-3),

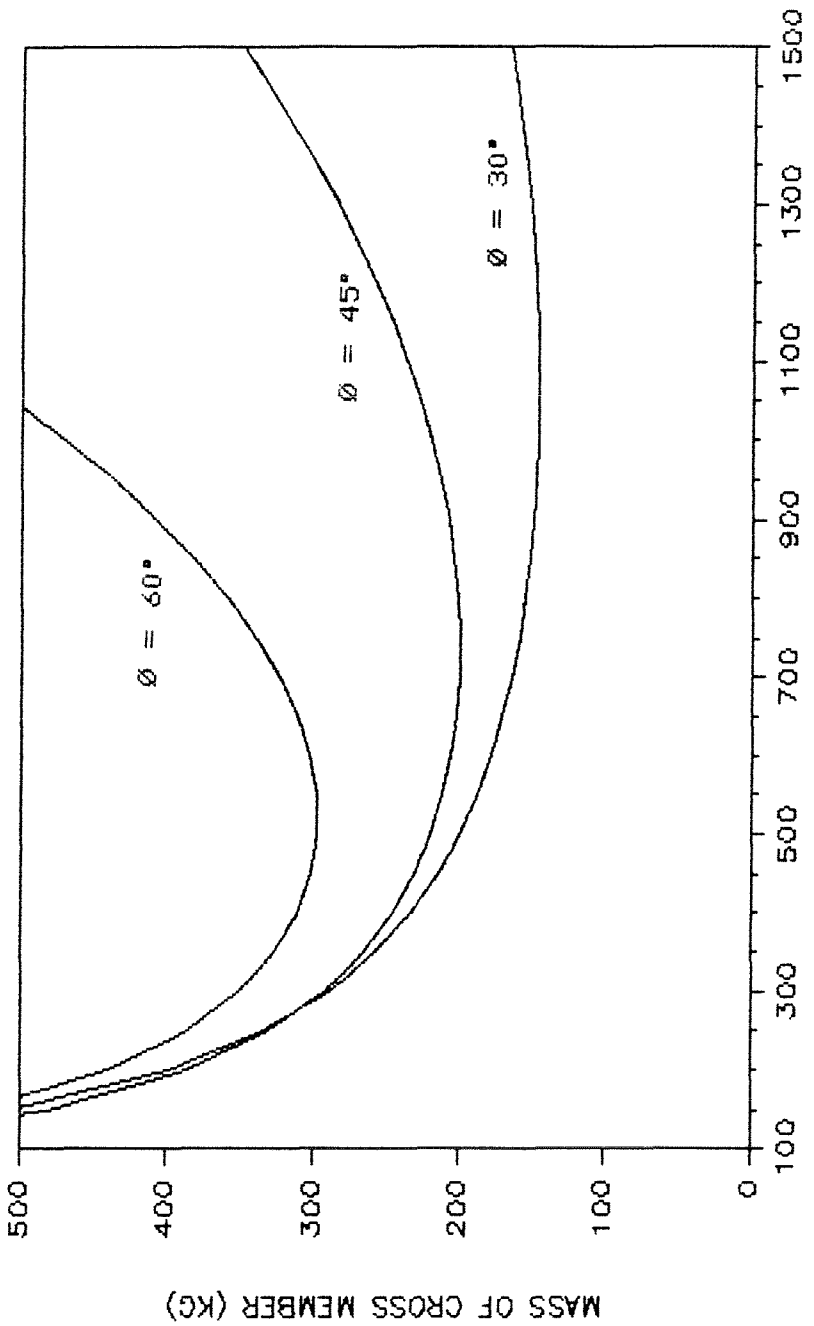

FIGURE 4-3. MASS OF CROSS MEMBER DEPENDS ON NUMBER OF BAYS AND ANGLE Ø.

the minimum mass of the truss column increases as the angle ϕ of the diagonals increases. An angle of $\phi = 30^{o}$ was chosen for the diagonals because it produced a lighter truss column than did the angles of $\phi = 45^{o}$ and $\phi = 60^{o}$.

Given these assumptions, the truss mass is minimum when the number of bays is approximately 1060. The resulting truss parameters for the cross member column are

$b = 1060$
$H_{cm} = 1.634$ m
$r_{l} = 2.622$ mm
$r_{d} = 0.709$ mm
$m_{cm} = 146.6$ kg

This truss will be used for all the tension-compression cross members in the preliminary antenna support structure shown in Figure (4-1).

4.4.3. Design of Diagonal Member Truss Column. The dependence on number of bays b and angle ϕ of the mass of a truss column diagonal member is shown in Figure (4-4). The longerons and diagonals are again assumed to be solid rods of graphite-epoxy composite. The axial load P is 3*(5.75 N) = 17.26 N. Column length l is 1118.0 m, and a/l is assumed to be 0.0025. For a diagonal angle of 30^{o}, the truss mass is a minimum when the number of bays is approximately 1050. The resulting truss parameters for the diagonal member column are

$l = 1118.0$ m
$b = 1050$
$H_{dm} = 1.844$ m
$r_{l} = 2.951$ mm
$r_{d} = 0.799$ mm
$m_{dm} = 207.8$ kg

This truss will be used for all the diagonal members in the preliminary antenna support structure shown Figure (4-1).

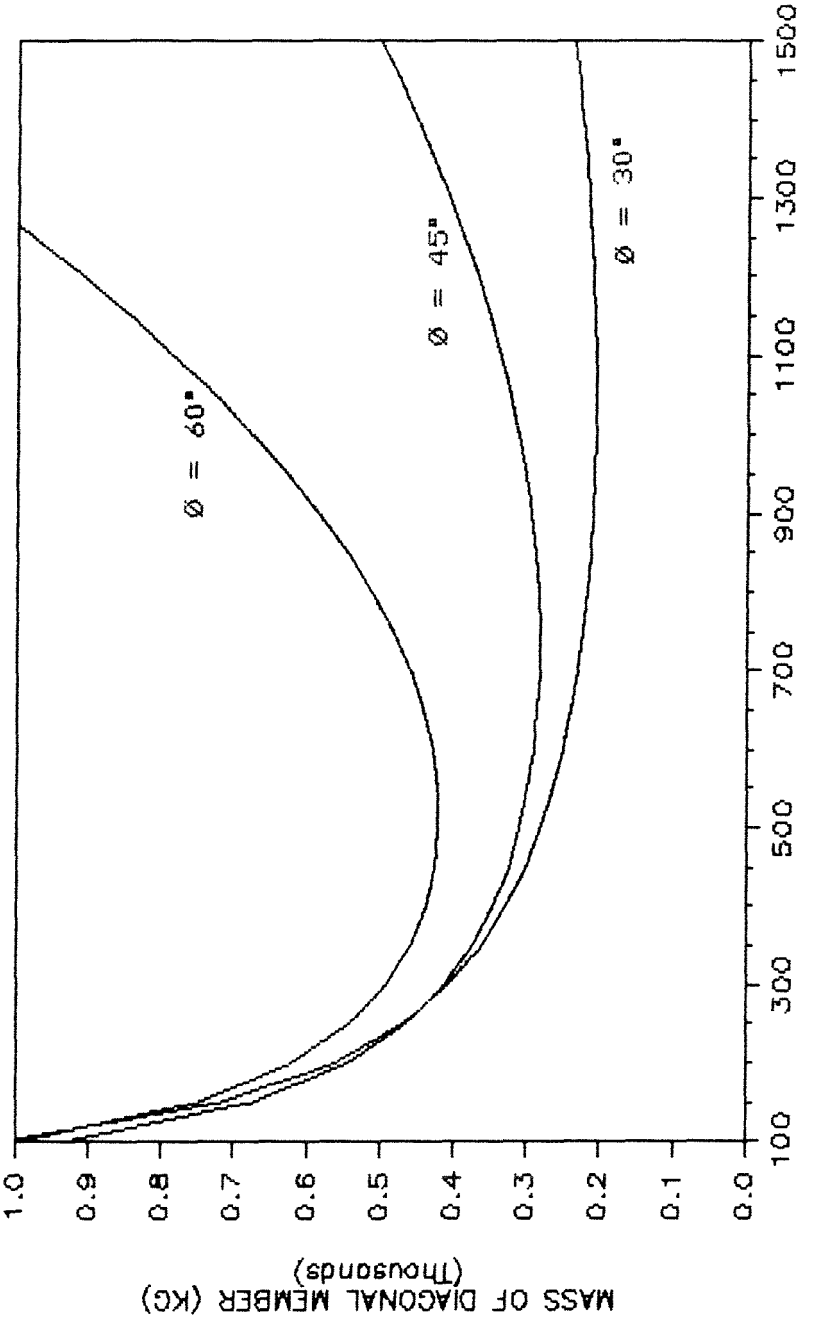

FIGURE 4-4. MASS OF DIAGONAL MEMBER DEPENDS ON NUMBER OF BAYS AND ANGLE Ø.

4.4.4. Design of Tension-Only Cross Member. Recall that the cross members carry the load induced by the centrifugal acceleration $\Omega^2 R$ acting on the mass of the antenna sticks. This component of the load carried by each cross member in the 21-member rigid-body model is given by

$$\sqrt{3} m_s \Omega^2 R/9 \tag{4.9}$$

where m_s is the mass of one antenna stick. When the two levels of tension-only cross members are added to the three levels of tension-compression cross members, this load estimate can be reduced by two-fifths. Given a spinrate of 12 rev/hr and the thin-walled round tube antenna stick mass (with antenna elements) of $m = 12{,}573$ kg for $L = 125$ m, and allowing a safety factor of 1.5, the load that the tension-only members must carry is

$$P_{TO} = 1.5(\tfrac{3}{5})(\sqrt{3} m_s \Omega^2 R/9) = 551.5 \text{ N} \tag{4.10}$$

This can be carried easily by a Kevlar cord with a diameter of 1 mm (the tensile strength of Kevlar fiber is approximately 1000 MPa) and a mass of about 1 kg. The tension-only cross members are virtually massless compared to the other members of the structure.

Chapter 5
FREE VIBRATION OF THE PRELIMINARY STRUCTURE

The periodic firing of control thrusters (required for spacecraft attitude control) excites structural vibration. Large space structures tend to have long vibrational periods (minutes are not uncommon) that make the spacecraft difficult to control. To accurately determine the position of each antenna element by analysis, it is necessary to understand the dynamics of the structure. The first step in characterizing the dynamics is to determine the natural frequencies and mode shapes. However, large space structures present a complex modeling problem. Although finite element dynamic analysis can be used to determine the structure's vibrational modes and frequencies, the number of elements needed to get reasonable results is so large that computer costs can become prohibitive. A simplified means of estimating modes and frequencies of the structure is therefore desirable.

The frequencies and mode shapes of the individual members of the structure are found in Section 5.1 by conventional analysis, which uses equations derived for a continuous beam (or a string, in the case of the tension-only cross members). Finite element analysis in Section 5.2 finds the frequencies and mode shapes of the overall structure of a simplified 27-degree-of-freedom (27-DOF) model, in which each member of the structure is represented by a single element. A more complicated 162-degree-of-freedom (162-DOF) model is also analyzed; it uses 12 elements on each tension-compression cross member and diagonal member. The results of the 162-DOF finite element analysis compare favorably to the results of conventional analysis and the 27-DOF finite element model, which indicates that simplified models can be used for design purposes to determine the vibrational dynamics of the structure.

5.1. Lateral Vibration of Members.

Per Meirovitch (reference 5), the natural frequencies ω_r in rad/sec of a simply-supported uniform beam (EI = constant, m(x) = mass per unit length = constant) in free bending vibration, are given by

$$\omega_r = (r\pi)^2 \sqrt{\frac{EI}{m(x)l^4}} , \qquad r = 1,2,... \tag{5.1}$$

where l is the length of the beam. This value must be divided by 2π to find the natural frequencies in Hertz. The normal mode shapes $Y_r(x)$ of bending vibration for the beam are given by

$$Y_r(x) = \sqrt{\frac{2}{m(x)l}} \sin\frac{r\pi x}{l} , \qquad r = 1,2,... \tag{5.2}$$

The modes in Equation (5.2) have been normalized according to $\int_0^L m(x)Y_r^2(x)dx = 1$ $(r = 1,2,...)$.

The above results neglect rotational inertia, and assume that shear deformation is small compared to the bending deformation. Thus rotary inertia and shear deformation effects are neglected. These assumptions are valid if the ratio between the beam characteristic length (in this case, one-half the vibrational wavelength) and beam width is large (greater than 10). Also, it is assumed that no axial load is acting on the beam.

The tension-only members are not beams, so Equations (5.1) and (5.2) do not apply to them. However, the natural frequencies and modes of a tension-only member can be found using the equations for vibration of a string. The natural frequencies ω_r in rad/sec are given by

$$\omega_r = r\pi \sqrt{\frac{T}{m(x)l^2}} , \qquad r = 1,2,... \tag{5.3}$$

where T is the tension in the string (N). The mode shapes $Y_r(x)$ are given by

$$Y_r(x) = A_r \sin\frac{r\pi x}{l} , \qquad r = 1,2,... \tag{5.4}$$

where A_r is the amplitude of the mode shape.

The tension-compression cross members can be modelled as strings when under axial tension if the magnitude of the tension is sufficiently high. This occurs when the spacecraft is spinning, and each cross member is therefore carrying an axial tensile load of $\sqrt{3}m_s\Omega^2R/15$. Given a spacecraft spinrate of Ω = 12 rev/hr and an antenna stick mass m_s of 12,573 kg, the tension carried by each cross member is 367.7 N. Using the data from Chapter 4, the lowest frequency of vibration for a "string" tension-compression cross member is 0.025 Hz.

A list of the five lowest frequencies of each member type are shown in Table (5-1). The data for the properties of each member are taken from the analyses in Chapter 4.

5.2. Finite Element Analysis of the Structure.

The equations that describe the natural frequencies and modes of a structure as complex as the preliminary design shown in Figure (4-1) are too involved to solve by conventional analysis. However, if the structure is represented by a simplified model, the natural frequencies and modes of the model can be determined numerically from the discrete forms of the equations. Finite element dynamic analysis does just that. The SDRC "SUPERB" finite element dynamic analysis software is capable of finding the frequencies and modes of a structure in free vibration. Beam elements are used to represent the members of the structure. In this code, a beam element has two nodes, one at each end, and includes the effects of shear deformation. The x-axis of the element lies on the line between the two nodes, so that the y- and

Table 5-1. FUNDAMENTAL FREQUENCIES AND HARMONICS FOR LATERAL VIBRATION OF THE STRUCTURAL MEMBERS. Found by conventional analysis.

	Lateral Vibration Frequency (Hz)			
Freq	Antenna Stick	T-C Cross Member	Diagonal Member	T-O Cross Member
ω_1	0.47176	0.00731	0.00660	0.30319
ω_2	1.8870	0.02926	0.02640	0.60638
ω_3	4.2459	0.06582	0.05940	0.90957
ω_4	7.5482	0.11702	0.10561	1.21277
ω_5	11.7940	0.18285	0.16501	1.51596

Note: The antenna stick segments are 250 m long.

z-axes form the plane of the element's cross-section. Given a Young's modulus E and Poisson's ratio ν, the code will calculate a value for the shear modulus G from the relation $G = E/2(1 + \nu)$.

A model of a simply-supported thin-walled cylindrical antenna stick segment composed of 25 beam elements serves as a test case of the modelling approach. Each element in the model is given the following properties:

mass density	= 1522 kg/m^3
Young's modulus	= 110.2 GPa
Poisson's ratio	= 0.360
length	= 250 m
cross-sectional area	= 0.0077 m^2
area moment of inertia $I_x = I_y$	= 0.040 m^4
shear area ratio $A_x = A_y$	= 2.0

These properties are representative of a thin-walled tube (t_m = 0.381 mm) of diameter 6.452 m, composed of a graphite-epoxy prepreg with one or two plies of fabric. Conventional analysis predicts a fundamental frequency of 0.487 Hz for this beam; finite element analysis yields an identical value.

5.2.1. 27-Degree-of-Freedom Model. In this model, each member of the structure is represented as a single beam element. The properties of the elements are given in Table (5-2). Note that they differ slightly from the properties calculated in Chapter 4. Because this model has no nodes other than the end nodes on the members, it cannot analyze the modes of the individual members; it can only analyze modes of the overall structure. The advantage of this simple model, however, is that it requires little CPU time to complete the dynamic analysis. This model therefore provides a good first estimate of the shape and frequencies of the structural modes.

TABLE 5-2. PROPERTIES GIVEN TO BEAM ELEMENTS IN THE 27-DEGREE-OF-FREEDOM FINITE ELEMENT DYNAMIC ANALYSIS. All elements are symmetrical about their x-axes, so that the shear area ratio and the area moment of inertia are the same about both the y- and z-axes.

Property	Antenna Stick	Cross Member	Diagonal Member
Young's Modulus (N/m^2)	1.102 E+11	1.102 E+11	1.102 E+11
Mass Density (kg/m^3)	1522	1522	1522
Poisson's Ratio	0.360	0.360	0.360
Cross-sectional Area (m^2)	7.72 E-03	6.649 E-05	8.710 E-05
Area Moment of Inertia (m^4)	4.019 E-02	2.959 E-05	5.120 E-05
Shear Area Ratio	2.0	2.0	2.0
Calculated ω_1 (Hz)	0.48795	0.00892	0.00820

The 27 natural frequencies found by this model are shown in Table (5-3). Note that the first six frequencies have been omitted, as they represent the six rigid body modes of the structure. Due to symmetry of the structure, some mode shapes have identical frequencies.

The orientation of the undeformed dynamic model appears in Figure (5-1). The cross members and antenna sticks are emphasized for clarity. The shapes of the first three structural modes are shown in Figures (5-2) , (5-3) , and (5-4), with the diagonal members omitted for clarity. Note that the natural frequencies of these three modes are in the range of the frequencies of the fourth and fifth modes of the diagonal members and tension-compression cross members. We would therefore expect to see these members, as well as the structure, vibrating at the first three structural frequencies. The lowest frequency of the antenna sticks is sufficiently high, however, that the antenna sticks will probably not be vibrating at the first three structural frequencies.

5.2.2. 162 Degree-of-Freedom Model. Additional beam elements are used in the 162-DOF model: each of the tension-compression cross members and the diagonal members is now composed of 12 beam elements. This allows the finite element program to determine numerically the natural frequencies of these members. Also, any coupling between the modes of these members and modes of the structure as a whole should be detected. Each 500 m antenna stick segment is still represented by a single beam element. The physical and material properties of the elements used in the 162-DOF analysis are shown in Table (5-4).

The analysis of this model produces 162 natural frequencies, many of which are similar or identical; some of them are listed in Table (5-5). The modal frequencies 7 and 19 represent the lowest natural frequency of the diagonal members and tension-compression cross members, respectively. Note that the first three structural frequencies (modes 97, 98, and 99) are higher than those found in the 27-DOF

TABLE 5.3 MODAL FREQUENCIES OF THE ANTENNA STRUCTURE FOUND BY FINITE ELEMENT DYNAMIC ANALYSIS OF THE 27-DEGREE-OF-FREEDOM MODEL. The first six modes are rigid body translation/rotation modes, and are omitted.

Mode	Frequency (Hz)
7	0.12299
8	0.17035
9	0.18752
10	0.18752
11	0.20019
12	0.20019
13	0.33117
14	0.33117
15	0.42228
16	0.42228
17	0.45033
18	0.49598
19	0.49598
20	0.55196
21	0.56884
22	4.5182
23	4.5605
24	4.5605
25	8.8955
26	8.8955
27	8.9031

FIGURE 5-1. ORIENTATION OF UNDEFORMED DYNAMIC MODEL.

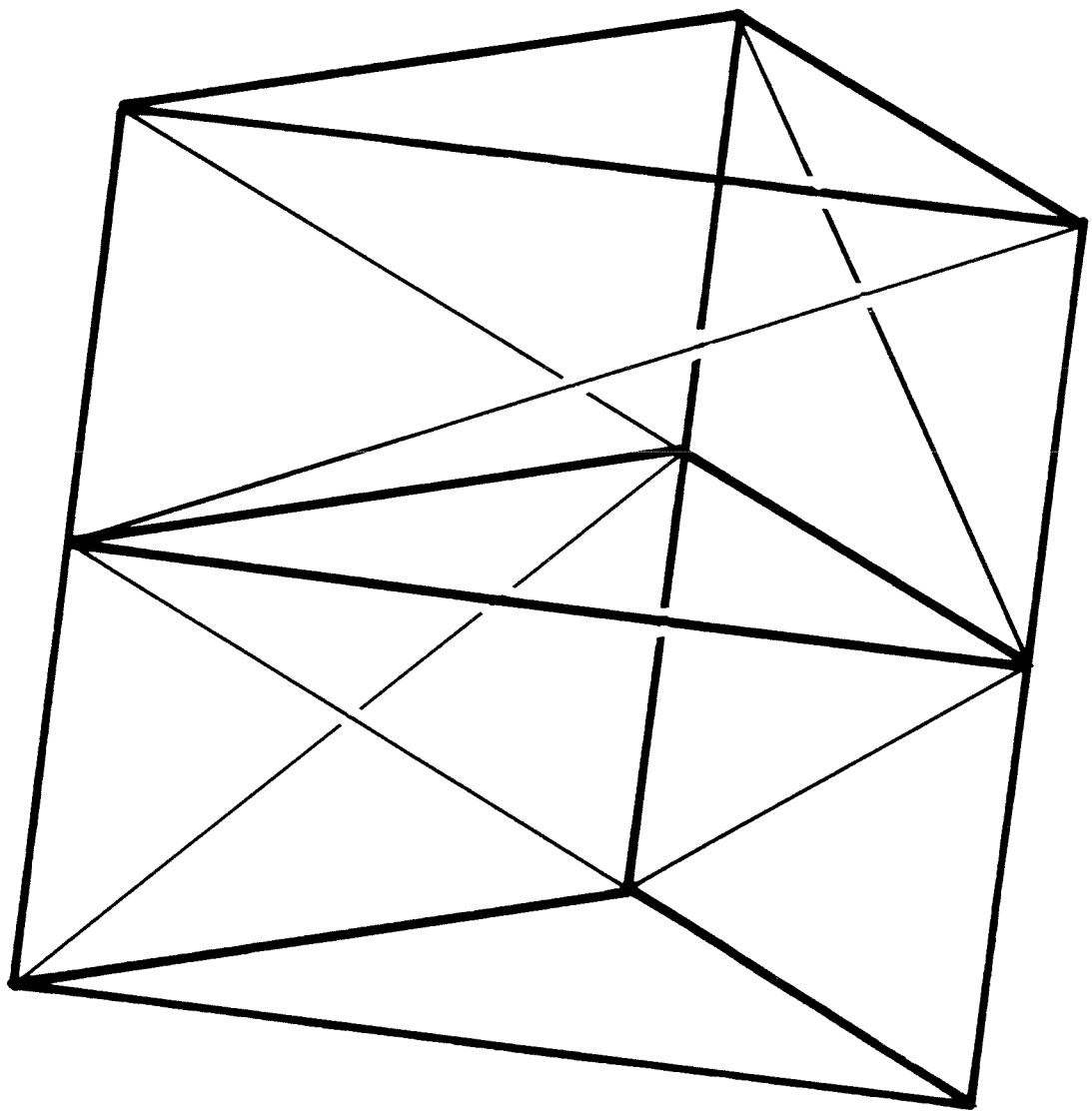

FIGURE 5-2. FIRST STRUCTURAL MODE SHAPE OF 27-DEGREE-OF-FREEDOM MODEL.

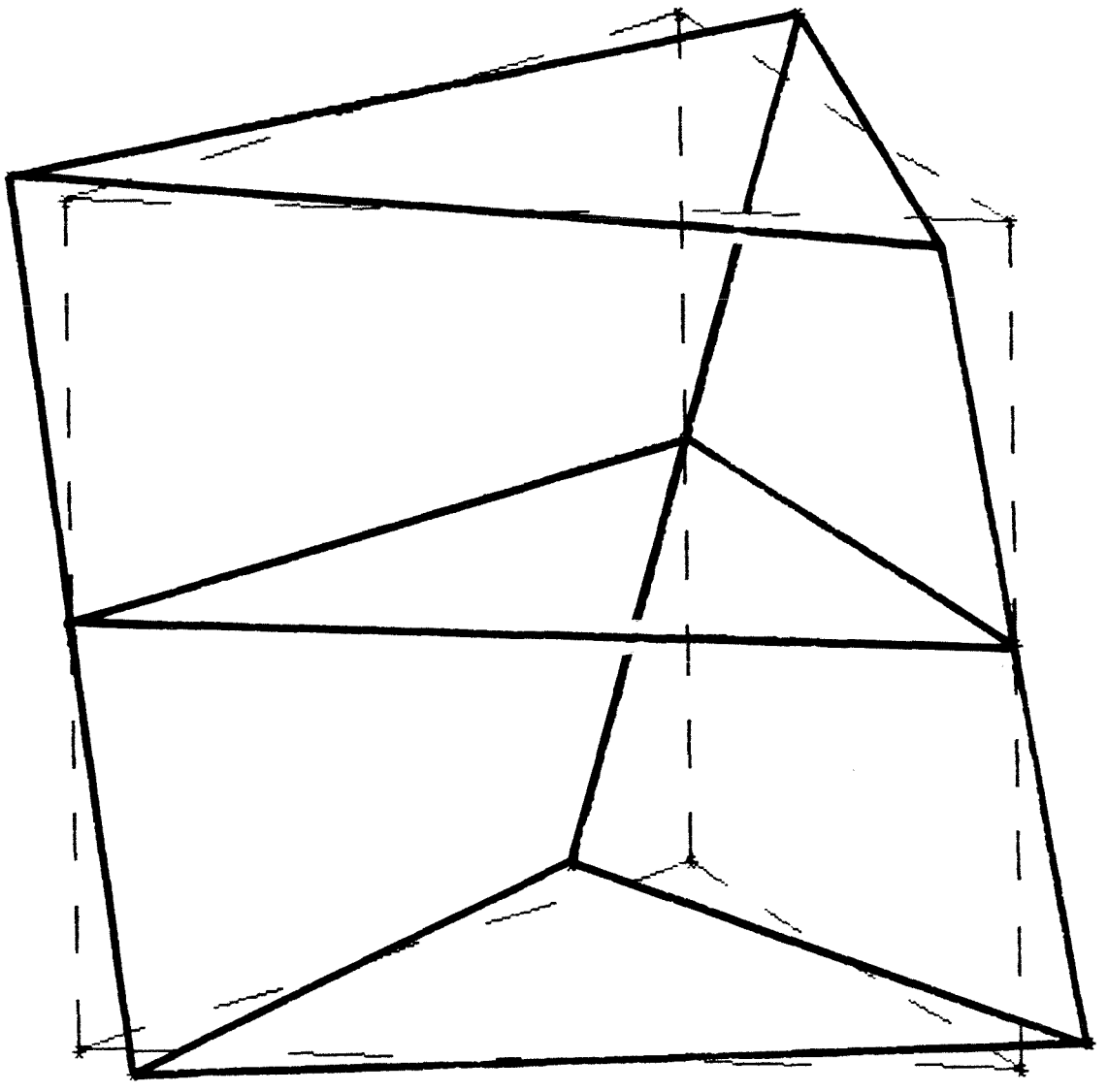

FIGURE 5-3. SECOND STRUCTURAL MODE SHAPE OF 27-DEGREE-OF-FREEDOM MODEL.

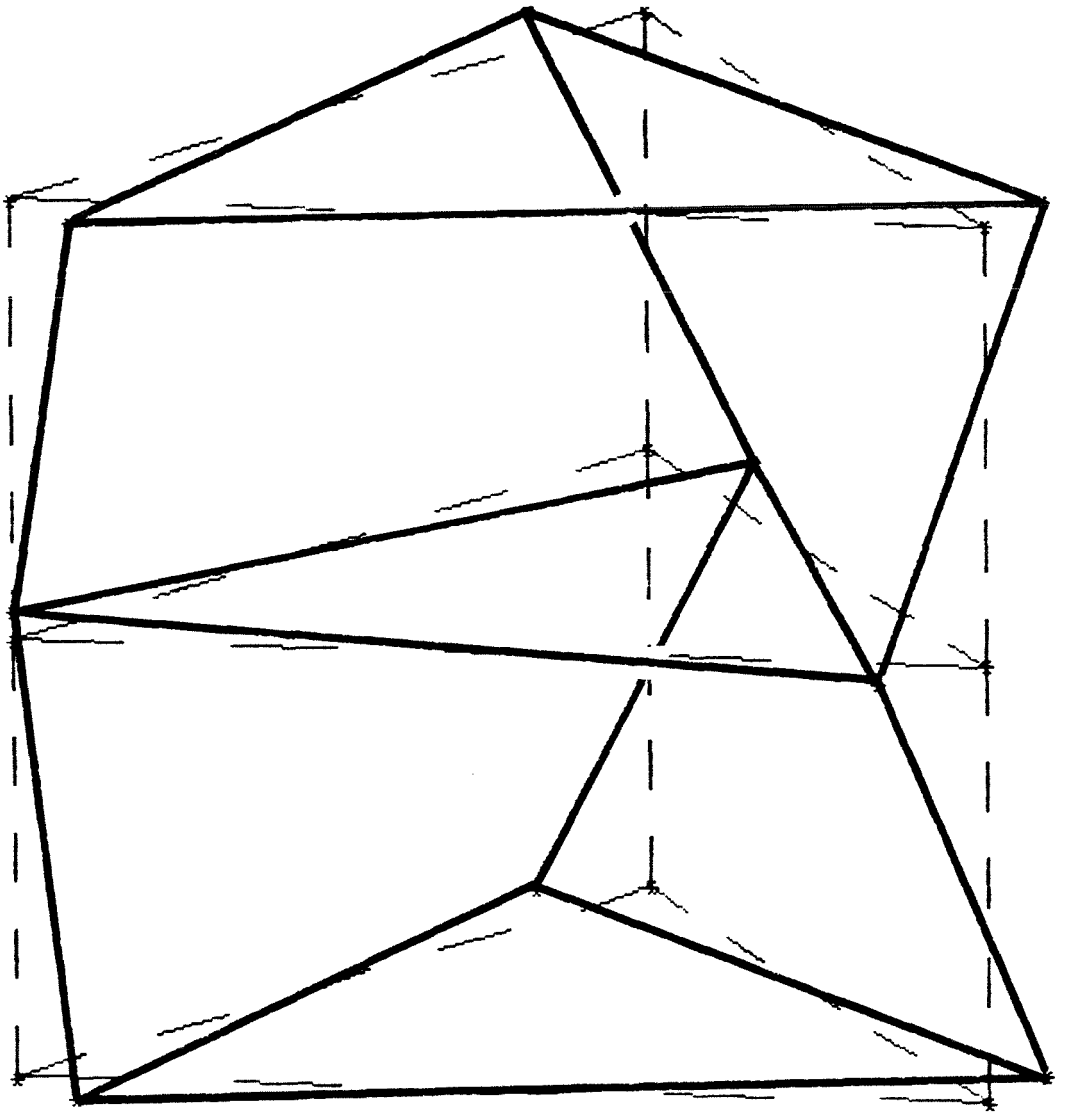

FIGURE 5-4. THIRD STRUCTURAL MODE SHAPE OF 27-DEGREE-OF-FREEDOM MODEL.

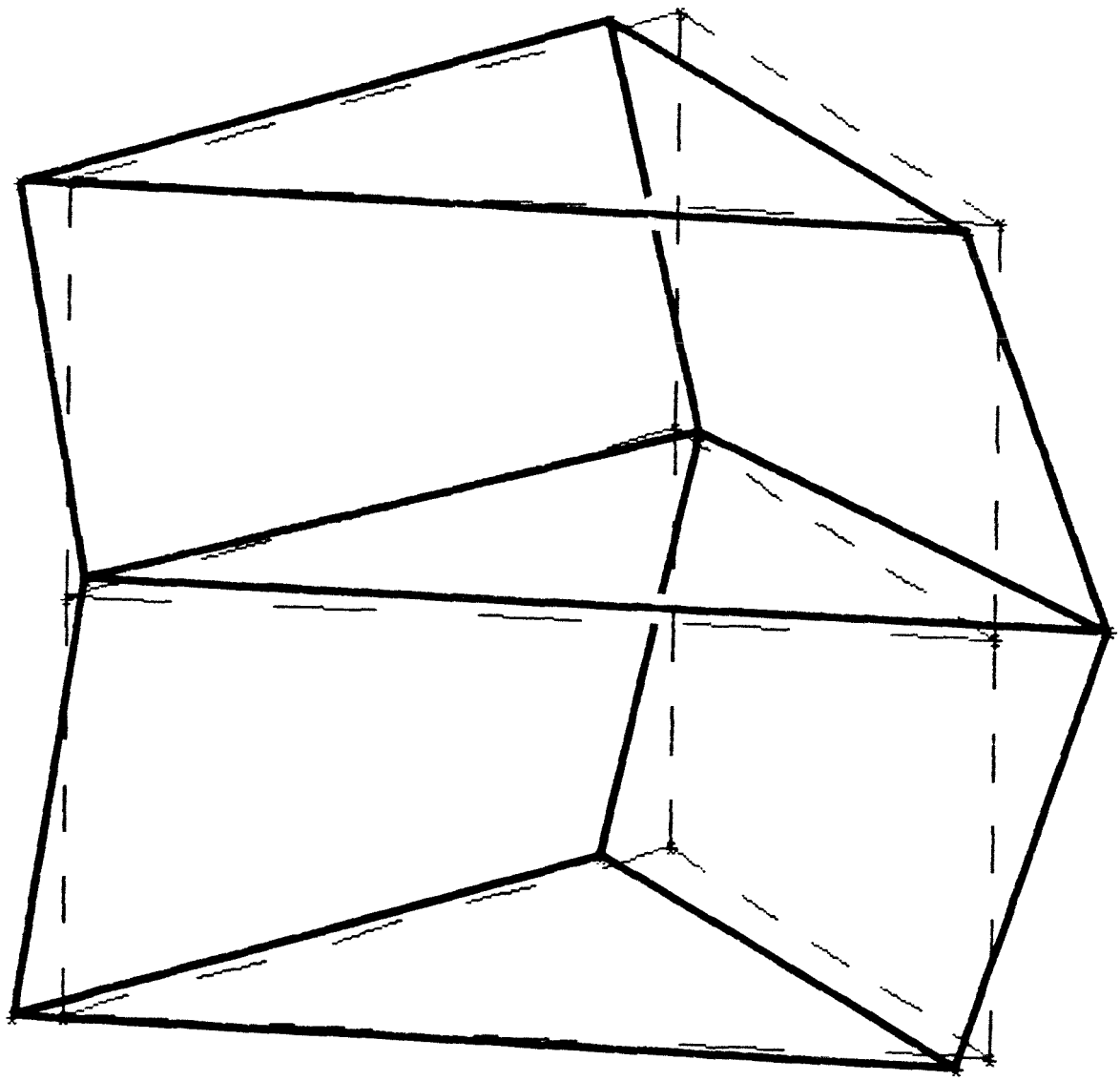

TABLE 5-4. PROPERTIES GIVEN TO BEAM ELEMENTS IN THE 162-DEGREE-OF-FREEDOM FINITE ELEMENT DYNAMIC ANALYSIS. All elements are symmetrical about their x-axes, so that the shear area ratio and the area moment of inertia are the same about both the y- and z-axes.

Property	Antenna Stick	Cross Member	Diagonal Member
Young's Modulus (N/m^2)	1.102 E+11	1.102 E+11	1.102 E+11
Mass Density (kg/m^3)	1522	1522	1522
Poisson's Ratio	0.360	0.360	0.360
Cross-sectional Area (m^2)	7.723 E-03	7.732 E-05	1.013 E-04
Area Moment of Inertia (m^4)	4.019 E-02	2.958 E-05	5.120 E-05
Shear Area Ratio	2.0	2.0	2.0
Calculated ω_1 (Hz)	0.48785	0.00827	0.00760

TABLE 5-5. SELECTED MODAL FREQUENCIES OF THE ANTENNA STRUCTURE, FOUND BY FINITE ELEMENT DYNAMIC ANALYSIS OF THE 162-DEGREE-OF-FREEDOM MODEL.

Mode	FEA Freq. (Hz)	Significance	Near Harmonics	Predicted Freq. (Hz)
7	0.0076093	First mode of diagonal members	1 * ω_d	0.00760
19	0.0082734	First mode of cross members	1 * ω_c	0.00827
39	0.030699	Second mode of diagonal members	4 * ω_d	0.03041
49	0.033379	Second mode of cross members	4 * ω_c	0.03307
67	0.072656	Third mode of diagonal members	9 * ω_d	0.6842
97	0.13436	First structural mode	16 * ω_c	0.12299
98	0.18798	Second structural mode	25 * ω_d	0.17035
99	0.20478	Third structural mode	25 * ω_c	0.18752

analysis. This is due in part to the different physical properties of the elements used in the two models. The first three structural mode shapes are shown in Figures (5-5) , (5-6) , and (5-7). As expected, the cross members and diagonal members, as well as the structure, are vibrating.

The frequencies found by this analysis compare favorably to the frequencies found by the 27-DOF analysis of the structure and by conventional analysis of the members. These results indicate that a complex finite element model is not needed for preliminary design purposes. Instead, a simplified finite element model that represents each member with a single element can be used to find the natural frequencies and mode shapes of the structure as a whole, and conventional analysis can be used to find the natural frequencies and mode shapes of the individual members.

FIGURE 5-5. FIRST STRUCTURAL MODE SHAPE OF 162-DEGREE-OF-FREEDOM MODEL.

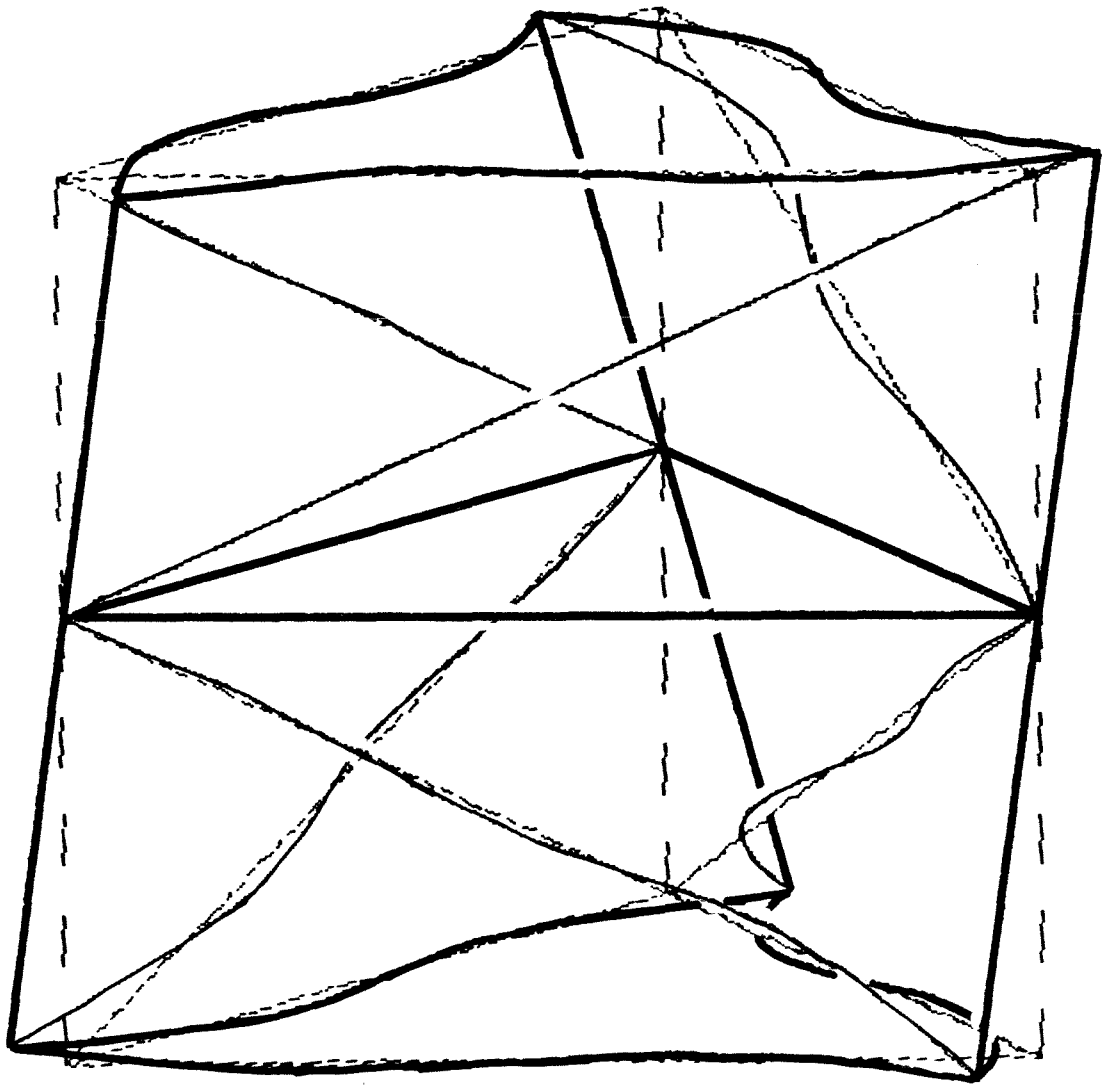

FIGURE 5-6. SECOND STRUCTURAL MODE SHAPE OF 162-DEGREE-OF-FREEDOM MODEL.

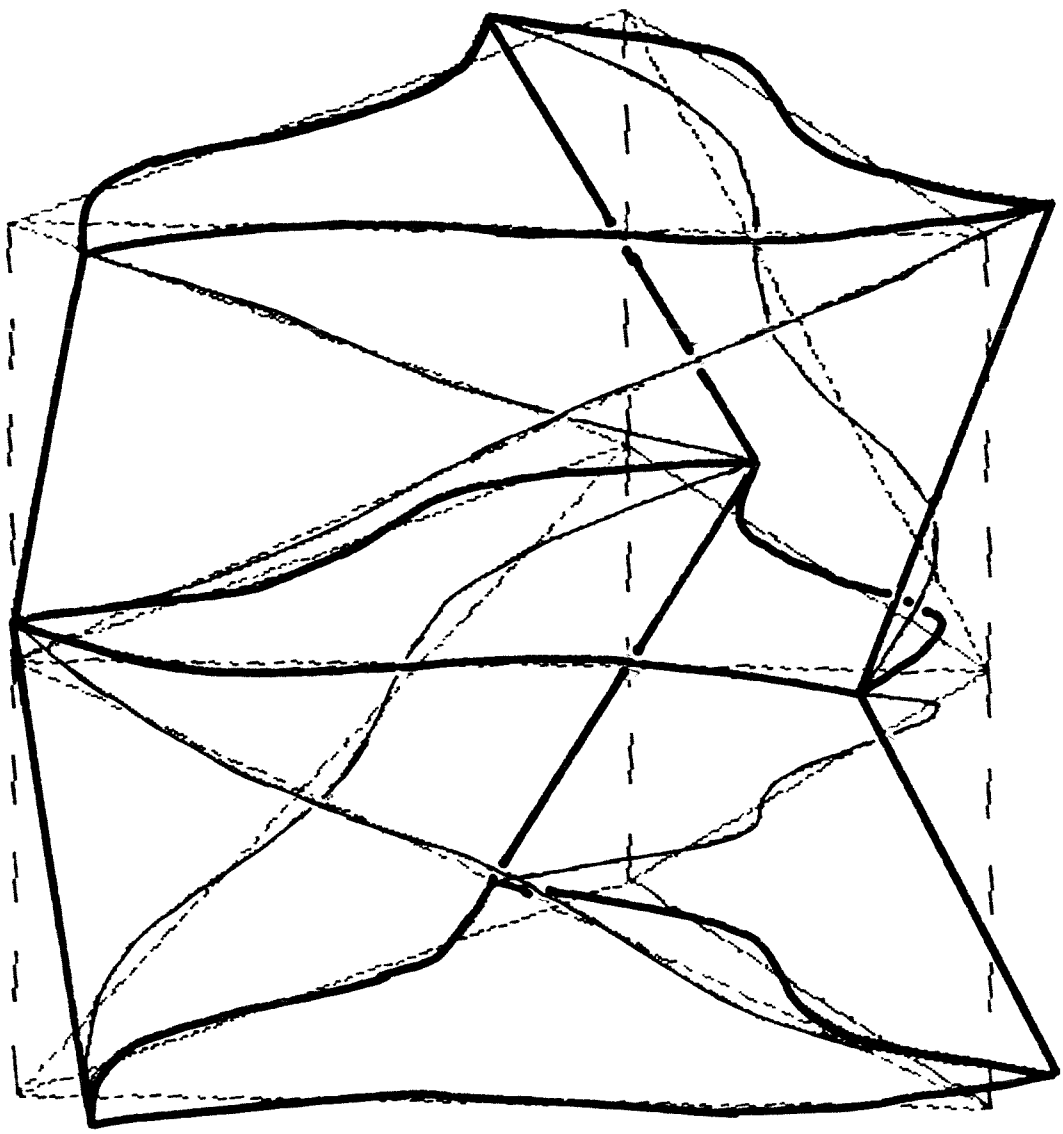

FIGURE 5-7. THIRD STRUCTURAL MODE SHAPE OF 162-DEGREE-OF-FREEDOM MODEL.

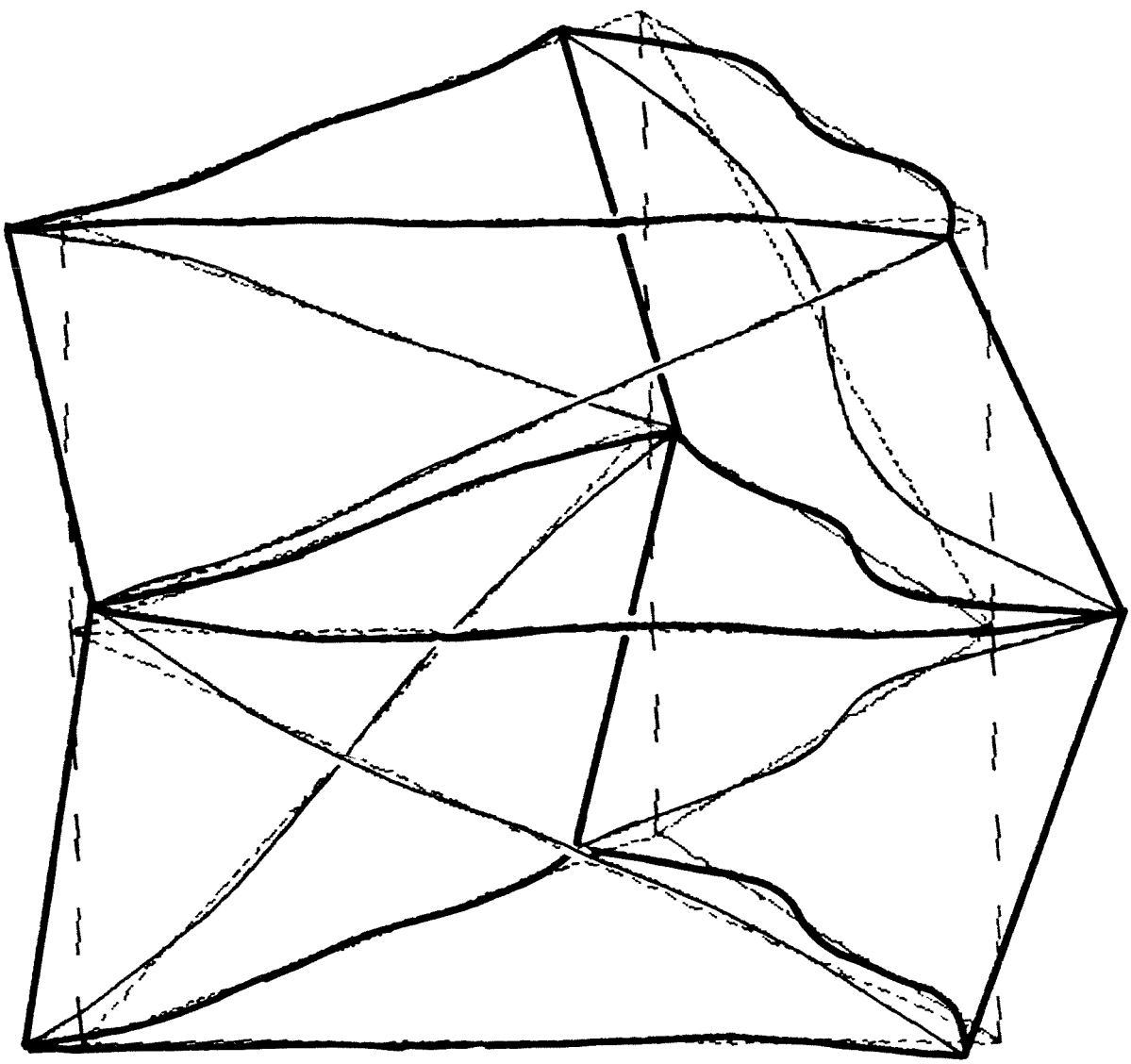

Chapter 6
CONCLUSIONS AND RECOMMENDATIONS

This study develops a preliminary structural design for the antenna sticks and support structure using performance requirements, static analysis, and consideration of environmental spacecraft torques. It represents the first step in the design cycle, with the corresponding data inconsistencies that arise when the design is in flux. The overview of the structure's free vibration modes in Chapter 5 is the beginning of the first design iteration.

The preliminary design phase must of necessity make assumptions. These assumptions should be checked by further analysis as the design cycle progresses. For instance, the antenna stick are designed based on the assumption that an accurate assessment of the joint positions can be made. Considerable development will be required, however, to design a system capable of performing this assessment within the limitations imposed by spacecraft configuration, environment, and power.

The quasi-static analysis that develops estimates of member axial loads implicitly assumes that the spacecraft spin axis is aligned with the spacecraft angular momentum vector. If significant nutation is present (as it may be with relatively low spinrates), this will not be the case. Additional analysis is thus desirable to verify the design loads used for the cross members and diagonal members. The axial loads induced in the antenna sticks should also be checked; the preliminary design assumes that axial loads are such that buckling does not occur.

The numerical analysis that helps determine a spinrate for the spacecraft (Chapter 3) is based on a "spacecraft" that consists only of the three antenna sticks. In future iterations, the analysis should use the complete preliminary structure as the model, as changes in the spacecraft's mass moments of inertia alter its response to

environmental torques.

Some problem areas have come to light during the preliminary design phase. One is the dependence of spacecraft spin stability on the structural mass moment of inertia ratios. Any spacecraft will tend to favor spinning about the principal body axis that has the highest mass moment of inertia. To insure that the spacecraft will spin about the z-axis, the ratios of mass moments of inertia I_{zz}/I_{xx} and I_{zz}/I_{yy} must have values greater than 1. In some "rigid" spacecraft, values of 1.05 for these ratios are sufficient. In a large flexible spacecraft such as this design, however, values of 2 or greater are desirable. In the preliminary design, these ratios have values of about 1.3, which is not sufficient to insure that the spacecraft will stay spinning about its z-axis. The preliminary configuration may have to be altered to remedy this. As the mass of the antenna sticks decreases (as it would if truss columns instead of thin-walled round tubes were used as antenna stick segments), I_{zz} decreases faster than I_{xx} or I_{yy}, which further reduces the value of the ratios. Any attempt to minimize the mass of structural members must therefore be tempered by consideration for spacecraft spin stability.

Another problem area is vibration: the preliminary spacecraft design may not be controllable. If this proves to be true, it may be necessary to redesign or relocate the members in order to raise their harmonic frequencies and decouple the vibrational modes. Some form of structural damping will be required. The response of the structure to forced vibration (such as that caused by thruster firing) needs to be studied in depth, as it may induce significant member loads (which have only been estimated in this work) and severely impact antenna stick displacement error.

A change in the basic support structure configuration may alleviate some of the problems. Surprisingly, limiting the mass of the spacecraft may not necessarily be important in this design. The

antenna stick segments can be made shorter so the number of cross members can be increased. Different diagonal configurations are possible as well. Lumped masses can be added at joints if necessary to increase moment of inertia ratios. Additional members may be inserted where helpful.

To keep this study to a manageable size, many issues vital to the design of a large spacecraft are not considered. Some of these issues are assembly in space, deployment, thermal distortion, controllability, and the placement and mass of necessary spacecraft components such as solar panels and thrusters.

REFERENCES

1. Mikulas, Martin M., Jr.: "Structural Efficiency of Long Lightly Loaded Truss and Isogrid Columns for Space Applications," NASA Technical Memorandum 78687, Langley Research Center, July 1978. (N78-33480)

2. "Interim Report for Study of Wrap-Rib Antenna Design," Lockheed Missiles and Space Company, July 17, 1981. (LMSC-D714653). Prepared for the Jet Propulsion Laboratory under contract 955345.

3. Timoshenko, Stephen P.; and Gere, James M.: Theory of Elastic Stability. 2nd Edition. McGraw-Hill Book Company, 1961.

4. Wertz, James R., ed.: Spacecraft Attitude Determination and Control. D. Reidel Publishing Company, 1984.

5. Meirovitch, Leonard M.: Elements of Vibration Analysis. McGraw-Hill Book Company, 1975.

6. Kaplan, Marshall H.: Modern Spacecraft Dynamics and Control. John Wiley and Sons, 1976.

APPENDIX A: DISPLACEMENT ERROR SENSITIVITY STUDY

The beam equation, which relates transverse displacement w(x) of a beam to its bending stiffness EI and transverse load per unit length Q, is

$$\frac{d^2}{dx^2}\left[E(x)I(x)\frac{d^2}{dx^2}w(x)\right] = Q(x) \tag{A.1}$$

For a beam of length 2L with a uniform bending stiffness $EI = E_oI_o$, subjected to a uniform transverse load per unit length Q_o, integration of the beam equation yields

$$w_o(x) = \frac{Q_o x^4}{24E_oI_o} + \frac{Ax^3}{6} + \frac{Bx^2}{2} + Cx + D \tag{A.2}$$

The four constants A, B, C, and D are found using the boundary conditions of the problem. For a simply-supported beam, the hinged ends dictate that both (a) beam displacement and (b) moment be zero at x = 0 (a hinged joint cannot support a moment). The other two boundary conditions arise from symmetry, and require that both (c) shear stress and (d) beam slope relative to the unloaded position be zero at x = L (the beam center). Slope, moment, and shear stress are proportional to the first, second, and third derivatives of the beam displacement, respectively. When substituted into (A.2), these boundary conditions determine the constants:

$$w(0) = 0 \rightarrow D = 0 \tag{A.3a}$$

$$w''(0) = 0 \rightarrow B = 0 \tag{A.3b}$$

$$w'''(L) = 0 \rightarrow A = -\frac{Q_o L}{E_o I_o} \tag{A.3c}$$

$$w'(L) = 0 \rightarrow C = \frac{Q_o L^3}{3E_o I_o} \tag{A.3d}$$

Thus the solution for the displacement $w_o(x)$ of a simply-supported beam that has both uniform bending stiffness and transverse load is

$$w_o(x) = \frac{Q_o L^4}{24E_o I_o}\left[\frac{x^4}{L^4} - \frac{4x^3}{L^3} + \frac{8x}{L}\right] \tag{A.4}$$

The maximum displacement occurs at the beam center (x = L), and is given by

$$w_o(x) = \frac{5Q_o L^4}{24E_o I_o} \tag{A.5}$$

The displacement w(x) for any beam with four distinct boundary conditions and uniform properties (both EI and Q constant) can be determined by the procedure outlined above. This fact can be used to determine the discrepancy between beam displacement calculations that assume a constant bending stiffness $E_o I_o$ and calculations that acknowledge the presence of an imperfection in EI. The discrepancy will be referred to as "displacement error." Displacement error is derived below for three cases:

Simply-supported beam with step imperfection in EI
Clamped beam with step imperfection in EI
Clamped beam with sinusoidal imperfection in EI

When the amplitude of the imperfection is equal for all three cases, the size of the displacement error is greater for the clamped beam with a step imperfection than for the clamped beam with the sinusoidal imperfection; displacement error is greatest for the

simply-supported beam with the step imperfection.

Simply-Supported Beam with Step Imperfection in EI

Assume that a simply-supported beam of length 2L has a step increase of amplitude δ and width 2α in its bending stiffness EI, as shown in Figure (2-1). We can use the symmetry of the beam properties to justify solving the beam equation over the interval x = 0 to x = L instead over the entire length of the beam.

Consider the beam section x = 0 to x = L to be composed of two different beams: Beam 1 has a bending stiffness of $EI = E_oI_o$, displacement $w_1(x)$, and exists over the interval x = 0 to $x = L(1-\alpha)$; Beam 2 has a bending stiffness of $EI = E_oI_o(1+\delta)$, displacement $w_2(x)$, and exists over the interval $x = L(1-\alpha)$ to x = L. By continuity, both beams must have the same displacement and derivatives at $x = L(1-\alpha)$. These conditions, combined with the simple support at end x = 0 and the symmetry condition at x = L, result in eight boundary conditions which determine the constants A_1, B_1, C_1, D_1 for $w_1(x)$ and A_2, B_2, C_2, D_2 for $w_2(x)$:

$$w_1(0) = 0 \rightarrow D_1 = 0 \tag{A.6a}$$

$$w_1''(0) = 0 \rightarrow B_1 = 0 \tag{A.6b}$$

$$w_2'''(L) = 0 \rightarrow A_2 = -\frac{Q_oL}{E_oI_o(1+\delta)} \tag{A.6c}$$

$$w_2'(L) = 0 \rightarrow C_2 = \frac{Q_oL^3}{3E_oI_o(1+\delta)} - B_2L \tag{A.6d}$$

$$w_1'''(L-L\alpha) = w_2'''(L-L\alpha) \rightarrow A_1 = -\frac{Q_oL}{E_oI_o(1+\delta)}[1+(1-\alpha)\delta] \tag{A.6e}$$

$$w_1''(L-L\alpha) = w_2''(L-L\alpha) \rightarrow B_2 = -\frac{Q_o L^2 (1-\alpha)^2 \delta}{2E_o I_o (1+\delta)} \qquad (A.6f)$$

$$w_1'(L-L\alpha) = w_2'(L-L\alpha) \rightarrow C_1 = \frac{Q_o L^3}{6E_o I_o (1+\delta)}[(2+\alpha)(1-\alpha)^2\delta + 2] \qquad (A.6g)$$

$$w_1(L-L\alpha) = w_2(L-L\alpha) \rightarrow D_2 = -\frac{Q_o L^4 (1-\alpha)^4}{24E_o I_o (1+\delta)} \qquad (A.6h)$$

The complete solutions for the two displacements are

$$w_1(x) = \frac{Q_o L^4}{24E_o I_o (1+\delta)} \left\{ \frac{x^4}{L^4}(1+\delta) - \frac{4x^3}{L^3}[1 + (1-\alpha)\delta] \right.$$

$$\left. + \frac{4x}{L}\left[\delta(2+\alpha)(1-\alpha)^2 + 2\right] \right\} \qquad (A.7a)$$

$$w_2(x) = \frac{Q_o L^4}{24E_o I_o (1+\delta)} \left\{ \frac{x^4}{L^4} - \frac{4x^3}{L^3} - \frac{6x^2}{L^2}(1-\alpha)^2\delta \right.$$

$$\left. + \frac{4x}{L}\left[2 + 3(1-\alpha)^2\delta\right] - (1-\alpha)^4\delta \right\} \qquad (A.7b)$$

These solutions can be verified by realizing that the substitution of $\delta = 0$ reduces both equations to the equation for $w_o(x)$ in (A.4). Verification can similarly be found by substituting $\alpha = 0$ into $w_1(x)$ and $w_2(L)$, or $\alpha = 1$ into $w_2(x)$ and $w_1(0)$.

The displacement error for the two beam sections is the difference between the displacements given by (A.7) and the displacement $w_o(x)$ from (A.4):

$$\epsilon_1(x) = w_o(x) - w_1(x) = \frac{Q_o L^4 \delta\alpha}{24E_o I_o(1+\delta)}\left[-\frac{4x^3}{L^3} + \frac{4x}{L}(3-\alpha^2)\right] \qquad (A.8a)$$

$$\epsilon_2(x) = w_o(x) - w_2(x) = \frac{Q_o L^4 \delta}{24E_o I_o(1+\delta)}\left[\frac{x^4}{L^4} - \frac{4x^3}{L^3} + \frac{6x^2}{L^2}(1-\alpha)^2\right.$$

$$\left. + \frac{4x}{L}(-1+6\alpha-3\alpha^2) + (1-\alpha)^4\right] \qquad (A.8b)$$

A plot of the normalized displacement error[1] over the beam half-length is shown in Figure (A-1) for four values of α. In this plot, the normalized value of $\epsilon_1(x)$ is plotted in the range $x = 0$ to $x = L(1-\alpha)$, and the normalized value of $\epsilon_2(x)$ is plotted in the range $x = L(1-\alpha)$ to $x = L$. The location on each curve where $x/L = (1-\alpha)$ is the location where the two beams meet. Note that for a given α, the maximum value of $\epsilon_2(x)$ is always greater that the maximum value of $\epsilon_1(x)$. This indicates that we can find the maximum displacement error for the simply-supported beam with a step imperfection in EI from $\epsilon_2(x)$ alone. A check of the first and second derivatives of $\epsilon_2(x)$ (with respect to x and, separately, with respect to α) confirms that the maximum value of $\epsilon_2(x)$ occurs for $\alpha = 1$ and $x = L$. Therefore, the maximum displacement error for a simply-supported beam with a step imperfection in EI of amplitude δ and width of 2α is given by

$$\max \epsilon = \frac{5Q_o L^4 \delta}{24E_o I_o(1+\delta)} = \frac{\delta}{(1+\delta)}\, w_o(L) \qquad (A.9)$$

---

1. The displacecement error is normalized by multiplying by

$$\frac{24E_o I_o(1+\delta)}{Q_o L^4 \delta}$$

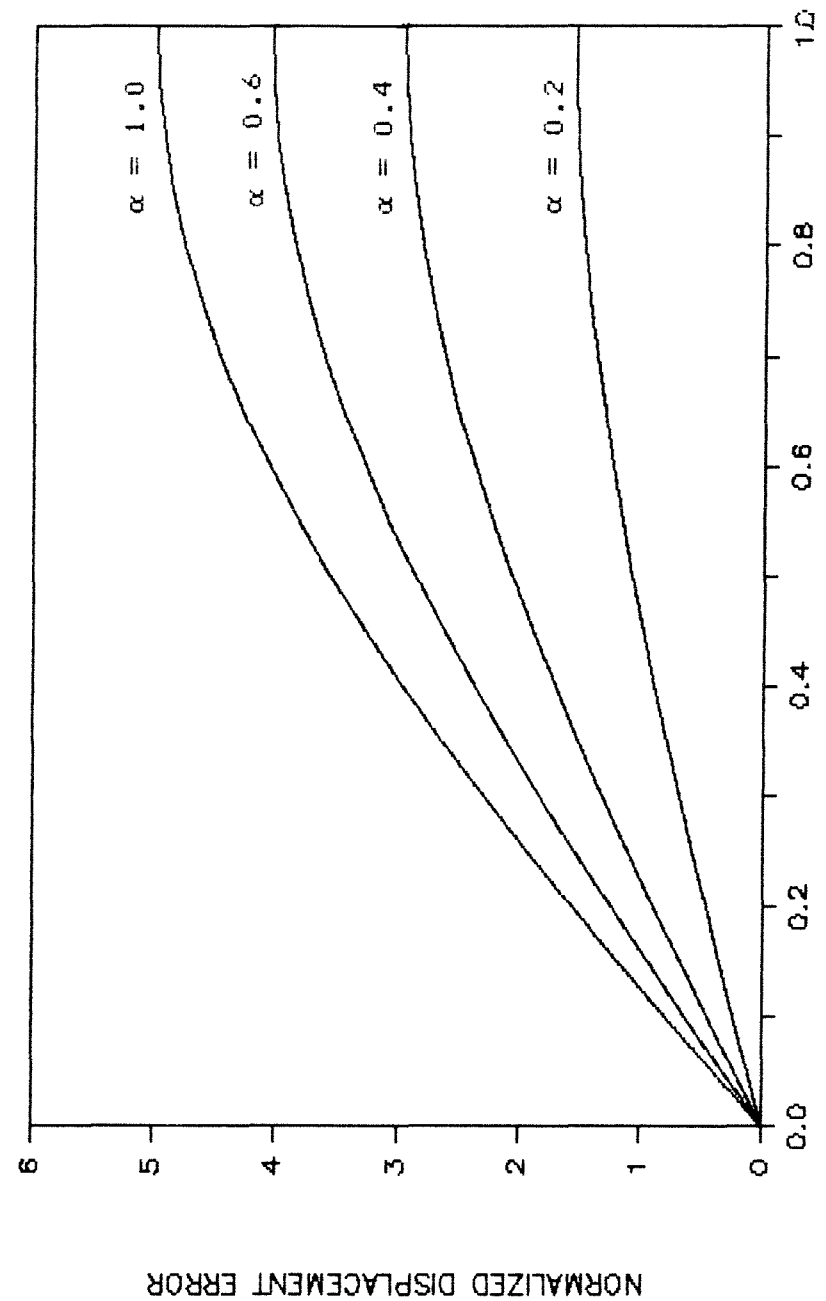

FIGURE A-1. DISPLACEMENT ERROR FOR A SIMPLY-SUPPORTED BEAM WITH A STEP IMPERFECTION IN BENDING STIFFNESS.

The sensitivy of displacement error ϵ to the amplitude of the imperfection in EI is of the form $\delta/(1+\delta)$, which reduces to a linear form for very small values of δ ($1>>\delta$).

Clamped Beam with Step Imperfection in EI

The solution for the displacement $w_o(x)$ of a clamped-clamped beam with length 2L, uniform bending stiffness, and uniform transverse load is

$$w_o(x) = \frac{Q_o L^4}{24 E_o I_o}\left(\frac{x^4}{L^4} - \frac{4x^3}{L^3} + \frac{4x^2}{L^2} \right) \qquad (A.10)$$

The maximum displacement occurs at the beam center, and is given by

$$w_o(L) = \frac{Q_o L^4}{24 E_o I_o} \qquad (A.11)$$

Consider a clamped-clamped beam of length 2L, with a step imperfection in EI identical that in the simply-supported case. Again, consider the beam section x = 0 to x = L to be composed of two different beams: Beam 1 has a bending stiffness of $EI = E_o I_o$, displacement $w_1(x)$, and exists over the interval x = 0 to x = L(1-α); Beam 2 has a bending stiffness of $EI = E_o I_o(1+\delta)$, displacement $w_2(x)$, and exists over the interval of x = L(1-α) to x = L. The boundary conditions at the center of the beam and at x = L(1-α) are the same as in Case 1. The clamped ends require that both (a) beam displacement and (b) slope be zero at x = 0. The resulting constants are

$$w_1(0) = 0 \rightarrow D_1 = 0 \qquad (A.12a)$$

$$w_1'(0) = 0 \rightarrow C_1 = 0 \qquad (A.12b)$$

$$w_2'''(L) = 0 \rightarrow A_2 = -\frac{Q_o L}{E_o I_o(1+\delta)} \tag{A.12c}$$

$$w_2'(L) = 0 \rightarrow C_2 = \frac{Q_o L^3}{3E_o I_o(1+\delta)} - B_2 L \tag{A.12d}$$

$$w_1'''(L-L\alpha) = w_2'''(L-L\alpha) \rightarrow A_1 = -\frac{Q_o L}{E_o I_o(1+\delta)}[1 + (1-\alpha)\delta] \tag{A.12e}$$

$$w_1''(L-L\alpha) = w_2''(L-L\alpha) \rightarrow B_1 = B_2 \tag{A.12f}$$

$$w_1'(L-L\alpha) = w_2'(L-L\alpha) \rightarrow B_1 = \frac{Q_o L^2}{3E_o I_o(1+\delta)}[(1-\alpha)^3\delta + 1] \tag{A.12g}$$

$$w_1(L-L\alpha) = w_2(L-L\alpha) \rightarrow D_2 = \frac{5Q_o L^4 \delta(1-\alpha)^4}{24E_o I_o(1+\delta)} \tag{A.12h}$$

The complete solutions for the two displacements, which can be verified in the same way as the displacements in the simply-supported case, are

$$w_1(x) = \frac{Q_o L^4}{24E_o I_o(1+\delta)}\left\{\frac{x^4}{L^4}(1+\delta) - \frac{4x^3}{L^3}[1+(1-\alpha)\delta] + \frac{4x^2}{L^2}[1+(1-\alpha)^3\delta]\right\} \tag{A.13a}$$

$$w_2(x) = \frac{Q_o L^4}{24E_o I_o(1+\delta)}\left\{\frac{x^4}{L^4} - \frac{4x^3}{L^3} + \frac{4x^2}{L^2}[1+(1-\alpha)^3\delta] - \frac{8x}{L}(1-\alpha)^3\delta + 5(1-\alpha)^4\right\} \tag{A.13b}$$

The corresponding displacement errors are

$$\epsilon_1(x) = \frac{Q_o L^4 \alpha\delta}{24E_o I_o(1+\delta)}\left[-\frac{4x^3}{L^3} + \frac{4x^2}{L^2}(3-3\alpha+\alpha^2)\right] \tag{A.14a}$$

$$\epsilon_2(x) = \frac{Q_o L^4 \delta}{24E_o I_o(1+\delta)}\left[\frac{x^4}{L^4} - \frac{4x^3}{L^3} + \frac{4x^2}{L^2}(3\alpha-3\alpha^2+\alpha^3) + \frac{8x}{L}(1-\alpha)^3 - 5(1-\alpha)^4\right] \tag{A.14b}$$

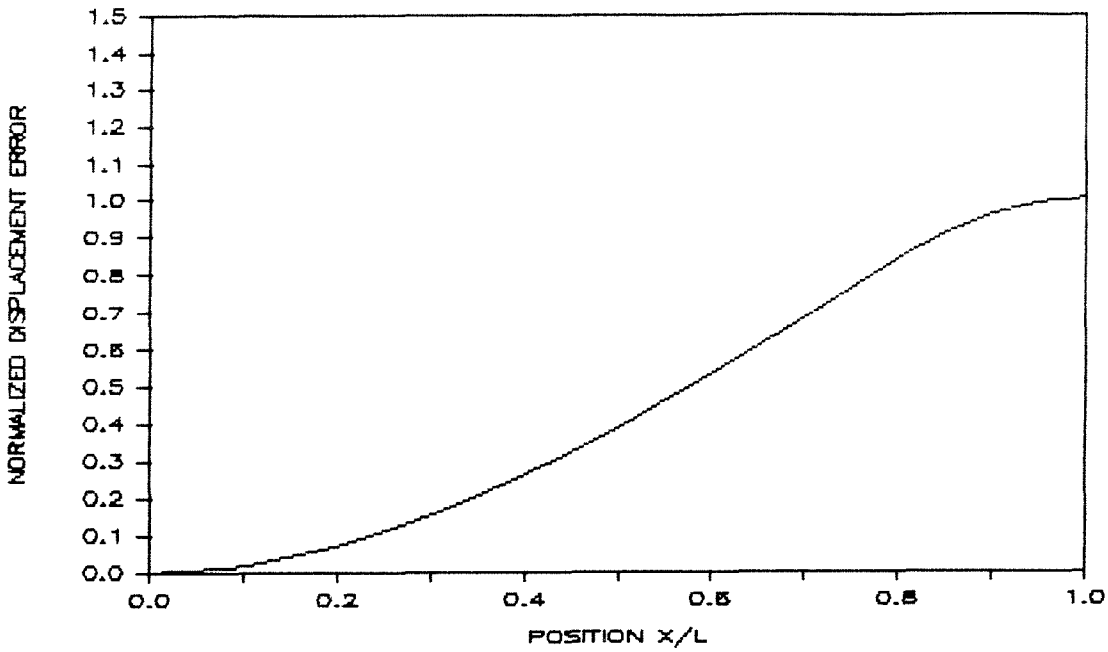

FIGURE A-2. DISPLACEMENT ERROR FOR A CLAMPED BEAM WITH A STEP IMPERFECTION OF WIDTH $\alpha = 0.2$ IN BENDING STIFFNESS.

FIGURE A-3. DISPLACEMENT ERROR FOR A CLAMPED BEAM WITH A STEP IMPERFECTION OF WIDTH $\alpha = 0.4$ IN BENDING STIFFNESS.

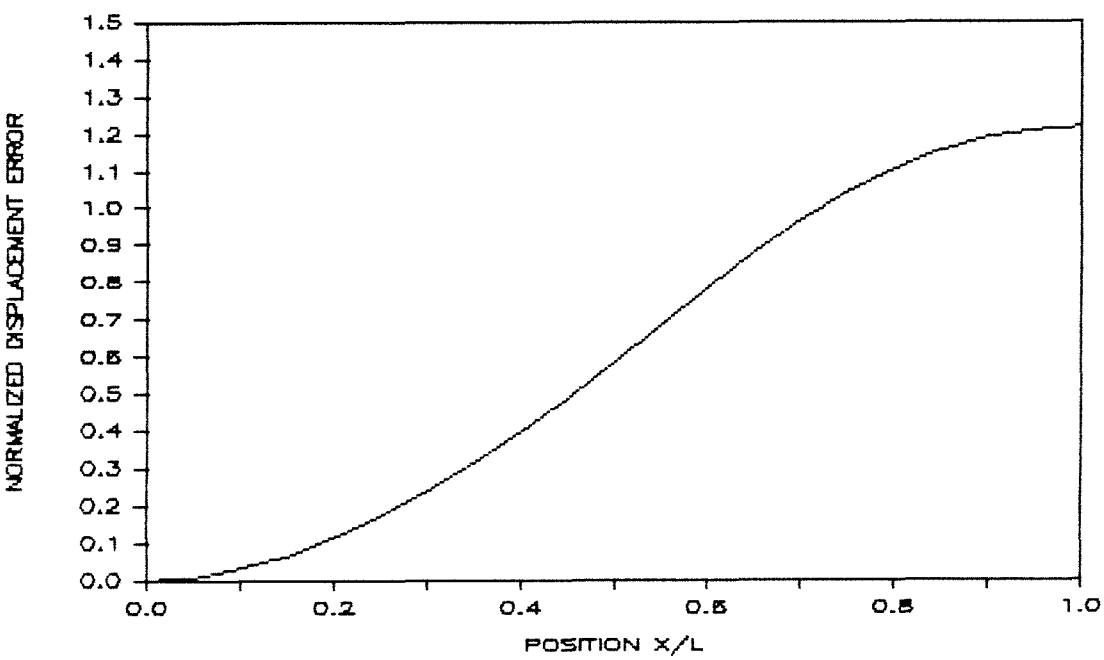

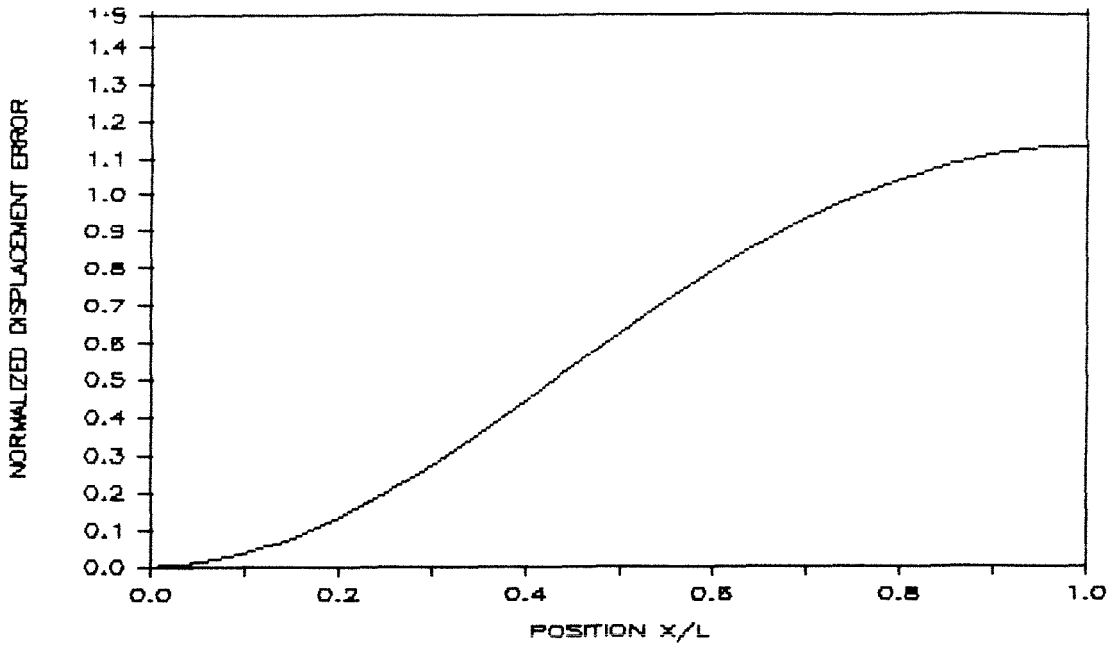

FIGURE A-4. DISPLACEMENT ERROR FOR A CLAMPED BEAM WITH A STEP IMPERFECTION OF WIDTH $\alpha = 0.6$ IN BENDING STIFFNESS.

FIGURE A-5. DISPLACEMENT ERROR FOR A CLAMPED BEAM WITH A STEP IMPERFECTION OF WIDTH $\alpha = 1.0$ IN BENDING STIFFNESS.

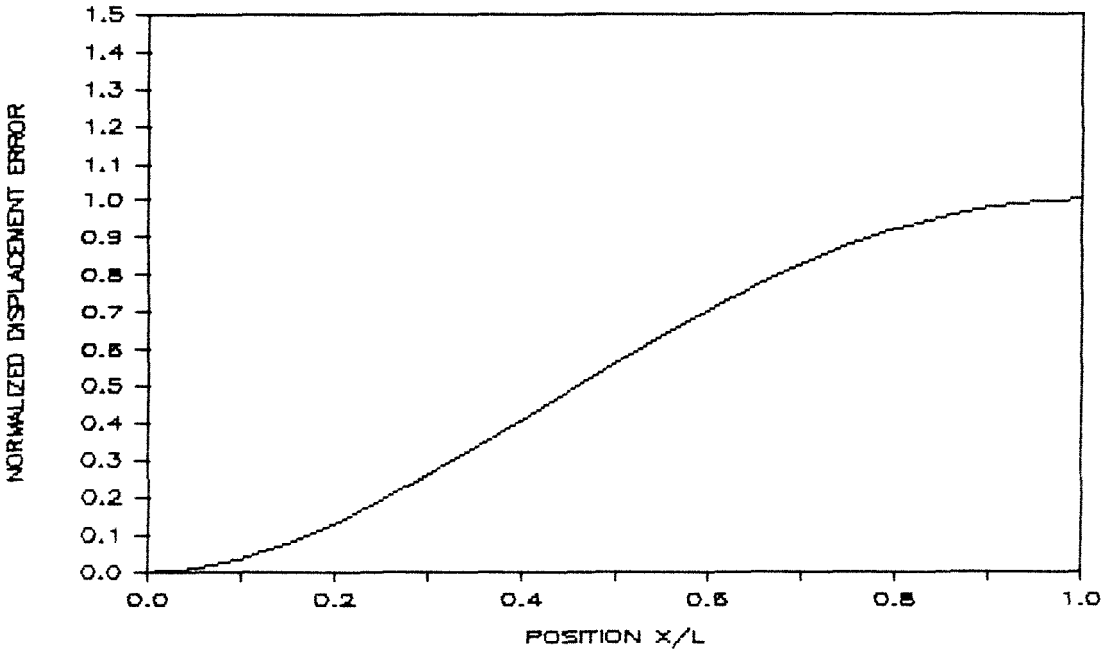

A plot of the normalized displacement error over the beam half-length is shown in Figures (A-2) to (A-5) for different values of α. Again, the maximum displacement error occurs in $\epsilon_2(x)$ at $x = L$. The error is maximum for $\alpha = 0.4$; this differs from the simply-supported case, in which the error is maximum for $\alpha = 1$. The maximum displacement error for a clamped beam with a step imperfection in EI of amplitude delta and width of 2α is given by

$$\max \epsilon = \frac{152}{125} \frac{Q_o L^4}{24 E_o I_o} \frac{\delta}{(1+\delta)} = \frac{152}{125} \frac{\delta}{(1+\delta)} w_o(L) \qquad (A.15)$$

Again, the sensitivy of displacement error ϵ to the amplitude of the imperfection in EI is of the form $\delta/(1+\delta)$.

Clamped Beam with Sinusoidal Imperfection in EI

Consider a beam of length 2L that has a sinusoidal imperfection in EI of the form

$$EI = E_o I_o (1 + \delta \sin \frac{n\pi x}{2L}) \qquad (A.16)$$

where n is the number of half-waves in the sinusoid (Figure A-6). Note that n must be odd to maintain symmetry of beam properties about $x = L$. Assume that the beam equation (A.1) can be solved using a perturbation solution of the form

$$w(x) = w_o(x) + \delta w_1(x) + \delta^2 w_2(x) + \ldots \qquad (A.17)$$

where $w_o(x)$ is the displacement for a clamped uniform beam given in (A.10). Assuming that the first perturbation term is satisfactory for an approximate solution, the displacement in (A.17) reduces to

FIGURE A-6. POSTULATED SINUSOIDAL IMPERFECTION IN BEAM BENDING STIFFNESS EI. Imperfection has the form $\sin(n\pi x/2L)$, with an amplitude of δ. Note that n must be an odd integer to maintain symmetry.

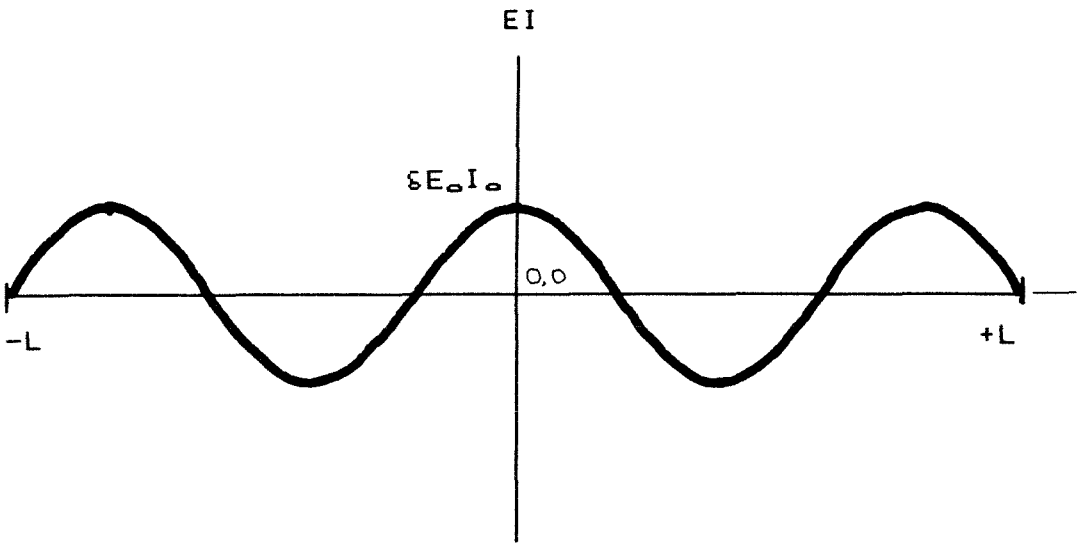

$$w(x) = w_o(x) + \delta w_1(x) \tag{A.18}$$

The four boundary conditions are

$$w(0) = 0 \tag{A.19a}$$

$$w'(0) = 0 \tag{A.19b}$$

$$w'(L) = 0 \tag{A.19c}$$

$$w'''(L) = 0 \tag{A.19d}$$

The resulting solution for $w_1(x)$ is

$$w_1(x) = \frac{Q_o L^4}{E_o I_o}\left\{\frac{4}{(n\pi)^2}\left[\frac{x^2}{2L^2} - \frac{x}{L} + \frac{1}{3} - \frac{12}{(n\pi)^2}\right]\sin\frac{n\pi x}{2L} + \frac{16}{(n\pi)^3}\left[1+\left[\frac{x}{L} - 1\right]\cos\frac{n\pi x}{2L}\right]\right.$$

$$\left. + \frac{1}{(n\pi)}\left[\frac{x^2}{L^2} - \frac{2x}{L}\right]\left[\frac{1}{3} - \frac{4}{(n\pi)^2}\right]\right\} \tag{A.20}$$

Note that as n tends to infinity, $w_1(x)$ tends to zero. The displacement error is found by subtracting $w_o(x)$ from the displacement $w(x)$ in (A.18), which results in

$$\epsilon(x) = \delta w_1(x) \tag{A.21}$$

Normalized plots of $\epsilon(x)$ vs. x/L for the first four values of n (Figures A-7 through A-10) show that the maximum displacement error always occurs at x = L. The maximum displacement error is greatest for n = 1. Thus, the maximum displacement error for a clamped-clamped beam with a sinusoidal imperfection of amplitude delta is

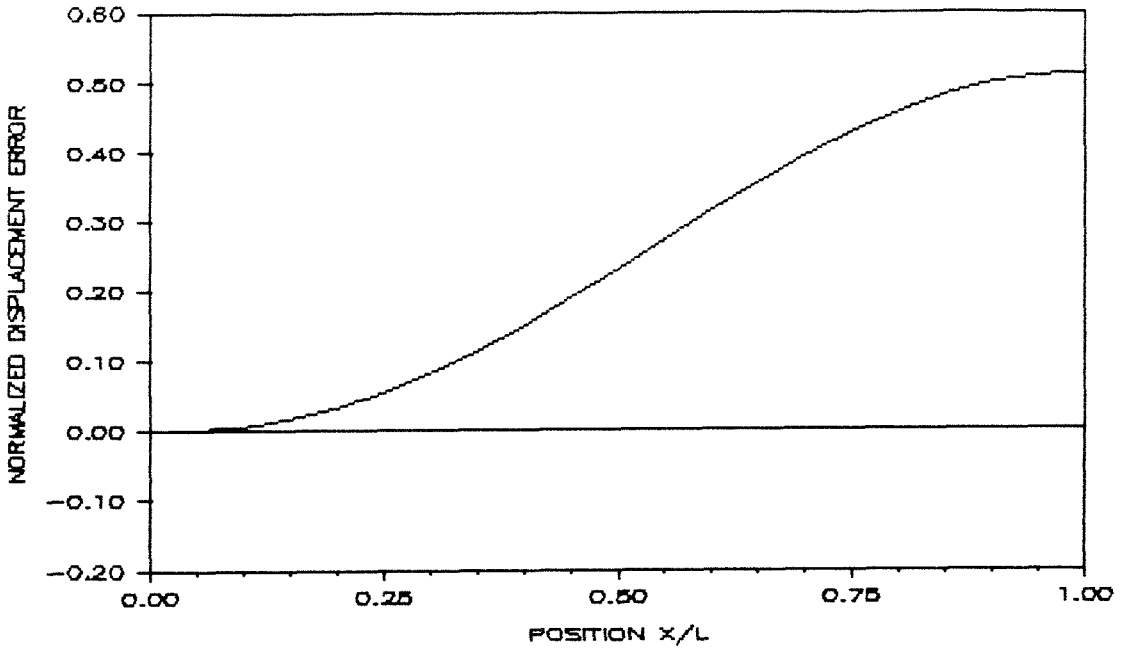

FIGURE A-7. DISPLACEMENT ERROR FOR A CLAMPED BEAM WITH A SINUSOIDAL IMPERFECTION IN BENDING STIFFNESS (n = 1).

FIGURE A-8. DISPLACEMENT ERROR FOR A CLAMPED BEAM WITH A SINUSOIDAL IMPERFECTION IN BENDING STIFFNESS (n = 3).

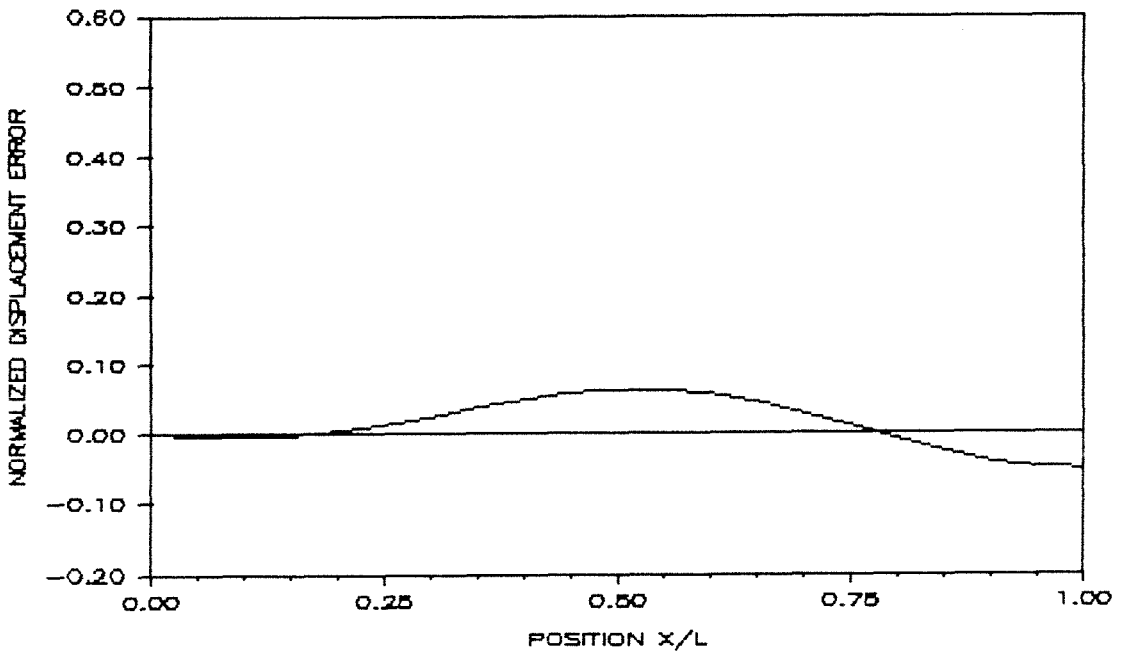

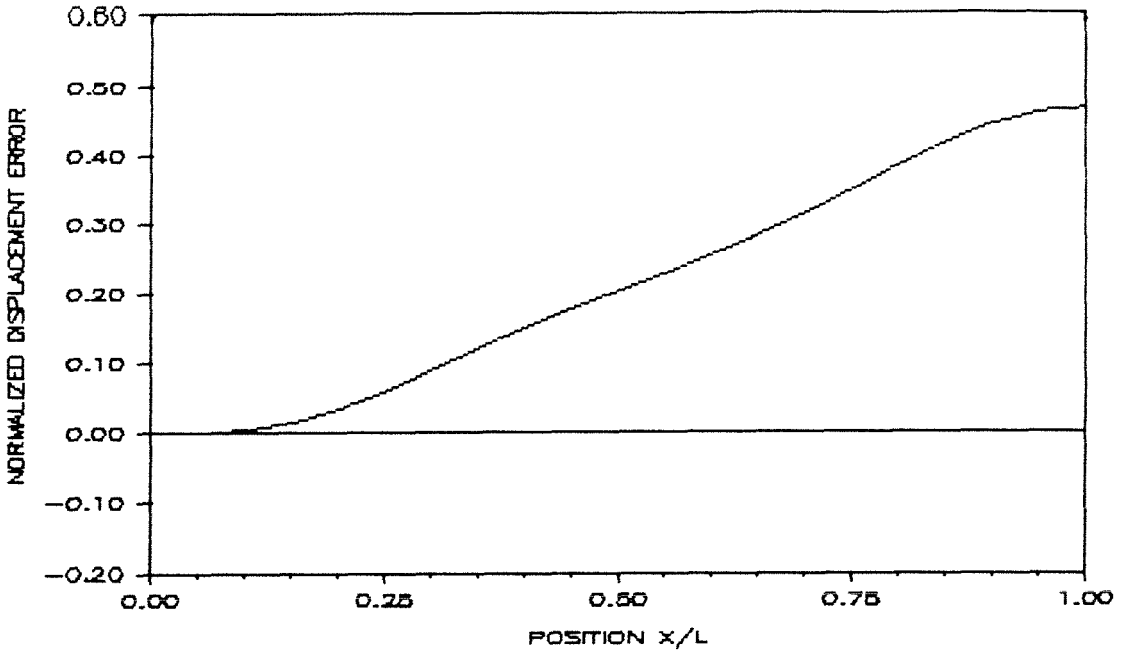

FIGURE A-9. DISPLACEMENT ERROR FOR A CLAMPED BEAM WITH A SINUSOIDAL IMPERFECTION IN BENDING STIFFNESS (n = 5).

FIGURE A-10. DISPLACEMENT ERROR FOR A CL
SINUSOIDAL IMPERFECTION IN BENDING STIFFN

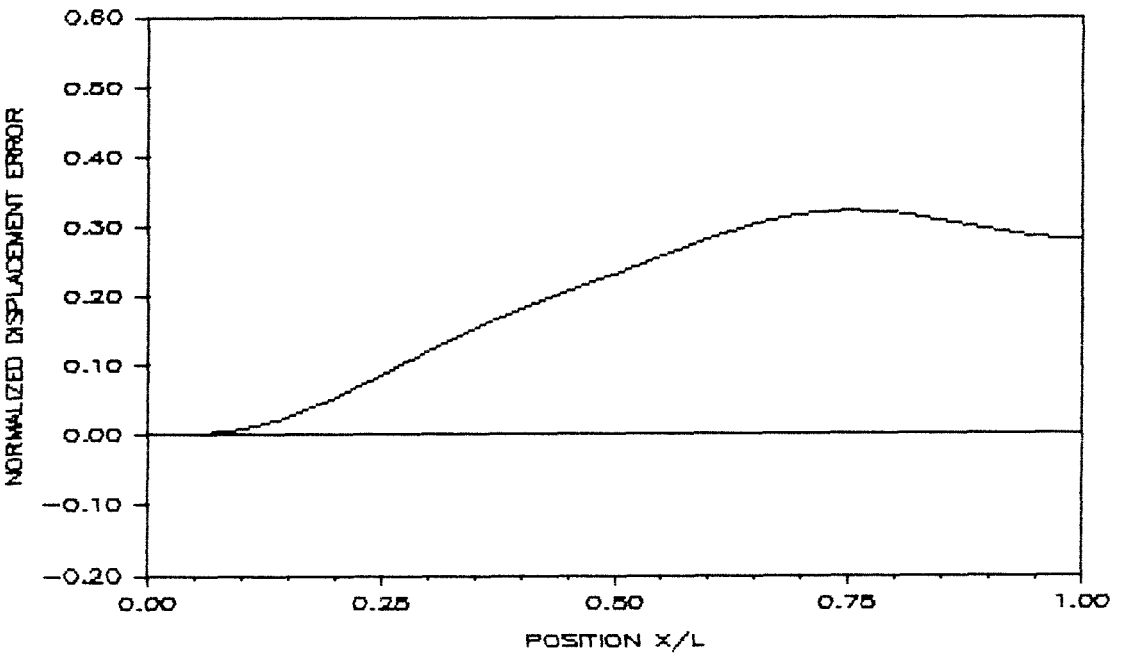

$$\max \epsilon = 0.021 \frac{Q_o L^4}{E_o I_o} \delta = 0.51 \delta w_o(L) \qquad (A.22)$$

Note that the dependence of $\epsilon(x)$ on δ for this case is linear. Recall, however, that this solution assumes that the value of δ is small.

APPENDIX B: INPUT DATA AND CALCULATED PRECESSION FOR SPINRATE DETERMINATION

Ω	Δt	radius	mass	I_{xx} (10^9)	I_{zz} (10^9)	precess
1	90	8.642	382.8	1.030	1.373	0.806
2	45	14.33	507.3	1.365	1.820	0.503
3	30	19.80	626.9	1.687	2.249	0.374
4	22	25.20	744.8	2.004	2.672	0.311
5	18	30.55	861.8	2.319	3.092	0.251
6	15	35.89	978.5	2.633	3.511	0.212
7	12	41.20	1095.0	2.947	3.929	0.191
8	11	46.52	1211.3	3.260	4.346	0.179
9	10	51.83	1327.3	3.572	4.762	0.155
10	9	57.15	1443.3	3.884	5.179	0.161
11	8	62.44	1559.4	4.169	5.595	0.130
12	7	67.74	1675.1	4.508	6.010	0.117
13	7	73.03	1791.2	4.820	6.427	0.112
14	6	78.35	1907.0	5.132	6.842	0.105
15	6	83.64	2022.7	5.443	7.257	0.102

Symbols:

Ω = spacecraft spinrate (rev/hr)

Δt = integration time step (sec) ≈ (spin period)/40

radius = radius of cylinder used to model antenna stick cross-sectional area (inches)

mass = total spacecraft mass (slugs) = $3(1.15)m_s$ (allows 15% for antenna stick joints)

I_{xx} = mass moment of inertia of spacecraft about its x-axis (slug-ft^2) = $I_{yy} = 3m_s s^2$

I_{yy} = mass moment of inertia of spacecraft about its spin axis (slug-ft^2) = $4m_s s^2$

precess = calculated spacecraft precession after 24 hours due to solar pressure and gravity gradient torques (deg)

APPENDIX C: QUASI-STATIC EQUILIBRIUM ANALYSIS OF A NINE-MASS RIGID BODY MODEL

The maximum axial loads carried by the members of the proposed structure can be estimated by analyzing the reaction of the structure to control thrusters in a quasi-static equilibrium state. The worst-case loads found from this analysis can be used as design loads for the structural members.

Assume the structure is a rigid body consisting of nine point masses and 21 massless connecting members (Figure 4-2) in equilibrium under the external load imposed by control thrusters (note that the tension-only cross members are excluded). The point masses are located at positions corresponding to the two ends and the center of each antenna stick. Each point mass has the mass of one-third of the antenna stick, or $m_s/3$. When a force is applied at some point in the structure, each point mass has inertial reactions to balance the applied translational and rotational loads. The massless connecting members of the structure must then carry internal loads to maintain equilibrium of the point masses.

If a control thruster is firing in a known direction at a known position in the structure, the inertial reactions of each point mass to the thruster load T can be determined. The translational acceleration acting on each point mass can be found by dividing the applied force T by the total mass of the structure m_B (note that $m_B = 3m_s$):

$$a_R = \frac{T}{m_B} = \frac{T}{3m_s} \qquad (C.1)$$

This translational acceleration acts on each point mass to produce an inertial reaction F_R of magnitude

$$F_R = \frac{m_s}{3} a_R = \frac{T}{9} \tag{C.2}$$

in the direction opposite of thruster load T.

The applied thruster load also creates a moment (or moments) about the center of gravity of the structure. Suppose that the thruster load T has a component that creates a moment M_u about a principal axis u that passes through the center of gravity. If the structure has a mass moment of inertia I_{uB} about u, then the moment M_u acts on the structure to produce an angular acceleration given by

$$\dot{\Omega}_u = \frac{M_u}{I_{uB}} \tag{C.3}$$

This angular acceleration acts uniformly on each point mass, so that a mass of $m_s/3$ with a moment arm of length r_u about axis u will experience an inertial reaction of magnitude

$$F_{\theta u} = \frac{m_s}{3} r_u \dot{\Omega}_u = \frac{m_s}{3} \frac{r_u M_u}{I_{uB}} \tag{C.4}$$

The moment vector of each inertial rotational reaction must oppose the applied moment vector. For example, if an applied load induces a positive moment, the inertial reaction at each point mass must be a negative moment.[1]

If the spacecraft is rotating with spinrate Ω (with Ω in rad/sec), an additional acceleration $\Omega^2 R$ acts in a radially outward direction on each point mass. This acceleration produces no net inertial reactions, because the force vectors it produces sum to zero.

---

1. The "right hand rule" is used in this analysis to determine the positive direction of rotational vectors.

The thruster loads, inertial reactions, and rotational loads at each joint reduce to three equations (one each in the x-, y-, and z-directions) that express the loads in terms of the thruster load T. Local equilibrium requires that the internal forces in the massless members connected to a joint exactly balance the external forces acting at that joint. Each of the nine joints has three local equilibrium equations (corresponding to the three applied load equations). This results in 27 simultaneous equations that determine the loads in the 21 massless members in terms of the thruster load T. The member loads are determined in this fashion for three load cases:

Thrusters firing at point 6 (center level)
Thrusters firing at point 3 (top level)
Thrusters firing at both point 6 and point 3

Thrusters Firing at Point 6

Assume that control thrusters are firing parallel to each of the three principal directions at point mass 6 on the center level of the structure. The principal axes of the nine-mass model correspond to the x-, y-, and z-axes of the model. One thruster is firing in the negative x-direction with thrust T_x, the second is firing in the positive y-direction with thrust T_y, and the third is firing in the negative z-direction with thrust T_z. The structure is spinning about the z-axis with spinrate Ω. Figure (C-1) shows the applied thruster loads and inertial reactions of the point masses for this load case.

Since the mass of each point mass is $m_s/3$, the inertial reactions to the translational force exerted by each thruster are the same at each point mass, and are given by

$$F_x = T_x/9 \qquad (C.5a)$$

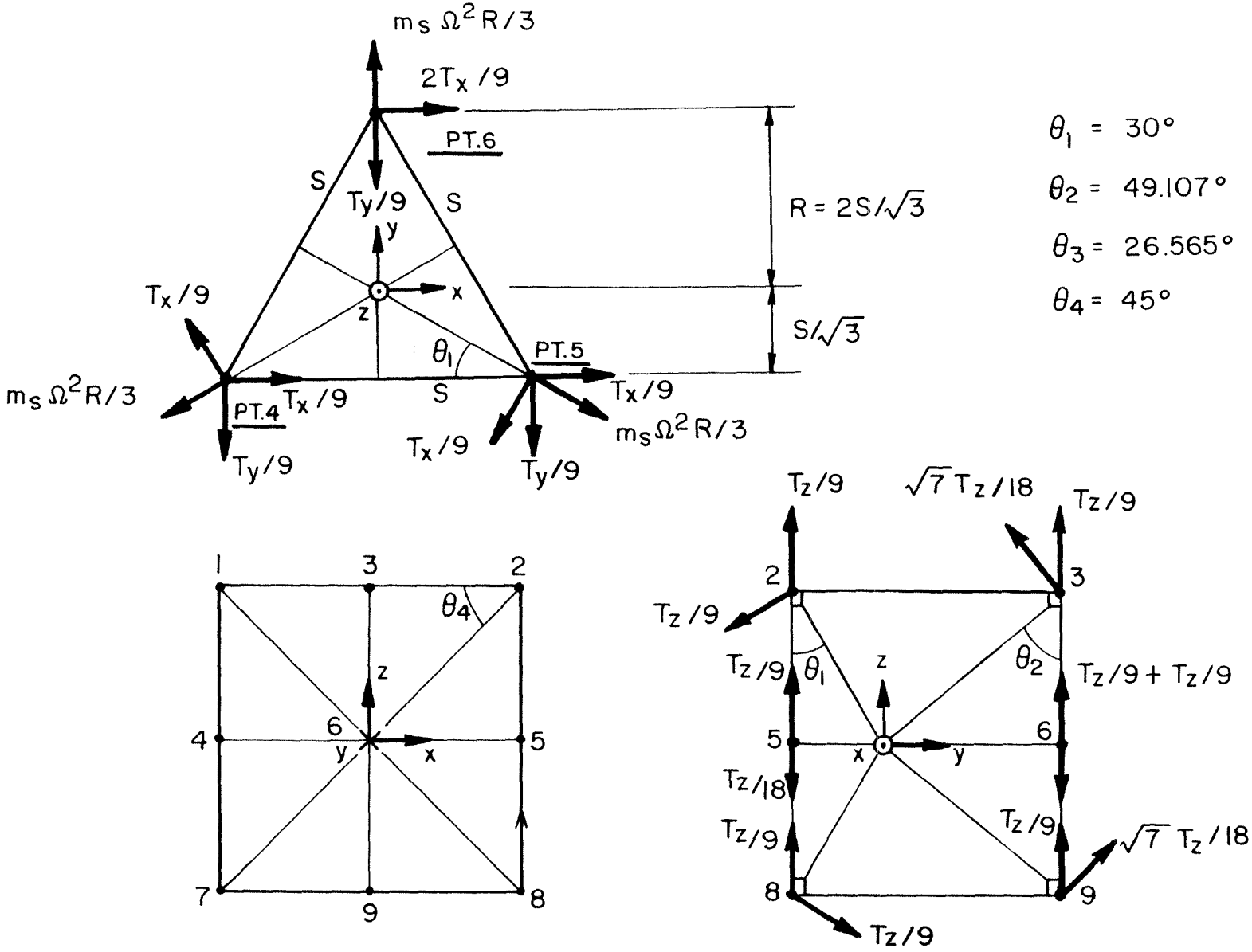

FIGURE C-1 INERTIAL REACTIONS OF THE NINE-MASS RIGID BODY MODEL TO THRUSTER LOADS APPLIED AT POINT 6

$$F_y = -T_y/9 \tag{C.5b}$$

$$F_z = T_z/9 \tag{C.5c}$$

where F_x and F_z act in the positive x- and z-directions, respectively, and F_y acts in the negative y-direction.

All the thruster loads are acting at a point on the y-axis; therefore, no rotational moment about the y-axis is created by the thrusters ($M_y = 0$, so $F_{\theta y} = 0$). However, the thrusters do create rotational moments about the x- and z-axes. T_x creates a positive moment $M_z = RT_x$ about the z-axis, while T_z creates a negative moment $M_x = RT_z$ about the x-axis.

Since each point mass has a moment arm of length R about the z-axis, each point mass has the same mass moment of inertia I_{zB} about the z-axis and the same inertial reaction to M_z. The mass moment of inertia I_{zB} of the structure is $I_{zB} = 3R^2m_s$; this, combined with the moment M_z, creates an angular acceleration about the z-axis of

$$\dot{\Omega}_z = \frac{M_z}{I_{zB}} = \frac{RT_x}{3R^2m_s} = \frac{T_x}{3}\,Rm_s \tag{C.6}$$

The resulting rotational reaction force at each point mass is given by

$$F_{\theta z} = \frac{m_s}{3}\,R\dot{\Omega}_z = \frac{m_s}{3}\,R\left\{\frac{T_x}{3Rm_s}\right\} = \frac{T_x}{9} \tag{C.7}$$

This force acts in a direction such that a negative torque is created about the z-axis.

The reaction to the applied moment about the x-axis is more difficult to find, because the point masses do not have the same moment arm about the x-axis. A list of the moment arms and mass moments of

inertia I_x for each point mass appears in Table (C-1). The mass moments of inertia of the individual point masses sum to a body moment of inertia I_{xB} of $4s^2m_s$ (recall that s is one-half the length of an antenna stick, so s = 500 m). The thruster T_z acts at distance $R = 2s/\sqrt{3}$ from the x-axis to create a uniform negative anguiar acceleration of

$$\dot{\Omega}_x = \frac{M_x}{I_{xB}} = \frac{(2s/\sqrt{3})T_z}{4s^2m_s} = \frac{T_z}{2\sqrt{3}sm_s} \qquad (C.8)$$

The resulting rotational reaction to M_x at points 1, 2, 7, and 8 is

$$F_{\theta x} = \left\{\frac{m_s}{3}\right\}\left\{\frac{2s}{\sqrt{3}}\right\}\left\{\frac{T_z}{2\sqrt{3}sm_s}\right\} = \frac{T_z}{9} \qquad (C.9a)$$

The rotational reaction to M_x at points 3 and 9 is

$$F_{\theta x} = \left\{\frac{m_s}{3}\right\}\left\{\frac{\sqrt{7}s}{\sqrt{3}}\right\}\left\{\frac{T_z}{2\sqrt{3}sm_s}\right\} = \frac{\sqrt{7}T_z}{18} \qquad (C.9b)$$

The rotational reaction to M_x are points 4 and 5 is

$$F_{\theta x} = \left\{\frac{m_s}{3}\right\}\left\{\frac{s}{\sqrt{3}}\right\}\left\{\frac{T_z}{2\sqrt{3}sm_s}\right\} = \frac{T_z}{18} \qquad (C.9c)$$

The rotational reaction to M_x at point 6 is

$$F_{\theta x} = \left\{\frac{m_s}{3}\right\}\left\{\frac{2s}{\sqrt{3}}\right\}\left\{\frac{T_z}{2\sqrt{3}sm_s}\right\} = \frac{T_z}{9} \qquad (C.9d)$$

The rotation of the spacecraft creates loads of magnitude $\Omega^2Rm_s/3$ which acts in a radially outward direction at each point mass.

TABLE C-1. MOMENT ARMS AND MASS MOMENTS OF INERTIA ABOUT X-AXIS IN NINE-MASS MODEL.

Point Mass	Moment Arm about X-Axis	I_x
1,2,7,8	$s\sqrt{1 + \tan^2 30°} = 2s/\sqrt{3}$	$4s^2m_s/9$
3,9	$s\sqrt{1 + 1/\cos^2 30°} = \sqrt{7}s/\sqrt{3}$	$7s^2m_s/9$
4,5	$s \cdot \tan 30° = s/\sqrt{3}$	$s^2m_s/9$
6	$s/\cos 30° = 2s/\sqrt{3}$	$4s^2m_s/9$

TABLE C-7. MOMENT ARMS AND MASS MOMENTS OF INERTIA ABOUT Y-AXIS IN NINE-MASS MODEL.

Point Mass	Moment Arm about Y-Axis	I_y
1,2,7,8	$\sqrt{2}s$	$2s^2m_s/3$
3,4,5,9	s	$s^2m_s/3$
6	0	0

The above loads can be separated into x, y, and z components for each point mass. The total load acting at each point mass (including thruster loads) is given in Table (C-2) in vector form, where the elements F_x, F_y, and F_z represent loads acting in the positive x-, y-, and z-directions, respectively. If we sum all the resulting loads and moments (including applied thruster loads) in their respective directions, we find that the sum of loads in each direction is zero, so that global equilibrium is satisfied.

Now that we have expressions for the external loads at each point mass, we need to relate the external loads to the loads carried by the massless members that connect to each point mass. Figure (C-2) shows the member numbering system used in the analysis. The 27 local equilibrium equations are given in Table (C-3). In the table, the designation $F_{x\#}$ indicates the external load in the u-direction at point mass number '#' (e.g., F_{x1} refers to the external load in the x-direction at point mass 1). The designation P_i indicates the tensile axial load in the i-th member.

The nine equations for points 1, 2, and 3 are solved as a set of simultaneous equations to find expressions for P_3, P_2, P_8, P_6, P_1, P_7, P_5, P_9, and P_4. The nine equations for points 7, 8, and 9 are solved as a set to find expressions for P_{21}, P_{19}, P_{18}, P_{13}, P_{16}, P_{14}, P_{20}, P_{17}, and P_{15}. These expressions are combined with the equations for F_x and F_y at point 4 and F_y at point 5 to find P_{10}, P_{11}, and P_{12}. All 27 of the equilibrium equations can be used to confirm the expressions found for the member axial loads. The 21 expressions for the member loads appear in Table (C-4). Note that only cross members carry the loads induced by spacecraft rotation. The maximum compressive load for each type of member can be found by setting the rotation rate Ω and selected thrusters loads in each equation to zero:

antenna sticks:

TABLE C-2. EXTERNAL LOADS ACTING ON POINT MASSES WHEN THRUSTERS ARE FIRING AT POINT 6.

Pt	F_x	F_y	F_z
1	$-m_s\Omega^2R/2\sqrt{3}+T_x/18$	$-m_s\Omega^2R/6+\sqrt{3}T_x/18- T_y/9-\sqrt{3}T_z/18$	$+ T_z/18$
2	$+m_s\Omega^2R/2\sqrt{3}+T_x/18$	$-m_s\Omega^2R/6-\sqrt{3}T_x/18- T_y/9-\sqrt{3}T_z/18$	$+ T_z/18$
3	$+2T_x/9$	$+m_s\Omega^2R/3 - T_y/9-\sqrt{3}T_z/18$	$+ 2T_z/9$
4	$-m_s\Omega^2R/2\sqrt{3}+T_x/18$	$-m_s\Omega^2R/6+\sqrt{3}T_x/18- T_y/9$	$+ T_z/18$
5	$+m_s\Omega^2R/2\sqrt{3}+T_x/18$	$-m_s\Omega^2R/6-\sqrt{3}T_x/18- T_y/9$	$+ T_z/18$
6	$-7T_x/9$	$+m_s\Omega^2R/3 +8T_y/9$	$- 7T_z/9$
7	$-m_s\Omega^2R/2\sqrt{3}+T_x/18$	$-m_s\Omega^2R/6+\sqrt{3}T_x/18- T_y/9+\sqrt{3}T_z/18$	$+ T_z/18$
8	$+m_s\Omega^2R/2\sqrt{3}+T_x/18$	$-m_s\Omega^2R/6-\sqrt{3}T_x/18- T_y/9+\sqrt{3}T_z/18$	$+ T_z/18$
9	$+2T_x/9$	$+m_s\Omega^2R/3 - T_y/9+\sqrt{3}T_z/18$	$+ 2T_z/9$

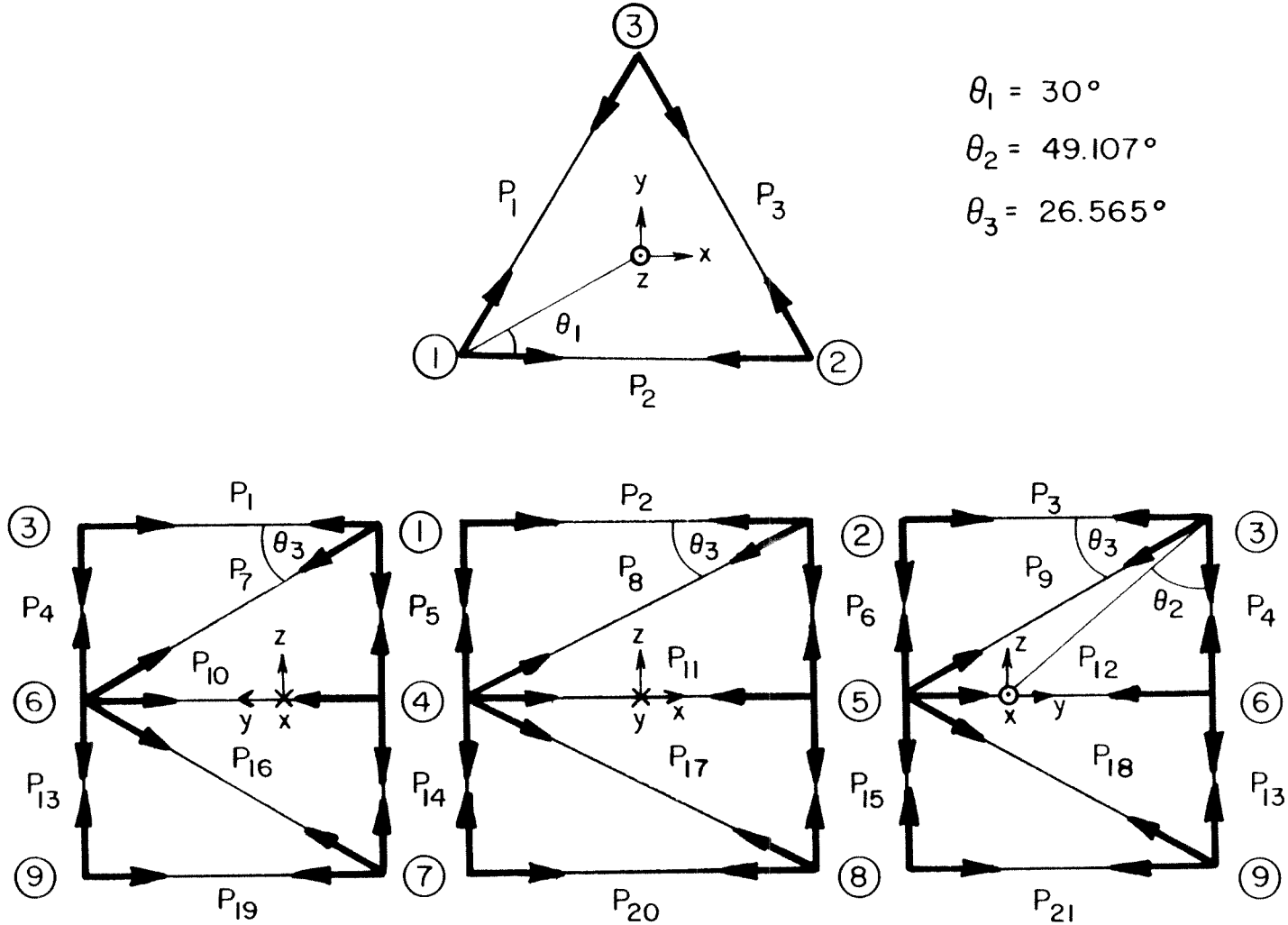

FIGURE C-2 MEMBER LOADS IN LOCAL EQUILIBRIUM FOR THE NINE - MASS RIGID BODY MODEL

TABLE C-3. LOCAL EQUILIBRIUM EQUATIONS FOR NINE-MASS RIGID BODY MODEL. "DIR" indicates the direction of force components summed on that line of the table.

PT	DIR	AXIAL TENSION IN MEMBER	
1	X	$+P_2+(P_1+2P_7/\sqrt{5})(1/2)$	$= -F_{X1}$
1	Y	$+(P_1+2P_7/\sqrt{5})(\sqrt{3}/2)$	$= -F_{Y1}$
1	Z	$-P_5-P_7/\sqrt{5}$	$= -F_{Z1}$
2	X	$-(P_2+2P_8/\sqrt{5})-P_3/2$	$= -F_{X2}$
2	Y	$+\sqrt{3}P_3/2$	$= -F_{Y2}$
2	Z	$-P_6-P_8/\sqrt{5}$	$= -F_{Z2}$
3	X	$+(P_3+2P_9/\sqrt{5})(1/2)-P_1/2$	$= -F_{X3}$
3	Y	$-\sqrt{3}P_1/2-(P_3+2P_9/\sqrt{5})(\sqrt{3}/2)$	$= -F_{Y3}$
3	Z	$-P_4-P_9/\sqrt{5}$	$= -F_{Z3}$
4	X	$+P_{11}+(P_8-P_{17})(2/\sqrt{5})+P_{10}/2$	$= -F_{X4}$
4	Y	$+\sqrt{3}P_{10}/2$	$= -F_{Y4}$
4	Z	$+P_5-P_{14}+(P_{18}-P_{17})(1/\sqrt{5})$	$= -F_{Z4}$
5	X	$-[P_{12}+(P_9+P_{18})(2/\sqrt{5})](1/2)-P_{11}$	$= -F_{X5}$
5	Y	$+[P_{12}+(P_9+P_{18})(2/\sqrt{5})](\sqrt{3}/2)$	$= -F_{Y5}$
5	Z	$+P_6-P_{15}+(P_9-P_{18})(1/\sqrt{5})$	$= -F_{Z5}$
6	X	$+[(P_{12}-P_{10})-(P_7-P_{16})(2/\sqrt{5})](1/2)$	$= -F_{X6}$
6	Y	$-[(P_{12}+P_{10})+(P_7+P_{16})(2/\sqrt{5})](\sqrt{3}/2)$	$= -F_{Y6}$
6	Z	$+P_4-P_{13}+(P_7-P_{16})(1/\sqrt{5})$	$= -F_{Z6}$
7	X	$+P_{20}+(P_{19}+2P_{16}/\sqrt{5})(1/2)$	$= -F_{X7}$
7	Y	$+(P_{19}+2P_{16}/\sqrt{5})(\sqrt{3}/2)$	$= -F_{Y7}$
7	Z	$+P_{14}+P_{16}/\sqrt{5}$	$= -F_{Z7}$
8	X	$-(P_{20}+2P_{17}/\sqrt{5})-P_{21}/2$	$= -F_{X8}$
8	Y	$+\sqrt{3}P_{21}/2$	$= -F_{Y8}$
8	Z	$+P_{15}+P_{17}/\sqrt{5}$	$= -F_{Z8}$
9	X	$+(P_{21}+2P_{18}/\sqrt{5})(1/2)-P_{19}/2$	$= -F_{X9}$
9	Y	$-(P_{21}+2P_{18}/\sqrt{5})(\sqrt{3}/2)-\sqrt{3}P_{19}/2$	$= -F_{Y9}$
9	Z	$+P_{13}+P_{18}/\sqrt{5}$	$= -F_{Z9}$

TABLE C-4. MEMBER LOADS INDUCED IN NINE-MASS MODEL WHEN THRUSTERS ARE FIRING AT POINT 6. "Type" refers to member type: S = antenna stick, C = cross member in support structure, D = diagonal member in support structure.

Pt	TYPE	AXIAL TENSION IN MEMBER
1	C	$+\sqrt{3}m_s\Omega^2R/9 + 2T_x/9 - \sqrt{3}T_y/27 - T_z/18$
2	C	$+\sqrt{3}m_s\Omega^2R/9 - \sqrt{3}T_y/27 - T_z/18$
3	C	$+\sqrt{3}m_s\Omega^2R/9 + T_x/9 + 2\sqrt{3}T_y/27 + T_z/9$
4	S	$+ T_x/6 + \sqrt{3}T_y/18 + 11T_z/36$
5	S	$+ T_x/6 - \sqrt{3}T_y/18 - T_z/36$
6	S	$+ T_z/18$
7	D	$-\sqrt{5}T_x/6 + \sqrt{15}T_y/18 + \sqrt{5}T_z/12$
8	D	0
9	D	$-\sqrt{5}T_x/6 - \sqrt{15}T_y/18 - \sqrt{5}T_z/12$
10	C	$+\sqrt{3}m_s\Omega^2R/9 - T_x/9 + 2\sqrt{3}T_y/27$
11	C	$+\sqrt{3}m_s\Omega^2R/9 - \sqrt{3}T_y/27$
12	C	$+\sqrt{3}m_s\Omega^2R/9 + 7T_x/9 + 8\sqrt{3}T_y/27$
13	S	$+ T_x/6 + \sqrt{3}T_y/18 - 11T_z/36$
14	S	$+ T_x/6 - \sqrt{3}T_y/18 + T_z/36$
15	S	$- T_z/18$
16	D	$-\sqrt{5}T_x/6 + \sqrt{15}T_y/18 - \sqrt{5}T_z/27$
17	D	0
18	D	$-\sqrt{5}T_x/6 - \sqrt{15}T_y/18 + \sqrt{5}T_z/12$
19	C	$+\sqrt{3}m_s\Omega^2R/9 + 2T_x/9 - \sqrt{3}T_y/27 + T_z/18$
20	C	$+\sqrt{3}m_s\Omega^2R/9 - \sqrt{3}T_y/27 + T_z/18$
21	C	$+\sqrt{3}m_s\Omega^2R/9 + T_x/6 + 2\sqrt{3}T_y/27 - T_z/9$

$$P_{13} = -11T_z/36 \qquad (T_x = T_y = 0) \tag{C.10a}$$

cross members:

$$P_2 = -\sqrt{3}T_y/27 - T_z/18 \qquad (\Omega = 0) \tag{C.10b}$$

diagonal members:

$$P_9 = -\sqrt{5}T_x/6 - \sqrt{15}T_y/18 - \sqrt{5}T_z/12 \tag{C.10c}$$

Verification of Loads by Finite Element Analysis

The loads found by the conventional analysis above are confirmed by static finite element analysis. The SDRC "SUPERB" finite element software is used for the analysis. The model consists of nine nodes, located at the "point mass" positions, and 21 linear beam elements, located at the "massless connecting member" positions. The bottom level nodes (corresponding to point masses 7, 8, and 9) are partially restrained to prevent rigid body motion, such that nodes 7 and 8 are allowed motion in the x-direction only, and node 9 is allowed motion in the y-direction only.

If the spinrate Ω is assumed to be zero, and all thruster loads are assumed to be 4.45 N (a one-pound thruster load), then numeric values can be calculated for external loads acting at all nine of the point masses (Table C-5). These loads are applied to the nodes in the appropriate directions to simulate the thruster and inertial reaction loads acting on the structure; however, no loads can be applied in the restrained directions on nodes 7, 8, and 9. The finite element analysis calculates the inertial reaction forces at each node, and gives an output listing of the resulting nodal force balance.

TABLE C-5. NODAL LOADS APPLIED TO FINITE ELEMENT MODEL TO SIMULATE THRUSTERS FIRING AT POINT 6 ($T_x = T_y = T_z = 4.45$ N, $\Omega = 0$).

Node	F_x (N)	F_y (N)	F_z (N)
1	0.24722	-0.49444	0.24722
2	0.24722	-1.3509	0.24722
3	0.98889	-0.92265	0.98889
4	0.24722	-0.06625	0.24722
5	0.24722	-0.92265	0.24722
6	-3.4611	3.95556	-3.4611
7	0.24722	0.36196*	0.24722*
8	0.24722	-0.49444*	0.24722*
9	0.98889*	-0.06625	0.98889*

* Because nodal motion is restrained in this direction, this load is not applied to the finite element model. Instead, this load appears as a reaction force in the finite element analysis output.

The member loads calculated by the finite element analysis for the structural members are compared to the loads found by conventional analysis (assuming 1 lb thrusters, with Ω=0) in Table (C-6).[2] The table shows that the finite element analysis confirms the load values conventional analysis to three significant digits.

Thrusters Firing at Point Mass 3

To find the member loads that are induced by control thrusters firing at point mass 3, conventional analysis is used (in a manner similar to the above analysis) to find the external loads acting on each point mass. Figure (C-3) shows the inertial reaction loads and spin loads for this analysis. The translational inertial reactions and spin loads are the same as if the thrusters are acting at point mass 6. However, some of the rotational reactions differ because the thrusters are no longer acting at a point on the y-axis.

The thruster load T_x acting at point 3 creates a moment $M_y = sT_x$ about the y-axis. The moment arm and mass moment of inertia I_y about the y-axis for each mass point are listed in Table (C-7). The mass moment of inertia I_{yB} of the structure is $4s^2m_s$, the same as I_{xB}. The angular acceleration created by M_y is $\dot{\Omega}_y = T_x/4sm_s$. The resulting negative rotational reaction at points 1, 2, 7, and 8 has a magnitude of

$$F_{\theta y} = T_x/6\sqrt{2} \qquad (C.11a)$$

The negative rotational reaction at points 3, 4, 5, and 9 has a magnitude of

2. The output listing of the finite element analysis contains some load values of magnitude 10^{-6} to 10^{-20}. These are considered to be numerical errors, and the affected values are taken to be zero.

TABLE C-6. MEMBER LOADS INDUCED BY THRUSTERS FIRING AT POINT 6 ($T_x = T_y = T_z = 4.45$ N, $\Omega = 0$)

Member	Conventional Analysis	Finite Element Analysis
P_1	+0.4562	+0.456
P_2	-0.5327	-0.533
P_3	+1.5598	+1.560
P_4	+2.5296	+2.53
P_5	+0.1901	+0.190
P_6	+0.2472	+0.247
P_7	+0.1283	+0.128
P_8	0	0.000
P_9	-3.4451	-3.445
P_{10}	+0.0765	+0.076
P_{11}	-0.2855	-0.285
P_{12}	+5.7449	+5.745
P_{13}	-0.1899	-0.190
P_{14}	+0.4371	+0.437
P_{15}	-0.2472	-0.247
P_{16}	-1.5301	-1.534
P_{17}	0	0.000
P_{18}	-1.7867	-1.784
P_{19}	+0.9506	+0.951
P_{20}	-0.0382	-0.038
P_{21}	+0.5709	+0.571

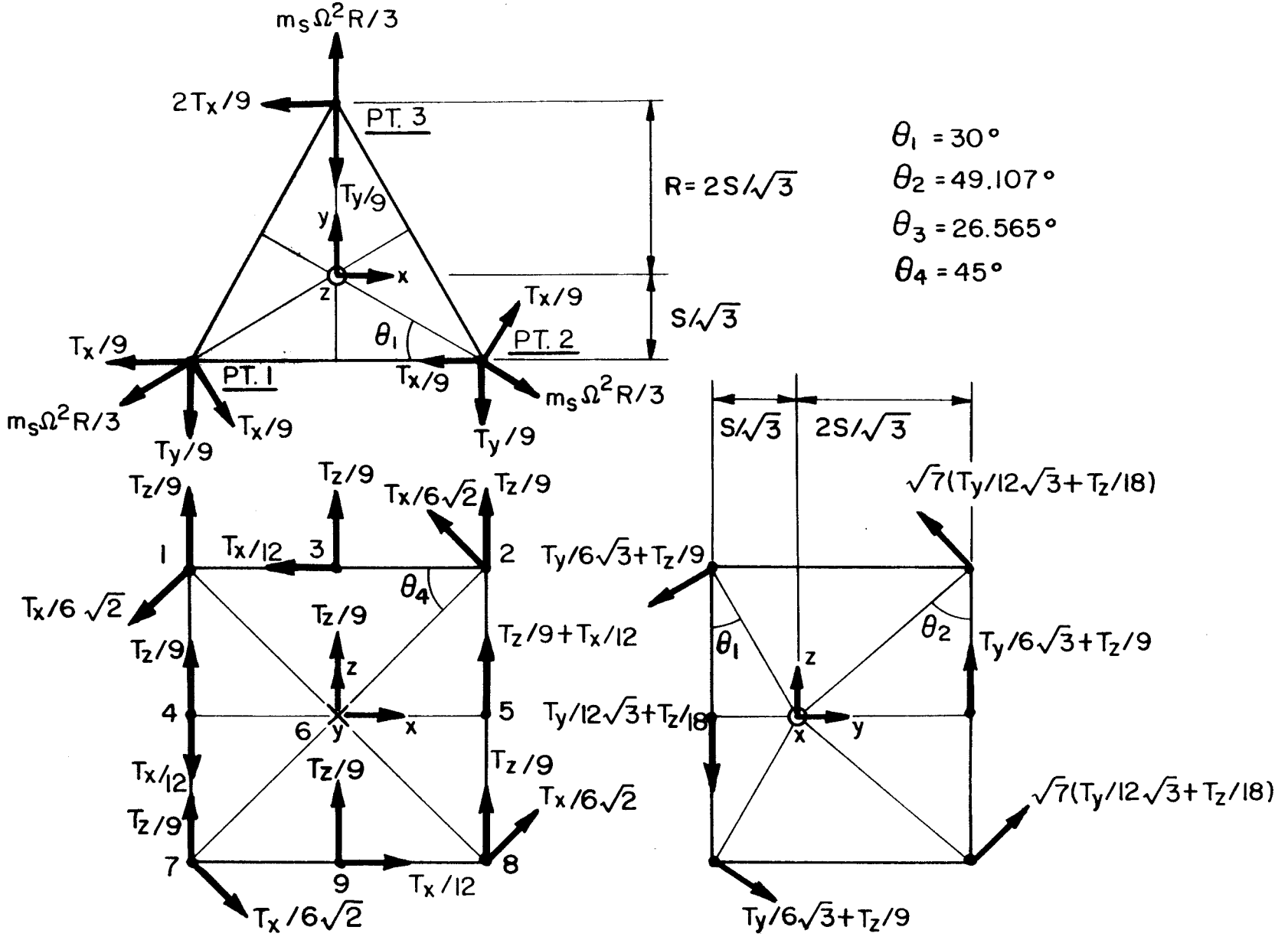

FIGURE C-3 INERTIAL REACTIONS OF THE NINE-MASS RIGID BODY MODEL TO THRUSTER LOADS APPLIED AT POINT 3

$$F_{\theta y} = T_x/12 \qquad (C.11b)$$

Note that point mass 6 lies on the y-axis, and has no reaction to the moment M_y.

Both T_z and T_y contribute to the moment M_x about the x-axis; M_x is a negative moment of magnitude

$$M_x = \left(\frac{\sqrt{7}s}{\sqrt{3}}\right)\left(\frac{\sqrt{3}T_y}{\sqrt{7}} + \frac{2T_z}{\sqrt{7}}\right) = s\left(T_y + \frac{2T_z}{\sqrt{3}}\right) \qquad (C.12)$$

The moment arms and mass moments of inertia about the x-axis are listed in Table (C-1). The rotational reaction to M_x at points 1, 2, 6, 7, and 8 is

$$F_{\theta x} = T_y/6\sqrt{3} + T_z/9 \qquad (C.13a)$$

The reaction to M_x at points 3 and 9 is

$$F_{\theta x} = \sqrt{7}(T_y/12\sqrt{3} + T_z/18) \qquad (C.13b)$$

The reaction to M_x at points 4 and 5

$$F_{\theta x} = T_y/12\sqrt{3} + T_z/18 \qquad (C.13c)$$

The angular acceleration $\dot{\Omega}_z$ created about the z-axis by T_x is the same as in the previous analysis, so the rotational reactions to M_z are the same. A summary of the external forces acting on each point mass is given in Table (C-8).

Finite element analysis (without conventional analysis) is used to find the member loads for this case. The nodal loads applied to the finite element model appear in Table (C-9). The model is the same as

TABLE C-8. EXTERNAL LOADS ACTING ON POINT MASSES WHEN THRUSTERS ARE FIRING AT POINT 3.

Pt	F_x	F_y	F_z
1	$-m_s\Omega^2R/2\sqrt{3}-5T_x/36$	$-m_s\Omega^2R/6-\sqrt{3}T_x/18-7T_y/12-\sqrt{3}T_z/18$	$-T_x/12-\sqrt{3}T_y/36+T_z/18$
2	$+m_s\Omega^2R/2\sqrt{3}-5T_x/18$	$-m_s\Omega^2R/6-\sqrt{3}T_x/18-7T_y/12-\sqrt{3}T_z/18$	$+T_x/12-\sqrt{3}T_y/36+T_z/18$
3	$+25T_x/9$	$+m_s\Omega^2R/3+29T_y/36-\sqrt{3}T_z/18$	$+\sqrt{3}T_y/18-7T_z/9$
4	$-m_s\Omega^2R/2\sqrt{3}-T_x/18$	$-m_s\Omega^2R/6-\sqrt{3}T_x/18-T_y/9$	$-T_x/12-\sqrt{3}T_y/36+T_z/18$
5	$+m_s\Omega^2R/2\sqrt{3}-T_x/18$	$-m_s\Omega^2R/6+\sqrt{3}T_x/18-T_y/9$	$+T_x/12-\sqrt{3}T_y/36+T_z/18$
6	$-2T_x/9$	$+m_s\Omega^2R/3-T_y/9$	$+\sqrt{3}T_y/18+2T_z/9$
7	$-m_s\Omega^2R/2\sqrt{3}+T_x/18$	$-m_s\Omega^2R/6-\sqrt{3}T_x/18-T_y/36+\sqrt{3}T_z/18$	$-T_x/12-\sqrt{3}T_y/36+T_z/18$
8	$+m_s\Omega^2R/2\sqrt{3}+T_x/18$	$-m_s\Omega^2R/6+\sqrt{3}T_x/18-T_y/36+\sqrt{3}T_z/18$	$+T_x/12-\sqrt{3}T_y/36+T_z/18$
9	$-5T_x/36$	$+m_s\Omega^2R/3-T_y/36+\sqrt{3}T_z/18$	$+\sqrt{3}T_y/18+2T_z/9$

TABLE C-9. NODAL LOADS APPLIED TO FINITE ELEMENT MODEL TO SIMULATE THRUSTERS FIRING AT POINT 3 ($T_x = T_y = T_z = 4.45$ N, $\Omega = 0$).

Node	F_x (N)	F_y (N)	F_z (N)
1	-0.61806	-1.72168	-0.33771
2	-0.61806	-0.86528	+0.40395
3	+3.09028	+3.15652	-3.03291
4	-0.24722	-0.92265	-0.33771
5	-0.24722	-0.06624	+0.40395
6	-0.98889	-0.49444	+1.41709
7	+0.12361	-0.12361*	-0.33771*
8	+0.12361	+0.73279*	+0.40395*
9	-0.61806*	+0.30459	+1.41709*

* Because nodal motion is restrained in this direction, this load is not applied to the finite element model. Instead, this load appears as a reaction force in the finite element analysis output.

that used above. Again, the output listing of nodal force balance confirms that the calculated point mass loads are correct. The resulting member beam loads (assuming 1 lb. thrusters and $\Omega = 0$) are given in Table (C-10).

Thrusters firing at Both Point 6 and Point 3

At some point during spacecraft maneuvers, it may be desirable to fire thrusters at more than one joint in the structure. The resulting member loads may exceed those calculated for a case in which thruster firing occurs at only one joint. To check this possibility, we can find the worst-case member loads induced when thrusters fire at both point mass 3 and point mass 6.

Finite element analysis can be used to calculate the member loads that result when a single thruster is fired at a given point mass location. When this analysis is run for the case of a single thruster firing at point mass 6 in each of 3 principal directions (i.e., positive F_x, F_y, and F_z), then the loads resulting from the firing of any combination of thrusters at point mass 6 can be determined simply by summing the appropriate member loads from the single thruster analyses. This process can be repeated to obtain member loads resulting when individual thrusters are firing at point mass 3.

Through the principle of superposition, the member loads calculated for the first case can be summed with the loads calculated for the second case to determine member loads that result when thrusters are firing at both points. The results of the superposition indicate that worst-case compressive member loads occur when thrusters are firing at more than one mass point. Calculating the member loads induced by all possible combinations of thruster firings is too time-consuming for a preliminary structural analysis. Therefore, the worst-case loads found by combining the two analyses are used as design loads for the structural members; a multiplicative "fudge factor" should be used with

TABLE C-10. MEMBER LOADS INDUCED BY THRUSTERS FIRING AT POINT 3 ($T_x = T_y = T_z = 4.45$ N, $\Omega = 0$)

Member	Finite Element Analysis	Type
P_1	-1.28	C
P_2	-1.12	C
P_3	+1.99	C
P_4	-4.50	S
P_5	-0.73	S
P_6	-0.71	S
P_7	+2.54	D
P_8	+0.83	D
P_9	+3.28	D
P_{10}	+0.08	C
P_{11}	-0.29	C
P_{12}	-1.27	C
P_{13}	-1.13	S
P_{14}	+0.42	S
P_{15}	+0.71	S
P_{16}	-1.83	D
P_{17}	-0.83	D
P_{18}	-0.65	D
P_{19}	+0.79	C
P_{20}	+0.55	C
P_{21}	+0.14	C

these results, however, to allow for the possibility that larger compressive member loads might be found if all possible combinations of thrusters were analyzed. The worst-case loads are given in Table (C-11).

TABLE C-11. WORST CASE MEMBER LOADS FOUND BY QUASI-STATIC EQUILIBRIUM ANALYSIS ($T_x = T_y = T_z = 4.45$ N, $\Omega = 0$). "$+T_x$" in "Point 3 Thrusters" column indicates a thruster load applied at point 3 in the positive x-direction.

MEMBER TYPE	POINT 3 THRUSTERS	POINT 6 THRUSTERS	MEMBER NUMBER	LOAD (N)
antenna stick	0	$-T_x + T_y - T_z$	P_4	- 4.50
antenna stick	0	$+T_x + T_z$	P_4	+ 4.39
cross member	$+T_x$	$+T_x$	P_{12}	- 4.44
cross member	0	$-T_x + T_y + T_z$	P_{12}	+ 5.74
diagonal member	$-T_x + T_y + T_z$	$-T_x + T_y + T_z$	P_{18}	- 5.75
diagonal member	$+T_x + T_y + T_z$	$+T_x + T_y + T_z$	P_{16}	+ 5.75